RÉPUBLIQUE ALGÉRIENNE DÉMOCRATIQUE ET POPULAIRE
MINISTÈRE DE L'ENSEIGNEMENT SUPÉRIEUR ET DE LA RECHERCHE SCIENTIFIQUE

École Nationale Polytechnique - Department of Civil Engineering

In collaboration with:

École des Ponts ParisTech - Research Center for Applied Mathematics

Rutgers University Camden - Department of Mathematical Sciences

CIRCLES Consortium

End-of-studies dissertation for obtaining the degree of **State Engineer** in **Civil Engineering**

Autonomous Vehicles and Mixed Traffic Flows for the Dissipation of Stop-and-go Waves in Multi-lane Ring Roads

---

By: **Tinhinane MEZAIR**

Under the direction of:

Internal supervisors: **Dr. Abdelmadjid TADJADIT** and **Pr. Latifa DEBBI**

External supervisors: **Dr. Amaury HAYAT** and **Pr. Benedetto PICCOLI**

Publicly defended on June 29^{th}, 2022, in front of the jury composed of:

President	Abderrahim BALI	Pr	ENP
Supervisor	Abdelmadjid TADJADIT	MC B	ENP
Co-supervisor	Latifa DEBBI	Pr	ENP
Co-supervisor	Amaury HAYAT	Maître de Conférences	ENPC
Examinator	Sana STIHI	MA A	ENP

ENP 2022

RÉPUBLIQUE ALGÉRIENNE DÉMOCRATIQUE ET POPULAIRE
MINISTÈRE DE L'ENSEIGNEMENT SUPÉRIEUR ET DE LA RECHERCHE SCIENTIFIQUE

École Nationale Polytechnique - Department of Civil Engineering

In collaboration with:

École des Ponts ParisTech - Research Center for Applied Mathematics

Rutgers University Camden - Department of Mathematical Sciences

CIRCLES Consortium

End-of-studies dissertation for obtaining the degree of **State Engineer** in **Civil Engineering**

Autonomous Vehicles and Mixed Traffic Flows for the Dissipation of Stop-and-go Waves in Multi-lane Ring Roads

---

By: **Tinhinane MEZAIR**

Under the direction of:

Internal supervisors: **Dr. Abdelmadjid TADJADIT** and **Pr. Latifa DEBBI**

External supervisors: **Dr. Amaury HAYAT** and **Pr. Benedetto PICCOLI**

Publicly defended on June 29^{th}, 2022, in front of the jury composed of:

President	Abderrahim BALI	Pr	ENP
Supervisor	Abdelmadjid TADJADIT	MC B	ENP
Co-supervisor	Latifa DEBBI	Pr	ENP
Co-supervisor	Amaury HAYAT	Maître de Conférences	ENPC
Examinator	Sana STIHI	MA A	ENP

ENP 2022

RÉPUBLIQUE ALGÉRIENNE DÉMOCRATIQUE ET POPULAIRE
MINISTÈRE DE L'ENSEIGNEMENT SUPÉRIEUR ET DE LA RECHERCHE SCIENTIFIQUE

École Nationale Polytechnique - Département de Génie Civil

En collaboration avec:

École des Ponts ParisTech - Centre de Recherche en Mathématiques Appliquées

Rutgers University Camden - Département des Sciences Mathématiques

CIRCLES Consortium

Mémoire de projet de fin d'études pour l'obtention du diplôme d'**Ingénieur d'État** en **Génie Civil**

Autonomous Vehicles and Mixed Traffic Flows for the Dissipation of Stop-and-go Waves in Multi-lane Ring Roads

---

Par: **Tinhinane MEZAIR**

Sous la direction de:

Encadrants internes: **Dr. Abdelmadjid TADJADIT** et **Pr. Latifa DEBBI**

Encadrants externes: **Dr. Amaury HAYAT** et **Pr. Benedetto PICCOLI**

Soutenu publiquement le 29 juin 2022 devant le jury composé de:

Président	Abderrahim BALI	Pr	ENP
Encadrant	Abdelmadjid TADJADIT	MC B	ENP
Co-encadrant	Latifa DEBBI	Pr	ENP
Co-encadrant	Amaury HAYAT	Maître de Conférences	ENPC
Examinatrice	Sana STIHI	MA A	ENP

ENP 2022

ملخص: في هذا العمل، نستخدم نموذج المرور المجهري Bando-FTL مع آلية تغيير المسار Treiber لوصف تحركات المركبات في طريق دائري متعدد المسارات، ونموذج $P\Delta P$ لتحديد استهلاك المركبات للوقود. نحن مهتمون بالمساهمة في تقديم فهم أفضل لأنظمة المرور على الطرق متعددة المسارات. على وجه الخصوص، في الجزء الأول من العمل، نثبت أن أنظمة المرور متعددة المسارات حساسة جدًا لمعاملات نموذج تغيير المسارات؛ وأنه من الممكن تبديد موجات التوقف والانطلاق، في حركة مرور متعددة المسارات بها سيارات عدوانية فقط، عن طريق إدخال مركبة مستقلة واحدة تسير وفقًا لقانون تسريع محدد وسط ازدحام شديد، والحصول على تخفيض يصل إلى 75% في استهلاك المركبات للطاقة. في الجزء الثاني، نوضح أنه، في تدفقات حركة مرور متعددة المسارات فيها سيارات تعاونية و أخرى عدوانية، على عكس أنظمة المسار الواحد، يمكن أن تكون نسبة السيارات التعاونية المنخفضة إلى 22% فعالة في تحسين سلاسة المرور. أخيرًا، في الجزء الثالث، ندرس نظام مرور متعدد المسارات حيث تتعايش شاحنات (مركبات طويلة ذات وزن ثقيل) مع سيارات عدوانية، ونوضح أن نسبة 29% من الشاحنات يمكن أن تكون فعالة في تبديد موجات التوقف والانطلاق.

الكلمات الدالة: التوقف و الإنطلاق، المركبات المستقلة، حركات المرور المختلطة، Bando-FTL ، Treiber ، $P\Delta P$.

Résumé: Dans ce travail, nous utilisons le modèle de trafic microscopique Bando-FTL avec le mécanisme Treiber et al. de changement de voie pour décrire les mouvements des véhicules dans une rocade à plusieurs voies, et le modèle $P\Delta P$ pour quantifier la consommation des véhicules en carburant. Nous nous intéressons à contribuer à une meilleure compréhension des systèmes de circulation routière à plusieurs voies. Dans une première partie du travail, nous prouvons que les systèmes de trafic multi-voies sont très sensibles aux paramètres de changement de voie; et qu'il est possible de dissiper les ondes stop-and-go, dans un trafic multi-voies de voitures agressives, en introduisant un seul véhicule autonome qui suit une loi d'accélération prescrite en forte congestion, et obtenir une réduction de la consommation d'énergie des véhicules pouvant aller jusqu'à 75 %. Dans une deuxième partie, nous montrons que, dans des flux de traffic multi-voies de voitures collaboratives et d'autres agressives, contrairement aux systèmes à une seule voie, une proportion de voitures collaboratives aussi faible que 22% peut être efficace pour dissiper les vagues stop-and-go. Enfin, dans une troisième partie, nous étudions un système de circulation multi-voies où coexistent des camions (véhicules longs et lourds) avec des voitures agressives, et nous montrons qu'une proportion de 29% de camions peut être efficace pour dissiper les vagues stop-and-go.

Mots clés: stop-and-go, voitures autonomes, trafics mixtes, Bando-FTL, Treiber, $P\Delta P$.

Abstract: In this work, we use the Bando-FTL microscopic traffic model with the Treiber et al. lane changing mechanism to describe the movements of vehicles in a multi-lane ring road, and the $P\Delta P$ model to quantify vehicular fuel consumption. We are interested in contributing to giving a better understanding of multi-lane road traffic systems. In a first part of the work, we prove that multi-lane traffic systems are very sensitive to lane changing parameters; and that it is possible to dissipate stop-and-go waves, in multi-lane traffic flows of aggressive cars, by introducing a single autonomous vehicle following a prescribed acceleration law in high congestion, and obtain a reduction in vehicular energy consumption of up to 75%. In a second part, we show that, in multi-lane traffic flows of collaborative and aggressive cars, in contrast with single-lane systems, a proportion of collaborative cars as low as 22% can be effective to smooth stop-and-go waves. Finally, in a third part, we study a multi-lane traffic system where coexist trucks (long heavy weight vehicles) with aggressive cars, and we show that a proportion of 29% of trucks can be efficient to dissipate stop-and-go waves.

Key words: stop-and-go, autonomous cars, mixed-traffic, Bando-FTL, Treiber, $P\Delta P$.

Dedication

I dedicate this thesis to my parents, my sister, and my brother, who have been a constant source of support and encouragement during all the challenges I have undertaken in my life in general and during this work.

Acknowledgements

I address many thanks to all the professors I had at École Nationale Polytechnique for everything that they taught me. I also thank the members of the jury for examining, reviewing, and improving this thesis.

I wish to thank my internal supervisors Dr. Abdelmadjid TADJADIT and Pr. Latifa DEBBI for giving me the chance to express my ideas freely, for their guidance, and for the time and patience that they granted me during this period. This work would not have been possible without their trust and support.

I wish to express my gratitude to Pr. Benedetto PICCOLI for giving me the opportunity to work on this ambitious project, providing me with all the necessary documentation and assistance, in addition to giving me the chance to exchange with the very talented members of his team. I would also like to express my sincere thanks to Dr. Amaury HAYAT for his interest in the development of my knowledge and all his time and guidance during the entire period of this work, and this with great sympathy despite his multiple occupations.

I would also like to extend my thanks to my friend Asmaa BOULATAFI for her immense support during this year, many of my projects would not have been possible without her help. I am very grateful for and proud of her friendship.

Finally, I would like to thank my parents, siblings, and anyone who has contributed directly or indirectly to the completion of this work.

Contents

List of Tables

List of Figures

List of Symbols

t_c	Last time that the considered vehicle i changed lane
t_f	Time of the end of the observation of the traffic flow
t^*	Time at which the traffic reaches an equilibrium flow
$\bar{v}^j$	Velocity of all the vehicles in the lane j at an equilibrium flow
$\bar{h}_i^j$	Distance at the equilibrium flow between two successive vehicles
n	Number of distinct types of vehicles on the road
N_j	Total number of vehicles in lane j
M	Total number of vehicles on the road
$\mathcal{M}_{n,p}(\mathbf{K})$	Set of matrices with n rows and p columns with coefficients in set $\mathbf{K}$
$C^p(\mathbf{K})$	Set of functions with p continuous successive derivatives in set $\mathbf{K}$
L	Length of the road
J	Number of lanes in the road
L_j	Length of the lane j
N	Total number of vehicles in each lane
$X_i^j(t)$	Position at time t of the vehicle i in lane j
$V_i^j(t)$	Velocity at time t of the vehicle i in lane j
$A_i^j(t)$	Acceleration at time t of the vehicle i in lane j
$H_i^j(t)$	Distance at time t between the geometric centers of two successive vehicles
τ_i^j	Cooldown time of lane change of the vehicle considering a lane change
$\Delta_I^{i,j}$	Acceleration incentive threshold of the vehicle considering a lane change
$\Delta_s^{i,j}$	Safety threshold of the vehicle considering a lane change
$\bar{A}_i^j(t)$	Expected acceleration of the vehicle in the new lane at time t
$\bar{A}_{\text{fol}}^{i,j}(t)$	Expected acceleration of the follower of the vehicle in the new lane at time t
α_i^j	Weight of the OV/Bando model
β_i^j	Weight of the FTL model
$V_{opt}^{i,j}(x)$	Optimal velocity preference function of the vehicle i in lane j
$V_{\max}^{i,j}$	Maximal preferred speed of the vehicle i in lane j
l_i^j	Length of the vehicle i in lane j
$l_{i+1}^j(t)$	Length of the vehicle directly in front of the vehicle i in lane j at time t
$d_0^{i,j}$	Minimal allowed distance between two successive vehicles
$\max_{acc}^{i,j}$	Maximal acceleration the vehicle i in lane j is capable of
$\max_{dec}^{i,j}$	Maximal deceleration the vehicle i in lane j is capable of
$power_i^j(t)$	Power consumption of the vehicle i in lane j at time t in $[kW]$
p_i^j	Absorption coefficient for power of the vehicle i in lane j in $[N]$
q_i^j	Absorption coefficient for power of the vehicle i in lane j in $[N \cdot s^2/m^2]$

LIST OF SYMBOLS

$mass_i^j$	Mass of the vehicle i in lane j in $[kg]$
$E^j(t)$	Energy consumption at time t in lane j in $[kW \cdot s/m]$
δt	Time step of a simulation
n_1	Number of the vehicles of population 1 in each lane
n_2	Number of the vehicles of population 2 in each lane
p	Penetration rate of the vehicles of population 1 on the road
$L_j(t)$	The length of the lane in which the considered vehicle is at a time t

Introduction

The average person spends 6 days a year in traffic jams [50]. How do traffic jams arise? We all have experienced those long hours of being stuck on the highway, wondering if an accident happened, or if there are works on the road; and suddenly, the traffic becomes fluid again, no car wrecks and no worksite gear to be seen, as if it all happened for no reason. This is called a phantom jam, a phenomenon that is caused by, apparently nothing. The existence of phantom jams has been demonstrated in 2008 by Sugiyama et al. [47], with a real life field experiment in which vehicles where asked to drive in a circle at a constant pace, the objective being to reproduce a road a bit dense in traffic but not too much. At the beginning, all the vehicles were driving at same speed and were equally spaced, the traffic was fluid, until a vehicle decides (by itself) to decelerate for no reason and produces a chain reaction, each vehicle brakes to not crash into the vehicle in its front. In seconds, a traffic jam is created and starts propagating back like a shock wave that was called a stop-and-go wave (see Figure 1). The real cause is the human time reaction, a driver always brakes stronger than does the vehicle in its front and always accelerates more slowly than does the vehicle in its front; if all the vehicles accelerated the same way at the same time, the traffic jam would disappear. An additional problem is our cognitive biases which can push us to act in irrational ways.

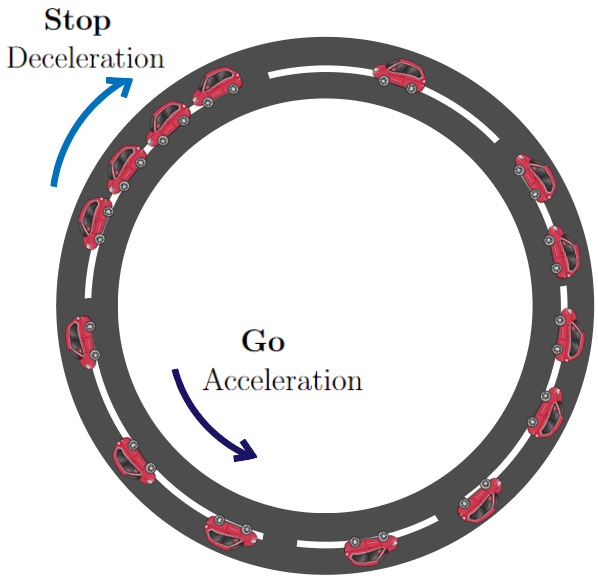

Figure 1 – Stop and go waves

Stop-and-go waves have been shown to increase fuel consumption in experiments conducted in [46], and shown to increase greenhouse emissions and degrade ambient air quality [8]. Speed variations, as drivers have to constantly brake and accelerate, strongly increase vehicular gas emissions and energy consumption compared to a state of constant speed (the equilibrium flow). Moreover, being frequently exposed to traffic jams leads to negative emotional health effects; mostly stress, nervousness, and aggressiveness; whereas long driving hours impact physical health; it mostly causes back pain, pain in the legs, headaches, and dizziness [1]. The economic impact of traffic congestion is also not negligible. Recent research conducted by the transport data company INRIX [22], on the state of congestion in 200 cities in 38 countries, showed the impact of traffic jams on the economy by looking at how much time and money it wastes. In the US, the total cost of lost productivity caused by traffic congestion, in 2020, was found to be $87 billion. In Algeria, there are reported cases of businesses closing or being relocated only because of road traffic congestion [44].

One could think that building new roads or widening existing roads would solve the problem. The roads would be less crowded and there would be less traffic jams. In reality, this could make things worse due to Braess's paradox [9]. In 1968, the city of Seoul in South-Korea built a 6 lane highway above the Cheonggycheon river, in an effort to improve traffic flow. After this road was made operational, the city became much more congested than it was. In 2005, the mayor of Seoul initiated a project to tear down the highway and revitalize the river. This was met with much controversy, as if this major road was already jammed up with cars, removing it would surely make traffic worse around the city. But to everyone's surprise, after closing the road, the traffic flow improved drastically in the city and travel times for the citizens of Seoul actually decreased. This is because almost all the drivers in the city where taking this new road, instead of splitting up into different roads, thinking that it would logically be the best choice since it is the largest one. Therefore, traffic (transportation) engineers work on developing more efficient solutions to control (regulate, improve) road traffic flow.

Traffic engineering is a branch of civil engineering that uses engineering techniques to achieve the safe and efficient movement of people and goods on roadways. It focuses mainly on research for safe and efficient traffic flow, such as road geometry, sidewalks and crosswalks, cycling infrastructure, traffic signs, road surface markings and traffic lights. Traffic engineering deals with the functional part of transportation systems, except the infrastructures provided. Traditional traffic control techniques include: traffic lights' control and coordination, traffic signals, ramp metering, and speed limit systems. The principal limitation of these infrastructure based traffic control solutions is their limited spatial resolution, as well as the need for driver compliance in the case of speed advisory based systems. New more efficient control paradigms are emerging thanks to the improvement of our understanding of road traffic at a rigorous mathematical level, in parallel with the advancements in vehicular technology. The latter are classified into levels of automation [43] which range from level one autonomous vehicles (AVs) available today, that provide the driver with minor technological assistance (stability control or lane correction assistance), to level five (AVs) which operate autonomously in all scenarios and in which humans cannot intervene. The ability of adaptive cruise controlled vehicles (level one automation) to smooth the traffic flow (to dissipate stop-and-go waves), i.e. increase the flow rate, was explored in [29, 48]. The use of vehicles as traffic controllers can also be combined with

more classical traffic control infrastructure techniques, such as ramp meters and variable speed limit systems [17, 37].

Traffic flow can be modeled at different scales, mainly at a microscopic level (by considering each vehicle individually), at a mesoscopic level (by considering the traffic in aggregate terms, while being interested in microscopic properties such as the distribution of the velocities and the accelerations), or at a macroscopic level (by only looking at the macroscopic properties, such as the density of the vehicles, the mean speed, or the flow rate). The vehicles can either circulate on a single-lane road, or be allowed to change lanes in a multi-lane road following a certain lane changing model/mechanism. This traffic flow can either be homogeneous, i.e. only contain one type of vehicles (all identical), and we refer to it as 1-phase traffic flow; or heterogeneous, i.e. contain n distinct populations of vehicles with $n \geq 2$, and we refer to it as mixed-traffic or n-phase traffic flow. In the literature, the problem of dissipating stop-and-go waves that are caused by irrational human driving behaviors has been very studied in a single-lane road context. The authors in [13], demonstrated from theoretical analysis and experiments, the efficiency of introducing a single autonomous vehicle following an appropriate acceleration law for dissipating stop-and-go waves, in a single-lane ring-road (i.e. a closed circular road as the one in Figure 1) where we have a 1-phase traffic flow only containing aggressive cars (aggressive drivers), with a reduction of fuel consumption of up to 40%. In [20], the authors proved that introducing a specific (critical) proportion (penetration rate) of collaborative cars (good drivers) into a 1-phase traffic flow of aggressive cars can dissipate stop-and-go waves and drastically improve the traffic flow. Moreover, they gave similar results for n-phase traffic flows with n being arbitrary large, still only for single-lane roads. However, they also showed that this critical penetration rate is a very large value (it is usually superior to 80%); therefore, this does not represent a realistic strategy to dissipate stop-and-go waves (introducing 80% of good drivers in a real traffic flow is almost impossible). The dissipation/smoothing of stop-and-go waves in a multi-lane road context has, to the best of our knowledge, not been studied theoretically yet. The authors in [19], studied the dissipation of stop-and-go waves with autonomous vehicles in a multi-lane system by performing a small number of numerical simulations (not enough **random** initial conditions to be able to draw conclusions).

In this work, we use the Bando-FTL microscopic traffic model [24] with the Treiber et al. lane changing mechanism [52] to describe the movements of vehicles in a multi-lane ring road, and the $P\Delta P$ model [45] to quantify vehicular fuel consumption. We are interested in contributing to giving a better understanding of multi-lane road traffic systems. In particular, in a first part of the work, we prove that multi-lane traffic systems are very sensitive to lane changing parameters, and that it is possible to dissipate stop-and-go waves, in multi-lane 1-phase traffic flows of aggressive cars, by introducing a single autonomous vehicle following a prescribed acceleration law in high congestion, and obtain a reduction in vehicular energy consumption of up to 75%. In a second part, we show that, in 2-phase multi-lane traffic flows of collaborative and aggressive cars, in contrast with single-lane systems, a proportion of collaborative cars as low as 22% can be effective to smooth stop-and-go waves. Finally, in a third part, we study a multi-lane 2-phase traffic system where coexist trucks (long heavy weight vehicles) with aggressive cars, and we show that a proportion of 29% of trucks can be efficient to dissipate stop-and-go waves.

We published the results obtained in the first part of this work in The European Physical Journal Special Topics - Springer.

> [24] Nicolas Kardous, Amaury Hayat, Sean T. McQuade, Xiaoqian Gong, Sydney Truong, **Tinhinane Mezair**, Paige Arnold, Ryan Delorenzo, Alexandre Bayen, and Benedetto Piccoli. A rigorous multi-population multi-lane hybrid traffic model for dissipation of waves via autonomous vehicles. Eur. Phys. J. Spec. Top., 2022.

The outline of this thesis is as follows.

Chapter 1: In this chapter, we introduce the lexic used to study road traffic, by giving the definitions related to describing the geometry of a road, and the composition of the traffic flow in terms of vehicles. We also expose the most common modeling approaches to describe the movements of the vehicles and to quantify their fuel consumption.

Chapter 2: In this chapter, we lay the mathematical foundations necessary to understand the rest of the thesis. We explain some fundamental concepts about dynamical systems, we give an introduction to stability theory and control theory, and we expose some of the applications of these concepts in road traffic that will be needed in the rest of this work.

Chapter 3: In this chapter, we introduce the main context of our study. We position ourselves in the specific traffic flow settings of our work: the geometry of the road, the composition of the traffic flow in terms of vehicles, and the parameters and models we choose to describe each vehicle's dynamics.

Chapter 4: In this chapter, we expose existing results and gaps in the literature of dissipating stop-and-go waves in road traffic, we detail the three problematics we contribute to address, and we expose our scientific approach and our findings.

Conclusions: Here, we summarize our results and talk about possible future research and perspectives.

Chapter 1

Definitions and Preliminaries about Road Traffic

In this chapter, we introduce the lexic used to study road traffic, by giving the definitions related to describing the geometry of a road, and the composition of the traffic flow in terms of vehicles. We also expose the most common modeling approaches to describe the movements of the vehicles and to quantify their fuel consumption.

1.1 Road geometries

While moving on the road, from time $t = 0$: beginning of the observation of the traffic flow, to time $t = t_f$: end of the observation of the traffic flow, the vehicles composing the observed traffic flow: all the vehicles that are on the observed road during $t \in [0, t_f]$, can either follow a single-lane or multi-lane closed or open road.

1.1.1 Single-lane and multi-lane roads

What we refer to as multi-lane roads and single-lane (single-track) roads, during $t \in [0, t_f]$, is given by the following definitions.

Single-lane roads:

We mean by a single-lane (single-track) road a simple road with one lane, in which all the vehicles are going in the same direction, and their order in the unique lane never changes during $t \in [0, t_f]$.

Figure 1.1 – Single-lane roads

Multi-lane roads:

In this work, we mean by a multi-lane road a road with at least two lanes but with the traffic moving in the same direction in all its lanes. In a multi-lane road, we have two possibilities: the vehicles can change lanes, or cannot.

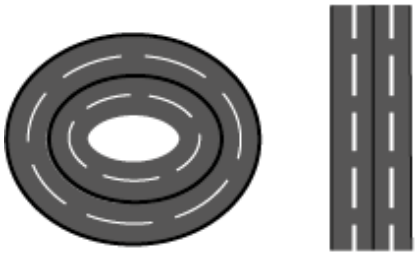

Figure 1.2 – Multi-lane roads

1.1.2 Closed and open roads

What we refer to as closed and open roads is given by the following definitions.

Closed roads:

We say that the observed vehicles follow a closed path, if there exists at least one vehicle on the observed road that rides on a place on the road that it was at at a time $t_i \in [0, t_f]$ at least once again at a time $t_j \in [0, t_f]$, with $t_j > t_i$.

Figure 1.3 – Closed roads

Remark 1.1.2.1. *A closed road can be a single-lane or a multi-lane road.*

Open roads:

We say that the observed vehicles follow an open path, if no vehicle on the observed road rides on a place on the road that it was at at a time $t_i \in [0, t_f]$ again at any time $t_j \in [0, t_f]$, such that $t_j > t_i$.

Figure 1.4 – Open roads

Remark 1.1.2.2. *An open road can be a single-lane or a multi-lane road.*

1.2 Composition of traffic flows

Depending on the composition of the traffic flow in terms of vehicles, we either have a uni-population or a mixed-population traffic flow.

1.2.1 Uni-population and mixed-population traffic flows

Two vehicles are considered to be from two distinct types/categories if they differ in at least one of these points:

– Their lengths.

– Their masses.

– The parameters of the equations governing their longitudinal dynamics.

– Their physical limits in terms of velocity and/or acceleration and/or deceleration.

– Their lane changing threshold parameters.

And based on this, we have the following definitions.

Uni-population (1-phase) traffic flows:

We refer to a traffic in which all the vehicles are of the same type as a uni-population or 1-phase traffic flow.

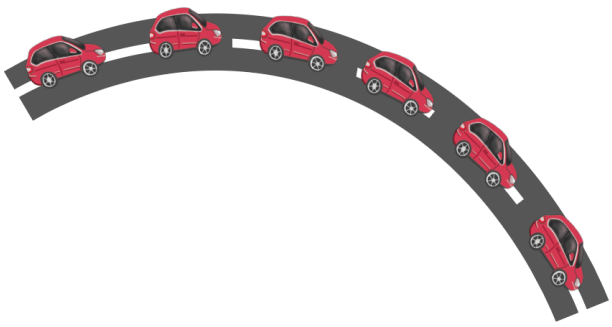

Figure 1.5 – Uni-population traffic flow on a single-lane open stretch of road

Remark 1.2.1.1. *We can have a uni-population traffic flow both in single and multi-lane roads, and both in open and closed roads.*

Mixed-population (n-phase) traffic flows:

We refer to a traffic in which the vehicles belong to n ($n \in \mathbb{N}$ and $n \geq 2$) distinct categories as a mixed-population or multi-population or n-phase traffic flow.

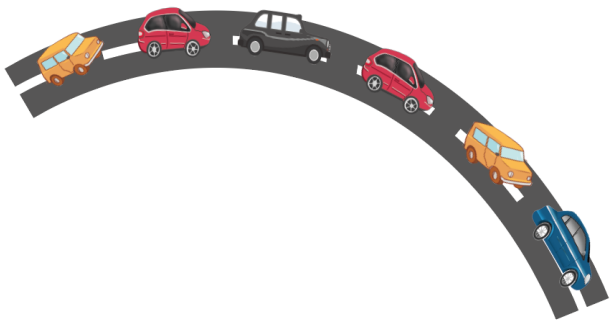

Figure 1.6 – Multi-population traffic flow on a single-lane open stretch of road

Remark 1.2.1.2. *We can have a mixed-population traffic flow both in single and multi-lane roads, and both in open and closed roads.*

1.3 Traffic modeling scales

A traffic flow can be studied and modeled at different scales. Consequently, road traffic models are grouped into categories depending on the scale at which they describe the traffic, including **microscopic**, **macroscopic**, and **mesoscopic** model categories. We give brief definitions of these modeling scales, and a summary of the important ideas in Table 1.1. We refer to [7, 15, 21, 38] for a detailed review of traffic modeling scales.

1.3.1 Microscopic models

A Microscopic model describes the behavior of a **single vehicle-driver unit** and its interaction with the rest of the vehicles-drivers, giving the relationship between the microscopic characteristics of the traffic stream (i.e. of a single vehicle-driver unit), such as: position, velocity, acceleration, lane changes, etc. The dynamics are represented by ordinary differential equations [15].

Because these models model each single vehicle-driver unit, when the number of vehicles on the road is very high, they become computationally expensive. We, however, use microscopic modeling in our study (see our motivations for this choice in Section 3.4).

Microscopic traffic models can be classified into two categories: cell automata models, which are discrete in time and space; and continuous models which are continuous in time. This last category is used for detailed studies of traffic instabilities and car-following behaviours [40].

1.3.2 Mesoscopic models

A mesoscopic traffic model bridges the gap between a microscopic and a macroscopic model, by describing the traffic flow in aggregate terms such as in probability distributions, but defining the behavioural rules for individual vehicles. In other terms, the dynamical variables are the **distributions** of **microscopic properties** such as: velocity, position, acceleration, etc. (see [27]).

Mesoscopic models apply gas-kinetic equations to describe the traffic flow. Recent research developments are making these models more realistic, and some theoretical results made them a starting point for many new macroscopic models [27].

1.3.3 Macroscopic models

A macroscopic model considers the general behavior of the **group of vehicles-drivers** on the road, instead of the individual behaviors. It gives the relationship between the macroscopic characteristics of the traffic stream, such as: density, flow, mean speed, etc. This model assumes a significantly large number of vehicles on the road. The dynamics are distributed and represented by partial differential equations [15].

Research works have proven the possibility of deriving a macroscopic model from a microscopic one by going to the large particle limit of the considered model [14].
The idea of macroscopic traffic models originated from the similarity between “traffic flow

on long crowded roads" and "flood movements in long rivers" that was highlighted by Lighthill and Whitham in 1955 [34] and complemented by the introduction of "shock-waves on the highway" by Richards in 1956 [42], which completed the LWR model [15].

Macroscopic models are generally classified according to the order of the mathematical model they obey.

1.3.4 Summary of modeling scales

One can summaries the fundamental ideas of each one of the three traffic modeling scales in a simple Table.

Modeling scale	Underlying principle	Dynamical variables
Microscopic	Car-following	Microscopic variables: position, velocity, acceleration, lane changes, etc.
Mesoscopic	Gas-kinetics	Distributions of microscopic variables: velocity, position, acceleration, etc.
Macroscopic	Fluid-dynamics	Macroscopic variables: density, flow, mean speed, etc.

Table 1.1 – Summary of traffic modeling scales

1.4 Longitudinal dynamics

In this section, we define the longitudinal dynamics of a vehicle, and give the commonly used models for these dynamics.

1.4.1 Definition of longitudinal dynamics

The simplest movement of vehicles to model is the car-following behavior, i.e. when the vehicles do not change lanes on the road. In this case, we say that they have one directional dynamics, **longitudinal dynamics**. See Figure 1.7.

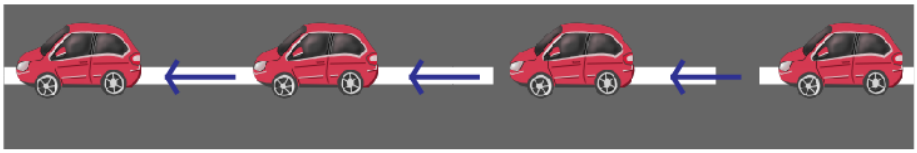

Figure 1.7 – Longitudinal dynamics

Remark 1.4.1.1. *This definition is valid for uni-population and mixed-population traffic flows.*

The general form of the system of equations governing the longitudinal dynamics of **each vehicle** on the road, when modeling traffic at a microscopic scale, is given, $\forall t \in]0, t_f[$, by:

$$\begin{cases} \dot{x}(t) = v(t), \\ \dot{v}(t) = f(h(t), \dot{h}(t), v(t)), \end{cases} \tag{1.1}$$

Where:

- $x(t)$: Is the position of the considered vehicle at a time t.
- $v(t)$: Is the velocity of the considered vehicle at a time t.
- $\dot{v}(t)$: Is the acceleration of the considered vehicle at a time t.
- $h(t)$: Is the distance between the front of the considered vehicle and the rear of the vehicle directly in front of it in the same lane at time t. The state $h(t) = 0$ represents a collision case.
- $\dot{h}(t)$: Is the derivative of $h(t)$ with respect to time at time t. It is also the difference between the velocity of the vehicle directly in front of the considered vehicle and its own velocity.
- $f : \mathbb{R}^3 \ni (x, y, z) \mapsto f(x, y, z) \in \mathbb{R}$ is a smooth real function satisfying the following conditions $\forall t \in [0, t_f]$ [20]:

$$\left.\frac{\partial f}{\partial x}\right|_{(h(t),0,v(t))} > 0, \tag{1.2}$$

$$\left.\frac{\partial f}{\partial y}\right|_{(h(t),0,v(t))} > 0, \tag{1.3}$$

$$\left.\frac{\partial f}{\partial z}\right|_{(h(t),0,v(t))} < 0. \tag{1.4}$$

The condition (1.2) means that:
For any given speed $v(t)$, when the difference in speed $\dot{h}(t) = 0$, the acceleration of the considered vehicle increases as the distance $h(t)$ increases.

The condition (1.3) means that:
For any given speed $v(t)$ and distance $h(t)$, the derivative of $f(\cdot)$ with respect to $\dot{h}(t)$ has

a strictly positive value when the difference of velocities $\dot{h}(t) = 0$.
The condition (1.4) means that:
For any given distance $h(t)$, when the difference in speed $\dot{h}(t) = 0$, the acceleration of the considered vehicle decreases as its velocity $v(t)$ increases.

Since we use microscopic modeling in our study (see our motivations for this choice in Section 3.4), we present the main longitudinal dynamics microscopic models [24], the **Intelligent Driver Model**, the **Optimal velocity or Bando** model, the **Follow the Leader** model, and the **Bando-Follow the Leader** model.

1.4.2 Intelligent Driver Model (IDM)

The Intelligent Driver Model (IDM) gives the general form of the longitudinal dynamics for a vehicle on the road, $\forall t \in]0, t_f[$, as [51]:

$$\begin{cases} \dot{x}(t) = v(t), \\ \dot{v}(t) = a\left(1 - \left(\frac{v(t)}{v_0}\right)^{\delta} - \left(\frac{s^*\left(v(t),\dot{h}(t)\right)}{h(t)}\right)^2\right), \\ s^*\left(v(t), \dot{h}(t)\right) = s_0 + Tv(t) + \frac{v(t)\dot{h}(t)}{2\sqrt{ab}}. \end{cases} \tag{1.5}$$

Where:

- v_0 : Is the desired speed when driving on a free road.
- T : Is the adaptation time of the driver when following other vehicles.
- a : Is the acceleration in everyday traffic.
- b : Is the comfortable braking deceleration in everyday traffic.
- s_0 : Is the minimum bumper-to-bumper distance to the front vehicle.
- δ : Is the exponent of the comparison between the actual speed of the vehicle $v(t)$ and its desired speed v_0.
- $s^*(\cdot)$: Is the desired dynamical distance.

1.4.3 Optimal Velocity or Bando (OV/Bando) model

The Optimal Velocity or Bando (OV/Bando) model gives the general form of the longitudinal dynamics for a vehicle on the road, $\forall t \in]0, t_f[$, as [24]:

$$\begin{cases} \dot{x}(t) = v(t), \\ \dot{v}(t) = V\left(h(t)\right) - v(t). \end{cases} \tag{1.6}$$

With the optimal velocity $V(\cdot)$ being a monotonically increasing bounded function. In

the literature, one can find several formulas for the optimal velocity function $V(\cdot)$, the common one is:

$$V\left(h(t)\right) = V_{\max}\left(\frac{\tanh\left(\frac{h(t)}{d_0} - 2\right) + \tanh(2)}{1 + \tanh(2)}\right). \tag{1.7}$$

Where:

- $V_{\max}$: Is the maximal preferred speed of the considered vehicle.
- d_0 : Is the minimal allowed distance between the considered vehicle and the vehicle directly in front of it in the same lane.

1.4.4 Follow the Leader (FTL) model

The Follow the Leader (FTL) model gives the general form of the longitudinal dynamics for a vehicle on the road, $\forall t \in]0, t_f[$, as [24]:

$$\begin{cases} \dot{x}(t) = v(t), \\ \dot{v}(t) = \frac{\dot{h}(t)}{h(t)^2}. \end{cases} \tag{1.8}$$

1.4.5 Bando-Follow the Leader (Bando-FTL) model

The Bando-Follow the Leader (Bando-FTL) model gives the general form of the longitudinal dynamics for a vehicle on the road as the combination of the Bando and FTL models, i.e. $\forall t \in]0, t_f[$ [24]:

$$\begin{cases} \dot{x}(t) = v(t), \\ \dot{v}(t) = \alpha\left(V\left(h(t)\right) - v(t)\right) + \beta\left(\frac{\dot{h}(t)}{h(t)^2}\right). \end{cases} \tag{1.9}$$

- α : Is a constant independent of time representing the weight of the optimal velocity term.
- β : Is a constant independent of time representing the weight of the follow the leader term.
- $V(\cdot)$: Is given by (1.7).

1.5 Traffic flow compositions and Bando-FTL

While adopting the Bando-FTL model, which is our case (see our motivations for this choice in Section 3.6), we have that the general form of the equations governing the dynamics of a vehicle k in the road is given, $\forall t \in [0, t_f]$ and $\forall k \in [1, M] \cap \mathbb{N}$ with M being the total number of vehicles on the road, by [20]:

$$\left\{ a_k(t) = f_k(h_k(t), \dot{h}_k(t), v_k(t)) = \alpha_k \cdot (V_k(h_k(t)) - v_k(t)) + \beta_k \cdot \frac{\dot{h}_k(t)}{(h_k(t))^2}, \right. \tag{1.10}$$

Where

$$V_k(\xi) = g_k(V_{\max_k}, \xi, d_{0_k}), \tag{1.11}$$

the functions $f_k : \mathbb{R}^3 \ni (x, y, z) \mapsto f_k(x, y, z) \in \mathbb{R}$ are smooth real functions satisfying the conditions (1.2)(1.3)(1.4), i.e. $\forall t \in [0, t_f]$:

$$\left.\frac{\partial f_k}{\partial x}\right|_{(h_k(t),0,v_k(t))} > 0, \quad \left.\frac{\partial f_k}{\partial y}\right|_{(h_k(t),0,v_k(t))} > 0, \quad \left.\frac{\partial f_k}{\partial z}\right|_{(h_k(t),0,v_k(t))} < 0 \tag{1.12}$$

and

- $a_k(t)$: Is the acceleration of the vehicle k at time t.
- $v_k(t)$: Is the speed of the vehicle k at time t.
- $h_k(t)$: Is the distance between the front of the vehicle k and the rear of the vehicle directly in front of it in the same lane at time t.
- $\dot{h}_k(t)$: Is the derivative of $h(t)$ with respect to time at time t.
- α_k : Is the weight of the OV/Bando model for the vehicle k.
- β_k : Is the weight of the FTL model for the vehicle k.
- $g_k(\cdot, \cdot, \cdot)$: Is the optimal velocity preference function of the vehicle k.
- $V_{\max_k}$: Is the maximal preferred speed of the vehicle k.
- d_{0_k} : Is the minimal allowed distance between the vehicle k and the vehicle directly in front of it in the same lane.

In [20], three typical cases are summarized:

1.5.1 Unified model

In this case, $f_k(\cdot,\cdot,\cdot)$ does not depend on k, i.e:

$$\alpha_k = \alpha \text{ and } \beta_k = \beta \text{ and } V_k(h_k(t)) = V(h_k(t)), \quad \forall k \in \{1, 2, \cdots, M\}. \tag{1.13}$$

That means that all the vehicles behave similarly. It is the case of 1-phase traffic flow.

1.5.2 Mixed traffic model

In this case, there are n different types of vehicles/drivers on the road, i.e.:

$$f_k \in \{F_m : m = 1, 2, \cdots, n\}, \quad \forall k \in \{1, 2, \cdots, n\} \text{ with } n \ll M, \tag{1.14}$$

i.e.:

$$(\alpha_k, \beta_k, V_k) \in \{(A_m, B_m, \mathcal{V}_m) : m = 1, 2, \ldots, n\}, \quad \forall k \in \{1, 2, \cdots, n\} \text{ with } n \ll M. \tag{1.15}$$

It is the case of n-phase traffic flow.

1.5.3 Mixed traffic with common velocity preference model

In this case, only $V_k(\cdot)$ is independent of k, while a_k and b_k have different values for the different types of vehicles, i.e.:

$$V_k(h_k(t)) = V(h_k(t)), \quad \forall k \in \{1, 2, \cdots, M\}, \tag{1.16}$$

but:

$$(\alpha_k, \beta_k) \in \{(A_m, B_m) : m = 1, 2, \ldots, n\}, \quad \forall k \in \{1, 2, \cdots, n\} \text{ with } n \ll M. \tag{1.17}$$

1.6 Bidirectional dynamics

In this section, we define the bidirectional dynamics of a vehicle, and give the commonly used models for the direction of movement that we have not discussed yet.

1.6.1 Definition of lateral dynamics

In multi-lane traffic systems when vehicles can change lanes, which are the systems that we study, we can say that the vehicles have **Bidirectional dynamics**. They still move forward on a lane following the vehicles in front of them in the same lane (longitudinal dynamics), and they can also change lane and go left or right to a neighboring lane; the later are the **lateral dynamics**. See Figure 1.8.

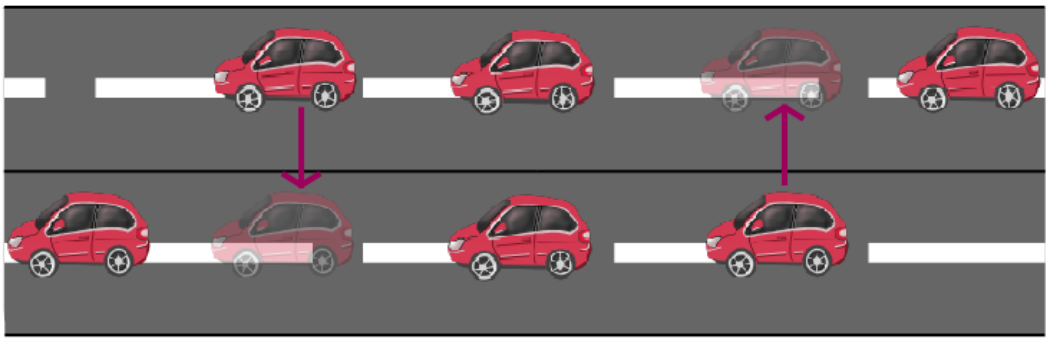

Figure 1.8 – Lateral dynamics

Remark 1.6.1.1. *This definition is valid for uni-population and mixed-population traffic flows.*

1.6.2 Modeling lane-changes/lateral-dynamics

Many lane changing models (also called lane changing mechanisms) have been proposed by researchers, and were subjects of review in [5, 35, 55]. A lane change, depending on the driver's motivation to change lane, can be classified as mandatory (MLC) or discretionary (DLC). A (MLC) is performed when the driver must leave its current lane for some reason (forced lane change), while a (DLC) is performed when the driver expects and wants to improve its acceleration/velocity in the new lane (free lane change).

Lane changing models either represent these two types of lane change by separate models, or combine them in one model, or only represent one of them.

Without distinction regarding how the lane changing mechanisms model the two types of lane change LC, these models are classified into [55]: Gipps-type LC models, Utility-theory based LC models, Cellular automata based LC models, Hazard-based (survival) LC models, Fuzzy logic based LC models, and Markov process based LC models.

In the following subsections, we give brief definitions of these types, extracted from [55].

1.6.3 Gipps-type LC models

These models consider the necessity, desirability and safety of lane changes. The driver is assumed to maintain a desired speed and be in the correct lane for an intended turning maneuver. When the turn is far away, the driver only concentrates on maintaining a desired speed. And when the turn is close, the driver only considers staying in the correct lane for the turning maneuver. If the turn is at a middle distance between these two scenarios, the driver only considers lane changes to the turning lanes or lanes that are adjacent to them. The above distance thresholds and the other parameters of the model are defined deterministically with no consideration for the variations in the driver's driving behaviours over time, or the difference in driving styles between drivers. A priority system is also defined deterministically to resolve conflicts when more than one lane is acceptable, considering the presence of heavy vehicles, speed gain, and the locations of obstructions. To the best of our knowledge, there has been no proposed method yet for making rigorous estimations of the model's parameters.

1.6.4 Utility-theory based LC models

In these models, the proposed LC structure consists of four latent (i.e., unobservable) levels of decision hierarchy. Taking into account the drivers heterogeneity and state dependence (the current choice's dependence on previous driving experiences and LC).

Tentatives have been made to estimate the parameters of the model for special cases, using for example vehicle trajectories: merging to the left lane from a freeway on-ramp, which only requires two decision levels, i.e., gap acceptance and LC execution.

1.6.5 Cellular automata based LC models

Like other approaches used to model LC, Cellular automata based LC models face several challenges. First of all, they are artifact-prone. One artifact induced by these models is that the LC duration is implicitly fixed as the length of one time step (typically not longer than $1s$), which is unrealistically short and inconsistent with observations. Another reported artifact is the infamous ping-pong traffic that vehicles laterally bounce back and forth between lanes without forward moving [36].

Although most of these reported artifacts can be avoided, e.g., the ping pong phenomenon can be eliminated by randomizing decisions of LC [36], vehicle movements need to be scrutinized before any conclusions should be drawn whenever cellular automata based LC models are used.

1.6.6 Hazard-based (survival) LC models

These models have seen the light as a response to the fact that the previously cited LC models neither sufficiently nor explicitly consider the stochasticity and possibly the unsafe character of the cognitive processes (e.g. perception, judgment and execution) followed by drivers. Thus, a hazard-based duration model was proposed.

Unlike rule-based LC models, the hazard-based duration model treats driver behaviors as a multiple duration process: free flow, car following, or lane change.

1.6.7 Fuzzy logic based LC models

The overall structure of fuzzy logic based LC models is similar to the LC models discussed previously (e.g. LC often categorized as either mandatory or discretionary. Two essential decisions are often considered: desirability (or necessity) of LC and gap acceptance), except that the LC rules are fuzzified as IF–THEN rules and presented in a natural language. The following is a typical IF–THEN LC rule: IF: (vehicle i is eligible for using the left lane) and (the gap between vehicle i and the leader in the left lane is large) and (the gap between vehicle i and the follower in the left lane is large) and (the speed in the current lane is low) and (the speed in the left lane is high). THEN: (vehicle i changes to the left lane).

Technically speaking, all the models that we discussed can be fuzzified.

1.6.8 Markov process based LC models

LC has also been modeled as a Markov process. These models aimed to reproduce LC frequency but cannot explain the decision process: why or why not LC occurs. Thus, they are not suitable for microscopic simulations. This limitation is overcome in [49] by integrating a hidden Markov model (HMM) with the utility theory based modeling framework.

1.6.9 The Treiber et al. lane changing mechanism

The Treiber et al. [52] lane changing mechanism, which is a variant of the Gipps-type models, reads as follows for a considered vehicle on the road at $\forall t \in [0, t_f]$:

$$\begin{cases} \bar{a}(t) > a(t) + \Delta_I \text{ (incentive)}, \\ \bar{a}(t) > -\Delta_s, \quad \bar{a}_{\text{fol}}(t) > -\Delta_s \quad \text{(safety)}, \\ t > t_c + \tau \quad \text{(cooldown time)}. \end{cases} \tag{1.18}$$

Where:

- Δ_I : Is the acceleration incentive threshold.
- Δ_s : Is the acceleration safety threshold.
- $a(t)$: Is the acceleration of the vehicle changing lane in the original lane at time t.
- $\bar{a}(t)$: Is the expected acceleration of the vehicle changing lane in the new lane at time t.
- $\bar{a}_{\text{fol}}(t)$: Is the expected acceleration of the follower of the vehicle changing lane in the new lane at time t.
- t_c : Is the last time that the considered vehicle changed lane, $t_c \in [0, t_f]$.
- τ : Is the cooldown time (the lane change time threshold), $\tau \in \mathbb{R}_+^*$.
- t : Is the time at which the considered vehicle is deciding a lane change.

Meaning that a vehicle changes lane if and only if:

(i) Doing so is safe: no huge braking is implied for the follower (in the new lane) of the vehicle changing lane.

(ii) It has an acceleration incentive: it will have a higher acceleration in the new lane compared to if it does not change lane.

(iii) A certain amount of time has passed since it last changed lane. This amount of time τ $\left(\tau \in \mathbb{R}_+^*\right)$ after which it can change lane again is called the cooldown time.

1.7 Modeling fuel consumption

Quantifying vehicular fuel consumption and gas emissions with precise models is very important to be able to study the effect of vehicular traffic on the environment. The authors in [41], give a brief review of the state-of-the-art and state-of-practice fuel consumption models and compare them. These models are divided into macroscopic and microscopic models:

- Macroscopic models use average aggregate network parameters to estimate network-wide emission rates.
- Microscopic models estimate instantaneous vehicle fuel consumption and emission rates, which are aggregated to estimate network-wide measures of effectiveness.

In all what follows in this document, we put the units of physical quantities either between [.] (e.g. the velocity is given in [m/s], meaning that the velocity is given in meter per second), or we write them directly next to the numerical value of the physical quantity (e.g. 1000s, meaning 1000 seconds).

The $P\Delta P$ model [45] is a power based microscopic model, which gives the power consumed by a considered vehicle at any given time $t \in [0, t_f]$ (in seconds) with the following formula:

$$power(t) = \left(p + q \cdot (v(t))^2 + mass \cdot \max\left(0, a(t)\right)\right) \cdot \frac{v(t)}{1000}, \quad \forall t \in [0, t_f]. \tag{1.19}$$

Where:

- $power(t)$: Is the power consumed by the considered vehicle at time t, in $[kW]$.
- p : Is the absorption coefficient for power, of the considered vehicle, in $[N]$.
- q : Is the absorption coefficient for velocity, of the considered vehicle, in $[N \cdot s^2/m^2]$.
- $mass$: Is the mass of the considered vehicle, in $[kg]$.
- $v(t)$: Is the velocity of the considered vehicle at time t, in $[m/s]$.
- $a(t)$: Is the acceleration of the considered vehicle at time t, in $[m/s^2]$.

We only detail the $P\Delta P$ model in this section and not the other existing models, since it is the model we use in our study (see our motivations for this choice in Section 3.11).

Chapter 2

Mathematical Background

In this chapter, we lay the mathematical foundations necessary to understand the rest of the thesis. We explain some fundamental concepts about dynamical systems, we give an introduction to stability theory and control theory, and we expose some of the applications of these concepts in road traffic that will be needed in the rest of this work.

2.1 Dynamical systems

In mathematics, a dynamical system is a system in which a function describes the time dependence of a point in an ambient space. Examples include the mathematical models that describe the swinging of a clock pendulum, the flow of water in a pipe, and the number of fish each springtime in a lake. The most general definition unifies several concepts in mathematics such as ordinary differential equations and ergodic theory by allowing different choices of the space and how time is measured. Time can be measured by integers, by real or complex numbers or can be a more general algebraic object, losing the memory of its physical origin, and the space may be a manifold or simply a set, without the need of a smooth space-time structure defined on it. Often the function is deterministic, that is, for a given time interval only one future state follows from the current state. However, some systems are stochastic, in that random events also affect the evolution of the state variables [25].

The figures below show some examples of dynamical system.

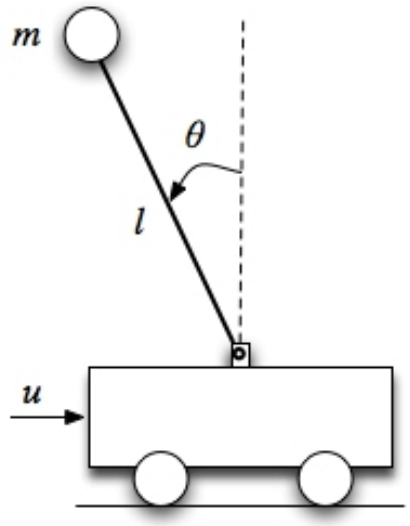

Figure 2.1 – Inverted pendulum on a cart (credit: [6])

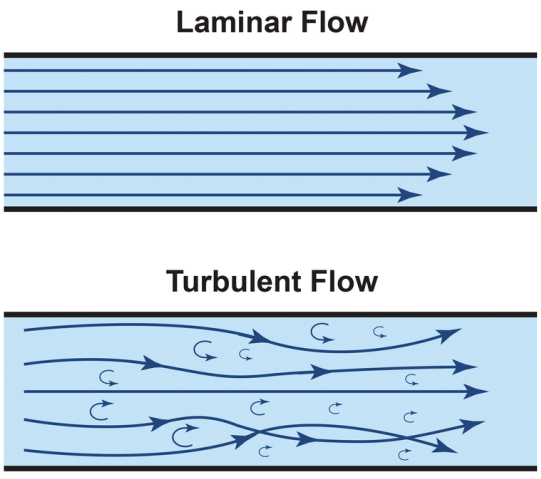

Figure 2.2 – Fluid flow (credit: [4])

In what follows, we are only talking about deterministic, continuous time, and autonomous systems. Where an autonomous system is a system for which the function describing the evolution over time does not "explicitly" depend on time, e.g. we consider a function $f(X(t), Y(t))$ but not a function $f(t, X(t))$.

Depending on if the function describing the evolution of the system over time is a linear or

nonlinear function, the dynamics of the system are said to be linear or nonlinear, and the system is said to be: a **linear dynamical system**, or a **nonlinear dynamical system**.

2.1.1 Linear dynamical systems

These systems can be solved exactly and have rich mathematical properties thanks to the fact that they satisfy the superposition principle.

The general form of the equations governing the dynamics of a linear system is given by:

$$\begin{cases} \dot{X}(t) = AX(t) = AX, \\ X(t_0) = X_0, \\ X : [t_0, t_1] \ni t \longmapsto \mathbb{R}^n, \\ n \in \mathbb{N}, \\ A \in \mathcal{M}_{n,n}(\mathbb{R}). \end{cases} \tag{2.1}$$

With:

$$X(t) = \begin{bmatrix} x_1(t) \\ x_2(t) \\ \vdots \\ x_n(t) \end{bmatrix}, \quad \forall t \in [t_0, t_1]. \tag{2.2}$$

$\mathcal{M}_{n,n}(\mathbb{R})$ is the set of matrices with n rows and n columns with coefficients in $\mathbb{R}$, $X = X(t)$ is the state vector of the system at time $t \in [t_{initial} = t_0, t_{final} = t_1]$, $\dot{X} = \dot{X}(t)$ is the derivative of $X = X(t)$ at the given time t, and $X(t_0) = X_0$ is the state of the system at the initial time. The system of equations (2.1) is called the **dynamics** of the system. The exact solution of a linear system is well-known and has the form:

$$X(t) = e^{At} X_0, \quad \forall t \in [t_0, t_1]. \tag{2.3}$$

The Figure 2.3 and the Figure 2.4 show examples of linear dynamical systems. For instance, the state vector of the system in Figure 2.3 can be chosen as $\forall t \in [t_0, t_1]$:

$$X(t) = \begin{bmatrix} \theta(t) \\ \dot{\theta}(t) \end{bmatrix}, \tag{2.4}$$

where $\theta(t)$ is the angle that the needle makes at time t with its vertical position, and $\dot{\theta}(t)$ is its angular velocity at time t.

Figure 2.3 – Metronome (credit: pianoreviewer.com)

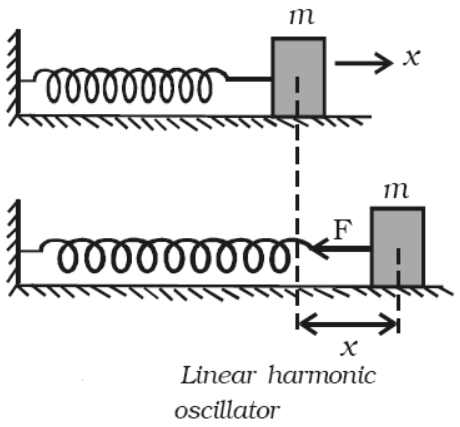

Figure 2.4 – Linear harmonic oscillator (credit: askiitians.com)

2.1.2 Nonlinear dynamical systems

In mathematics and applied sciences, a nonlinear system is a system in which the change of the output is not proportional to the change of the input. Most systems are inherently nonlinear in nature. Nonlinear dynamical systems, describing changes in variables over time, may appear to be chaotic [26], unpredictable, or counter-intuitive. Contrasting with linear systems, for most nonlinear systems we do not have an exact solution or we do not have a solution at all, the study of many of their properties is also relatively complicated [54].

A nonlinear system is given by:

$$\begin{cases} \dot{X}(t) = f(X(t)) = f(X), \\ X(t_0) = X_0, \\ X : [t_0, t_1] \ni t \longmapsto \mathbb{R}^n, \\ n \in \mathbb{N}, \\ f : \ \mathbb{R}^n \longmapsto \mathbb{R}^n. \end{cases} \tag{2.5}$$

With:

$$X(t) = X = \begin{bmatrix} x_1(t) \\ x_2(t) \\ \vdots \\ x_n(t) \end{bmatrix} \text{ and } f(X) = \begin{bmatrix} f_1\left(x_1, x_2, \cdots, x_n\right) \\ f_2\left(x_1, x_2, \cdots, x_n\right) \\ \vdots \\ f_n\left(x_1, x_2, \cdots, x_n\right) \end{bmatrix}, \quad \forall t \in [t_0, t_1]. \tag{2.6}$$

Such that at least one of the elements $f_i(\cdot)$ of $f(\cdot)$, for $i \in \{1, 2, \cdots, n\}$, is a nonlinear function; $X = X(t)$ is the state vector of the system at time $t \in [t_0, t_1]$; $\dot{X} = \dot{X}(t)$ is the derivative of $X = X(t)$ at the given time t; and $X(t_0)$ is the state of the system at time t_0. The system of equations (2.5) is called the **dynamics** of the system.

Remark 2.1.1. *In the case where $f(X) = AX$, the system of equations 2.5 prescribes the dynamics of a linear dynamical system. If we do not impose a constraint on the expression of $f(\cdot)$, the general form of the dynamics of dynamical systems (either linear or nonlinear systems) can be given by the system of equations 2.5.*

The figures below show examples of nonlinear systems.

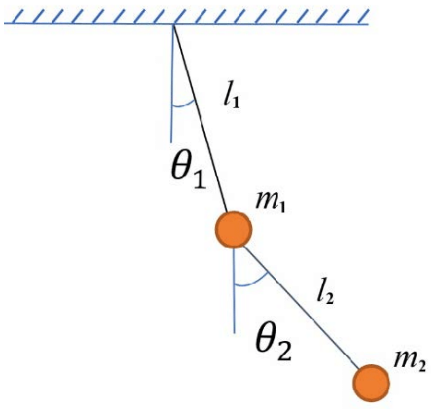

Figure 2.5 – Double pendulum (credit: [23])

Figure 2.6 – Earth's climate (credit: Rowan Griffiths)

2.2 Equilibrium points

An equilibrium of a dynamical system is a value of the state variables when the state variables do not change. In other words, an equilibrium is a solution that does not change with time. This means if the system starts at an equilibrium, the state will remain at the equilibrium forever [53].

For both linear and nonlinear systems, at an equilibrium $\bar{X}$, if there are no external perturbations, we have:

$$0 = f(\bar{X}) \text{ the 0 of } \mathbb{R}^n, \quad \forall t \in [t_0, t_1]. \tag{2.7}$$

For continuous time dynamical systems, to find the equilibrium point one can solve the following equation:

$$\frac{\mathrm{d}X}{\mathrm{d}t} = \dot{X}(t) = 0, \text{ i.e. } f(X(t)) = 0, \text{ such that 0 is the 0 of } \mathbb{R}^n, \quad \forall t \in [t_0, t_1]. \tag{2.8}$$

This is why equilibrium points are also called stationary or steady-states.

2.3 Existence and uniqueness of the solution of the dynamics equation

If $f(\cdot)$ is **locally Lipschitz at the neighborhood** X_0, we know that the dynamics:

$$\begin{cases} \dot{X} = f(X(t)) = f(X), \\ X(t_0) = X_0, \\ X: \ t \in [t_0, t_1] \longmapsto \mathbb{R}^n, \\ n \in \mathbb{N}, \\ f: \ \mathbb{R}^n \longmapsto \mathbb{R}^n, \end{cases} \tag{2.9}$$

make sense mathematically and physically, i.e. for an initial condition $X_0 \in \mathbb{D}$ ($\mathbb{D} \subset \mathbb{R}^n$), the ssystem "have up to some time" a solution which is "unique" [53].

Theorem 2.3.1. *(Sufficient conditions for existence and uniqueness)*
For $t \in [t_0, t_1]$, if:

(i) $f(\cdot)$ satisfies the local Lipschitz condition:

$\forall r \in \mathbb{R}^+$, $\exists L_r > 0$ *such that* $\forall X, Y \in B = \{X \in \mathbb{R}^n \mid ||X - X_0|| \leq r\}$:
$||f(X) - f(Y)|| \leq L_r ||X - Y||$, $\forall t \in [t_0, t_1]$, $||.||$ *is any norm in* $\mathbb{R}^n$.

*Then there **exists** a **unique** solution $X(t)$ for the initial value problem (2.9), defined on $t \in [t_0, t_0 + \delta]$ for some $\delta \in \mathbb{R}_+^*$ **(local existence and uniqueness result)**. And we say that $f(\cdot)$ is locally Lipschitz in the neighborhood of X_0.*

Theorem 2.3.2. *If:*

(i) $f(\cdot)$ is continuous on $\mathbb{D} \subset \mathbb{R}^n$ for $\forall t \in [t_0, t_1]$.

(ii) Given the formula of the Jacobian of $f(\cdot)$ (when it exists):

$$\frac{Df}{DX} = \begin{bmatrix} \frac{\partial f_1}{\partial x_1} & \frac{\partial f_1}{\partial x_2} & \dots & \frac{\partial f_1}{\partial x_n} \\ \frac{\partial f_2}{\partial x_1} & \frac{\partial f_2}{\partial x_2} & \dots & \frac{\partial f_2}{\partial x_n} \\ \vdots & \vdots & \dots & \vdots \\ \frac{\partial f_n}{\partial x_1} & \frac{\partial f_n}{\partial x_2} & \dots & \frac{\partial f_n}{\partial x_n} \end{bmatrix}, \tag{2.10}$$

if the Jacobian exists and all its elements are continuous and bounded on $\mathbb{D}$ for $\forall t \in [t_0, t_1]$.

Then $f(\cdot)$ is locally Lipschitz on $\mathbb{D}$.

We have the following definitions about $f(\cdot)$:

- Locally Lipschitz on $\mathbb{D}$: if locally Lipschitz in the neighborhood of all points X_0 in $\mathbb{D}$ and the Lipschitz constant L_r depends on r.
- Lipschitz on $\mathbb{D}$: if locally Lipschitz on $\mathbb{D}$ and $\forall r > 0$ we have $L_r = L$ with $L > 0$.
- Globally Lipschitz : if Lipschitz on $\mathbb{R}^n$.

2.4 Stability theory

What follows is mainly inspired from [10]. All the following definitions and results concern a particular equilibrium point (it is an equilibrium point of the system that has these properties or not, not the system). We only define notions that are relevant to our work, and we consider, to simplify the notations with no loss of generality, the equilibrium point of interest to be $\bar{X} = 0$ (the 0 of $\mathbb{R}^n$). Knowing that this can be any equilibrium point with the appropriate change in reference. We denote by $X(t, X_0)$ the response of the dynamical system at time t to the initial condition X_0.

2.4.1 Stability

$X = 0$ is **stable** if and only if:

$$\forall \varepsilon > 0 \quad \exists \delta(\varepsilon) > 0 \quad \text{such that } ||X_0|| < \delta \implies ||X(t, X_0)|| < \varepsilon, \quad \forall t > t_0. \tag{2.11}$$

Which means that if the equilibrium point $X = 0$ is stable, for any open ball around the origin ($X = 0$) with radius ε, it should always be possible to find an open ball around the origin with radius δ, such that if the system starts inside this last ball, it will stay inside the ball of radius ε for all future time. In other words, if the system starts close to a stable equilibrium point it should stay close.
The figure below is a visual interpretation for the 2D case (n=2).

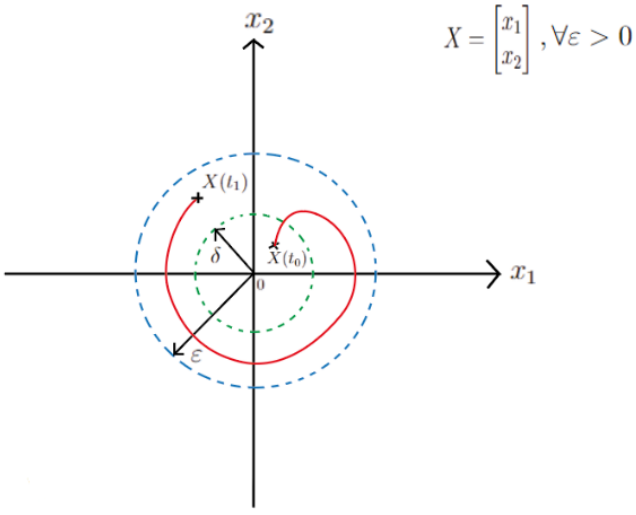

Figure 2.7 – Visual interpretation of stability for the 2D case

2.4.2 Local asymptotic stability

If the equilibrium point $X = 0$ is **locally asymptotically stable**, the system will not only stay close to this equilibrium if it starts close, but it will also converge to this equilibrium point when $t \to +\infty$.

In other terms, the equilibrium point $X = 0$ is locally asymptotically stable iff (if and only if):

(i) It is stable.

(ii) $\exists r > 0$ such that $||X_0|| < r \implies \lim_{t\to+\infty} X(t) = 0$ **(convergence property)**.

The **region of attraction** $B_r(0)$ of the equilibrium $X = 0$ is the centered ball of radius r defined as:

$$B_r(0) = \{X_0 \in \mathbb{R}^n \mid ||X_0|| < r\} \cap \mathbb{D}. \tag{2.12}$$

With r here being the largest positive real number satisfying the convergence property stated just above.

2.4.3 Global asymptotic stability

The equilibrium point $X = 0$ is **globally asymptotically stable** if and only if:

(i) It is locally asymptotically stable.

(ii) $B_r(0) = \mathbb{R}^n$.

Remark 2.4.3.1. *This implies that $X = 0$ is the only equilibrium point of the system. Because if there was another equilibrium point (EP), if the system starts at the other (EP) it will stay at it and will not be attracted to $X = 0$ which will mean that $B_r(0) \neq \mathbb{R}^n$.*

2.4.4 Local exponential stability

This is a stronger property than asymptotic stability. The equilibrium point $X = 0$ is **locally exponentially stable** if and only if:

$$\exists r, k, \lambda > 0 \text{ such that } ||X_0|| < r \implies ||X(t)|| \leq k||X_0||e^{-\lambda t}, \quad \forall t \geq t_0. \tag{2.13}$$

This means that the distance between $X(t)$ and the origin $X = 0$ is exponentially decaying from its initial value X_0 to $X = 0$.

The **region of attraction** $E_r(0)$ of the equilibrium $X = 0$ is the centered ball of radius r defined as:

$$E_r(0) = \{X_0 \in \mathbb{R}^n \mid ||X_0|| < r\} \cap \mathbb{D}. \tag{2.14}$$

With r here being the largest positive real number satisfying (2.13).

2.4.5 Global exponential stability

The equilibrium point $X = 0$ is **globally exponentially stable** if and only if:

$$\exists k, \lambda > 0 \text{ such that } \forall X_0 \in \mathbb{R}^n : \quad ||X(t)|| \leq k||X_0||e^{-\lambda t}, \quad \forall t \geq t_0. \tag{2.15}$$

Remark 2.4.5.1. *This implies that $X = 0$ is the only equilibrium point of the system.*

2.4.6 Routh Hurwitz criterion

In this subsection, we state the Routh Hurwitz criterion for linear systems for which the matrix A is **diagonalizable**, since we need it to understand the article [20] which gives fundamental results that we cite and use in Chapter 4.

For a **linear** system (2.1) with solution:

$$X(t) = e^{At}X_0, \quad t \in [t_0, t_1], \tag{2.16}$$

to be able to imagine the exponential of a matrix, take the Taylor series of $exp(x)$ around the equilibrium point $X = 0$ and replace x by At:

$$e^{At} = \sum_{m \geq 0}^{+\infty} \frac{(At)^m}{m!}. \tag{2.17}$$

We have:

$$AT = TD. \tag{2.18}$$

With T being a matrix containing the eigenvectors of A as columns corresponding to the appropriate eigenvalues in D, with D being a diagonal matrix containing the eigenvalues of A, i.e.:

$$D = \begin{bmatrix} \varphi_1 & 0 & \dots & 0 \\ 0 & \varphi_2 & \ddots & \vdots \\ \vdots & \ddots & \ddots & 0 \\ 0 & \dots & 0 & \varphi_n \end{bmatrix}, \quad T = [\omega_1, \omega_2, \dots, \omega_n]. \tag{2.19}$$

With ω_i being the eigenvector of the matrix A corresponding to the eigenvalue φ_i of matrix A, with $i \in \{1, 2, \cdots, n\}$. So:

$$T^{-1}AT = D. \tag{2.20}$$

If we choose to make the following change of variable:

$$X = TZ, \quad \forall t \in [t_0, t_1]. \tag{2.21}$$

We have from (2.1), that $\forall t \in [t_0, t_1]$:

$$\dot{X} = T\dot{Z} = AX \implies T\dot{Z} = ATZ \implies \dot{Z} = T^{-1}ATZ \implies \dot{Z} = DZ. \tag{2.22}$$

This is a simpler system because D is diagonal, and its solution is given by:

$$Z(t) = e^{Dt}Z(t_0) = \begin{bmatrix} e^{\varphi_1 t} & 0 & \dots & 0 \\ 0 & e^{\varphi_2 t} & \ddots & \vdots \\ \vdots & \ddots & \ddots & 0 \\ 0 & \dots & 0 & e^{\varphi_n t} \end{bmatrix} Z(t_0), \quad \forall t \in [t_0, t_1]. \tag{2.23}$$

Using $A = TDT^{-1}$ to simplify (2.17), we get $\forall t \in [t_0, t_1]$:

$$e^{At} = e^{TDT^{-1}t} = T\sum_{m\geq 0}^{+\infty} \frac{(AD)^m}{m!}T^{-1} \implies e^{At} = Te^{Dt}T^{-1}. \tag{2.24}$$

So $\forall t \in [t_0, t_1]$:

$$X(t) = Te^{Dt}T^{-1}X_0. \tag{2.25}$$

And given that:

$$e^{Dt} = \begin{bmatrix} e^{\varphi_1 t} & 0 & \dots & 0 \\ 0 & e^{\varphi_2 t} & \ddots & \vdots \\ \vdots & \ddots & \ddots & 0 \\ 0 & \dots & 0 & e^{\varphi_n t} \end{bmatrix}, \quad \forall t \in [t_0, t_1]. \tag{2.26}$$

And writing the eigenvalues in the form :

$$\varphi_i = a_i + jb_i, \quad a_i, b_i \in \mathbb{R}, \forall i \in \{1, 2, \cdots, n\}, \ j \text{ is the complex number } j = \sqrt{-1}. \tag{2.27}$$

Implies $\forall t \in [t_0, t_1]$:

$$e^{\varphi_i t} = e^{a_i t}(\cos(b_i t) + j \sin(b_i t)), \quad \forall i \in \{1, 2, \cdots, n\}. \tag{2.28}$$

And by writing:

$$X(t) = \begin{bmatrix} x_1(t) \\ x_2(t) \\ \vdots \\ x_n(t) \end{bmatrix}, \quad \forall t \in [t_0, t_1]. \tag{2.29}$$

We can deduce the following results:

(i) If $\exists i \in \{1, 2, \cdots, n\}$ such that a_i, the real part of the eigenvalue φ_i, is strictly larger than 0, there $\exists x_i(t)$ that exponentially blows to infinity when t is big enough. In other terms, X diverges from $X = 0$, and therefore, the equilibrium point $X = 0$ is unstable. The $x_i(t)$ follows a similar behavior as in Figure 2.8.

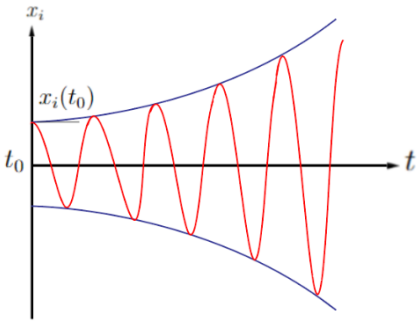

Figure 2.8 – Exponential divergence of $x_i(t)$

(ii) If $\forall i \in \{1, 2, \cdots, n\}$ we have $a_i < 0$, all $x_i(t)$ converge exponentially to the origin when t goes to infinity. Therefore, the equilibrium point $X = 0$ is exponentially stable. All the elements $x_i(t)$ of X follow a similar behavior as in Figure 2.9.

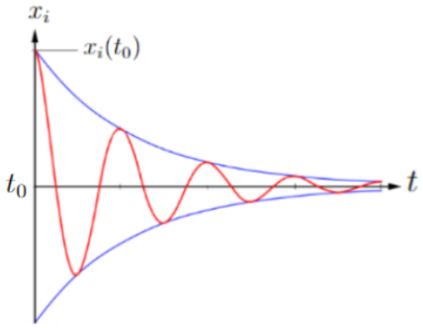

Figure 2.9 – Exponential convergence of $x_i(t)$ to 0

Summary 2.4.6.1. *If all the eigenvalues of matrix A have negative real parts, the equilibrium point of the linear system $\dot{X} = AX$ is exponentially stable. And if there exists at least one eigenvalue of A with a positive real part, the equilibrium point of the linear system $\dot{X} = AX$ is unstable.*

2.4.7 Some good facts to know

In this section, we state some important remarks and we leave the proofs for the interested readers to look for:

(i) Linear systems have at most one equilibrium point. While nonlinear systems can have one or many equilibrium points.

(ii) For linear systems, if the equilibrium point is stable it is always exponentially stable.

(iii) For linear systems, the convergence to the equilibrium point property defined in Section 2.4.2, implies the stability of the equilibrium point. But, for nonlinear systems, convergence does not always imply stability.

(iv) For both linear and nonlinear systems, exponential stability (local or global) always implies stability.

(v) For both linear and nonlinear systems, exponential stability always implies asymptotic stability.

2.5 Linearizing around an equilibrium point

Given the complexity of nonlinear systems, to study them, we generally linearize the original system around an equilibrium point then study the linear version and deduce local results around the considered equilibrium point $\bar{X}$ from linear theories.
If we write:

$$X(t) = \begin{bmatrix} x_1(t) \\ x_2(t) \\ \vdots \\ x_n(t) \end{bmatrix}, \quad \forall t \in [t_0, t_1]. \tag{2.30}$$

For the nonlinear system $\dot{X} = f(X)$ we have $\forall t \in [t_0, t_1]$:

$$\begin{cases} \dot{x}_1 = f_1(x_1, x_2, \cdots, x_n), \\ \dot{x}_2 = f_2(x_1, x_2, \cdots, x_n), \\ \vdots \\ \dot{x}_n = f_n(x_1, x_2, \cdots, x_n). \end{cases} \tag{2.31}$$

The Jacobian of the system at the equilibrium point $X = \bar{X}$ is then given by:

$$\left.\frac{Df}{DX}\right|_{X=\bar{X}} = \begin{bmatrix} \left.\frac{\partial f_1}{\partial x_1}\right|_{X=\bar{X}} & \left.\frac{\partial f_1}{\partial x_2}\right|_{X=\bar{X}} & \cdots & \left.\frac{\partial f_1}{\partial x_n}\right|_{X=\bar{X}} \\ \left.\frac{\partial f_2}{\partial x_1}\right|_{X=\bar{X}} & \left.\frac{\partial f_2}{\partial x_2}\right|_{X=\bar{X}} & \cdots & \left.\frac{\partial f_2}{\partial x_n}\right|_{X=\bar{X}} \\ \vdots & \vdots & \cdots & \vdots \\ \left.\frac{\partial f_n}{\partial x_1}\right|_{X=\bar{X}} & \left.\frac{\partial f_n}{\partial x_2}\right|_{X=\bar{X}} & \cdots & \left.\frac{\partial f_n}{\partial x_n}\right|_{X=\bar{X}} \end{bmatrix}. \tag{2.32}$$

The linearized system around the considered equilibrium point $\bar{X} = 0$ is given by:

$$\dot{X} = \left.\frac{Df}{DX}\right|_{X=\bar{X}=0} X, \quad \forall t \in [t_0, t_1]. \tag{2.33}$$

To give an intuition of where does this come from, assume $\bar{X} = 0$, then around $\bar{X} = 0$ we have for $m \in \mathbb{N}$:

$$\begin{aligned}(\dot{X} - \dot{\bar{X}}) &= f(X - \bar{X}) \\ &\approx f(\bar{X}) + \frac{Df}{DX}\bigg|_{X=\bar{X}} (X - \bar{X}).\end{aligned} \tag{2.34}$$

When $X \to \bar{X}$ and $\bar{X} = 0$ we have $f(\bar{X}) = 0$ (recall (2.7)) and $(X - \bar{X}) = X$, which gives (2.33).

Theorem 2.5.1. *(Hartman Grobman)*
If all the eigenvalues of $\frac{Df}{DX}\big|_{X=\bar{X}}$ *have a non-zero real part, the linear system:*

$$\dot{X} = f(\bar{X}) + \frac{Df}{DX}\bigg|_{X=\bar{X}} (X - \bar{X}), \tag{2.35}$$

describes well the behavior of the original nonlinear system $\dot{X} = f(X)$ *around* $\bar{X}$*.*

In other terms, this theorem states that the behavior of a dynamical system in a domain near a hyperbolic equilibrium point is qualitatively the same as the behaviour of its linearisation near this equilibrium point, where hyperbolicity means that no eigenvalue of the linearisation has real part equal to zero. Therefore, when dealing with such dynamical systems one can use the simpler linearisation of the system to analyse its behaviour around equilibria.

2.6 Some control theory

In this section, we introduce some basic concepts of control theory [53] that are needed in this work. For further reading on control theory we recommend [31, 53].

Control theory deals with driving a dynamical system to a desired state, while sometimes minimizing some criteria (such as time, energy, or something else).

When being able to measure the response of the system to a given control, and then re-adapt the control to the received feedback, we say that we have a closed-loop system and that we are performing feedback control. This process is explained visually in Figure 2.10.

A typical feedback control system is written as:

$$\dot{X}(t) = f(X(t)) + u(t, X(t)), \quad \forall t \in [t_0, t_1]. \tag{2.36}$$

Where $u(t, X(t))$ is the control term, also called a control law or a controller. There exists many controllers in the literature, such as: proportional controllers (P), proportional

integral controllers (PI), and proportional integral derivative controllers (PID).

The simplest controller is the (P) controller, it is the one we use in our work, and it is given by:

$$u(t, X(t)) = -kX(t), \quad k \in \mathcal{M}_{n,n}(\mathbb{R}), \text{ for } t \in [t_0, t_1]. \tag{2.37}$$

It is shown in Figure 2.10.

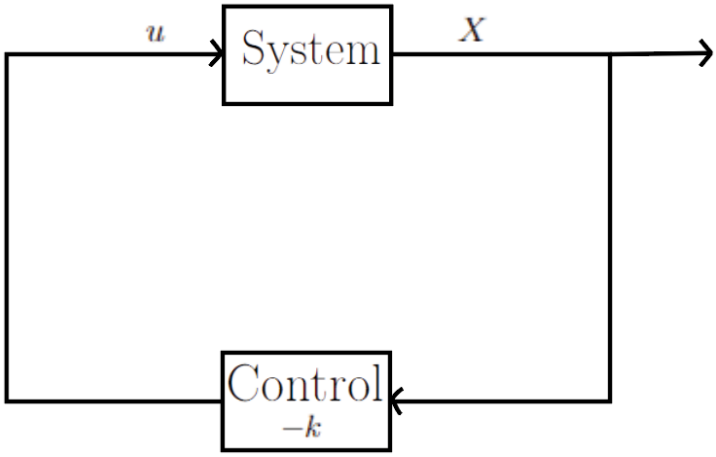

Figure 2.10 – Proportional feedback control

The Figure 2.10 illustrates how the control law u acts on the system to make it produce a response X, that we observe and take into account to improve the control law u (feedback control) after multiplying it by $-k$ (proportional controller).

The goal of control can be to stabilize an equilibrium point. We give an intuition of how this is performed using a linear system, and it is the same idea for nonlinear systems. Take the typical linear system with equilibrium point $\bar{X} = 0$:

$$\begin{cases} \dot{X} = AX(t) = AX, \\ X(t_0) = X_0, \\ X : \ t \in]t_0, t_1] \longmapsto \mathbb{R}^n, \\ n \in \mathbb{N}, \\ A \in \mathcal{M}_{n,n}(\mathbb{R}). \end{cases} \tag{2.38}$$

The controlled version with the (P) controller (2.37) is given by:

$$\dot{X} = AX - kX = (A - k)X, \quad \forall t \in [t_0, t_1]. \tag{2.39}$$

It becomes a new dynamical system with matrix $(A-k)$ instead of A and with equilibrium point $\bar{X} = 0$. By appropriately choosing k, this new system's equilibrium point can be

stable (by having a matrix $(A - k)$ with all eigenvalues of strictly negative real parts).

For a general system for which the equilibrium point $\bar{X}$ is not the origin, we can choose $u(t, X(t)) = -k(X - \bar{X})$ instead of $u(t, X(t)) = -kX$, and the previous idea still applies by seeing that we can write $Z = X - \bar{X}$ at any time $t \in [t_0, t_1]$ and go back to an equivalent linear system with equilibrium point $\bar{Z} = 0$.

Controlling a system and stabilizing its equilibrium point is not always possible. Now, we define controllability and stabilizability:

- Controllability: Controllability is defined as the ability of a control system to reach a desired state from a fixed (initial) state. And there are ways for studying the controllability of a system, which we do not cover here. We just note that if we could steer a system towards a certain state/direction with control, it means that this direction is a controllable direction of the system (a reachable direction with control).
- Stabilizability: A system is stabilizable if all of its unstable directions (the x_i elements of X which blow to infinity, as explained in Subsection 2.4.6) are controllable.

For nonlinear systems, if they could be linearized, and if the linear version is controllable, a very used approach to control them is to design controllers for the linearized version first and then test if it gives the suitable results on the nonlinear original system.

2.7 Applications to road traffic

In this section, we introduce applications in road traffic that we need in this work for the notions we have seen in this chapter. Other application are discussed in Chapter 4.

2.7.1 Definition of equilibrium flow

We say that the road traffic is at an **equilibrium flow** starting from a time t^*, such that $t^* \in [0, t_f]$, if $\forall i \in [1, N_j] \cap \mathbb{N}$ and $\forall j \in [1, J] \cap \mathbb{N}$, where N_j is the total number of vehicles on lane j and J is the total number of lanes on the observed road, if we have [30]:

(i) The velocity $V_i^j(t)$, of each vehicle i in the lane j of the observed road, equals the same constant velocity $\bar{v}^j$ when $t \in [t^*, t_f]$, $\forall j \in [1, J] \cap \mathbb{N}$.

(ii) The distance $h_i^j(t)$, between the front of the vehicle i in the lane j and the rear of the vehicle directly in front of it in the same lane, equals a constant $\bar{h}_i^j$ when $t \in [t^*, t_f]$, $\forall j \in [1, J] \cap \mathbb{N}$.

(iii) There are no lane changes when $t \in [t^*, t_f]$.

Mathematically, at the equilibrium flow, $\forall i \in [1, N_j] \cap \mathbb{N}$ and $\forall j \in [1, J] \cap \mathbb{N}$ and $\forall t \in [t^*, t_f]$, we have:

$$\begin{cases} V_i^j(t) = \bar{v}^j, \\ h_i^j(t) = \bar{h}_i^j. \end{cases} \tag{2.40}$$

Meaning that at an equilibrium flow, all the vehicles that are in the same lane j ($\forall j \in [1, J] \cap \mathbb{N}$) have the same velocity $\bar{v}^j$, but different distances between each other $\bar{h}_i^j$ which stay constant over time ($\forall j \in [1, J] \cap \mathbb{N}$ and $\forall i \in [1, N_j] \cap \mathbb{N}$).

The couple $\left(\bar{v}^j, \bar{h}_i^j\right)$, $\forall i \in [1, N_j] \cap \mathbb{N}$ and $\forall j \in [1, J] \cap \mathbb{N}$, is referred to as the equilibrium flow in this work. In the case of a single-lane road ($J = 1$), we denote it just by $\left(\bar{v}, \bar{h}_i\right)$, $\forall i \in [1, N] \cap \mathbb{N}$, such that N is the total number of vehicles in the single-lane road.

Remark 2.7.1.1. *An equilibrium flow does not always exist for the road traffic system.*

Theorem 2.7.1.1. *The equilibrium flows of the road traffic system are* ***equilibrium points of the system****, which means that if the system starts at such a state or reaches it at a certain time $t^* \in [0, t_f]$, it stays at it forever, this justifies the name of equilibrium flow [30].*

2.7.2 Uniqueness of equilibrium flow and its value

In the mixed traffic model with common velocity preference **with no lane changes**, the equilibrium flows are the same as the equilibrium flows in the unified model if they exist. This is because, at an equilibrium flow, we have (after recalling the system of equations (1.10) in Section 1.5):

$$\begin{cases} a_k(t) = f_k\left(h_k(t), \dot{h}_k(t), v_k(t)\right) = 0, \\ \dot{h}_k(t) = 0, \end{cases} \quad \forall t \in [t^*, t_f] \text{ and } \forall k \in [1, M] \cap \mathbb{N} \tag{2.41}$$

Which implies that when $t \in [t^*, t_f]$:

$$V_k(h_k(t)) - v_k(t) = 0 \text{ and } V_k(h_k(t)) = v_k(t) = \bar{v}, \quad \forall k \in \{1, 2, \cdots, n\} \text{ with } n \ll M. \tag{2.42}$$

Which means that $\bar{v}$ is independent of a_k and b_k, and the equations (2.41)(1.12) imply that when an equilibrium flow exists, it is unique (i.e. $\bar{h}_k = V_k^{-1}(\bar{v})$, $\forall k \in [1, M] \cap M$, in other terms, an equilibrium flow velocity $\bar{v}$ is associated to only one possible equilibrium flow inter-vehicular distance $\bar{h}$ for each vehicle on the road), and this is true in the three

models of traffic flow seen in Section 1.5 when there are **no lane changes**. Thus, since in the mixed traffic with common velocity preference model, we have $V_k(h_k(t)) = V(h_k(t))$ for $\forall k \in [1, M] \cap \mathbb{N}$, the equilibrium flow is the same as the equilibrium flow in the unified model.

Theorem 2.7.2.1. *When an equilibrium flow exists, in case there are* ***no lane changes****, it is unique, and this is true in the three traffic flow cases [20].*

Theorem 2.7.2.2. *When an equilibrium flow exists for the mixed traffic with common velocity model where there are* ***no lane changes****, it also exists for the unified model* ***with no lane changes*** *and vice versa. Moreover, the equilibrium flow is the same in the two cases [20].*

2.7.3 Linearizing around an equilibrium flow

The general traffic model given by (1.10) (1.11) (1.12), can be nonlinear. As seen in Section 2.5, the study of the linearized system around the equilibrium point can give us local stability results about the real nonlinear system.

After calculating the Jacobian of the system of equations (1.10) (1.11) (1.12), for a considered vehicle k with $k \in [1, M] \cap \mathbb{N}$, in a single-track road, [11] gave the following results for the considered vehicle $\forall t \in [0, t_f]$:

$$a_k^{(1)} = \left.\frac{\partial f_k}{\partial x}\right|_{(\bar{h}_k, 0, \bar{v})}, \quad a_k^{(2)} = \left.\frac{\partial f_k}{\partial y} - \frac{\partial f_k}{\partial z}\right|_{(\bar{h}_k, 0, \bar{v})}, \quad a_k^{(3)} = \left.\frac{\partial f_k}{\partial y}\right|_{(\bar{h}_k, 0, \bar{v})}. \tag{2.43}$$

The perturbations in velocity and distance from the considered equilibrium point $(\bar{v}, \bar{h}_k)$, $\forall k \in [1, M] \cap \mathbb{N}$, for a considered vehicle k on the road, $\forall t \in [0, t_f]$ and $\forall k \in [1, M] \cap \mathbb{N}$, are denoted by:

$$\begin{cases} Y_k(t) = h_k(t) - \bar{h}_k, \\ U_k(t) = v_k(t) - \bar{v}. \end{cases} \tag{2.44}$$

And the equation (1.10) becomes equivalent to:

$$\dot{U}_k(t) = f_k\left(\bar{h}_k + Y_k(t), \dot{Y}_k(t), \bar{v} + U_k(t)\right), \quad \forall t \in [0, t_f] \text{ and } \forall k \in [1, M] \cap \mathbb{N}. \tag{2.45}$$

Where $\dot{Y}_k(t)$ is the derivative of $Y_k(t)$ at time $t \in [0, t_f]$, and $\dot{U}_k(t)$ is the derivative of $U_k(t)$ at time $t \in [0, t_f]$. In the case of a closed single-track road, $Y_{M+1}(t) = Y_1(t)$ and $U_{M+1}(t) = U_1(t)$, $\forall t \in [0, t_f]$, the following condition is satisfied:

$$\sum_{k=1}^{M} Y_k(t) = \sum_{k=1}^{M} h_k(t) - \sum_{k=1}^{M} \bar{h}_k = 0, \quad \forall k \in [1, M] \cap \mathbb{N} \text{ and } \forall t \in [0, t_f]. \tag{2.46}$$

The linearization around the equilibrium point, given in [11], gives us the linearized version of the equation (2.45):

$$\dot{U}_k(t) = a_k^{(1)} \cdot Y_k(t) - a_k^{(2)} \cdot U_k(t) + a_k^{(3)} \cdot U_{k+1}(t), \quad \forall t \in [0, t_f] \text{ and } \forall k \in [1, M] \cap \mathbb{N}. \tag{2.47}$$

With the vehicle $k+1$ being the vehicle directly in front of the considered vehicle k, and $U_{k+1}(t) = v_{k+1}(t) - \bar{v}$. In the case of a closed single-lane road, the equation (2.46) is satisfied.

Note that $a_k^{(1)}$, $a_k^{(2)}$, and $a_k^{(3)}$ are independent of time.

2.7.4 Stability of equilibrium flow

The authors in [11], studied the stability of the **unified model** (i.e. the case where $\forall k \in [1, M] \cap \mathbb{N}$ we have: $f_k(\cdot) = f(\cdot)$ and $a_k^{(1)} = a^{(1)}$ and $a_k^{(2)} = a^{(2)}$ and $a_k^{(3)} = a^{(3)}$) in a closed single-lane road setting and gave the following results:

Theorem 2.7.4.1. *The equilibrium flow* $\left(\bar{h}_k, \bar{v}\right)_{\forall k \in [1,M] \cap \mathbb{N}} = \left(\bar{h}, \bar{v}\right)$, *of the system (1.10) (1.11) (1.12) in the case of a unified model, is:*

- *Locally stable, if:*
$$(a^{(2)})^2 - (a^{(3)})^2 - 2 \cdot (a^{(1)}) \geq 0. \tag{2.48}$$
- *Unstable, provided M sufficiently large, if:*
$$(a^{(2)})^2 - (a^{(3)})^2 - 2 \cdot (a^{(1)}) < 0. \tag{2.49}$$

Chapter 3

The Context of The Study

In this chapter, we introduce the main context of our study. We position ourselves in the specific traffic flow settings of our work: the geometry of the road, the composition of the traffic flow in terms of vehicles, and the parameters and models we choose to describe each vehicle's dynamics.

3.1 Description of the road

We propose to study a traffic flow on a multi-lane ring-road. In other words, the observed road has a closed circular shape, and is composed of a finite number of lanes J ($J \in \mathbb{N}^*$), with each lane having the same width of $3m$. The reference length L ($L \in \mathbb{R}_+^*$) is the length of the line situated in the inner extremity of lane J. The length L_j of the line situated in the inner extremity of lane j ($\forall j \in [1, J] \cap \mathbb{N}$), which we call the length of the lane j, is computed by:

$$L_j = \left(\frac{L}{2\pi} + 3J - 3j \right) 2\pi, \quad \forall j \in [1, J] \cap \mathbb{N}. \tag{3.1}$$

We refer to L as the length of the road. The outer lane of the road (lane 1) is the longest lane, and the length of each lane is smaller the closer it is to the center of the road. See Figure 3.1 for clarification.

The reasons for considering a ring road are explained in [11], and we cite them:

(i) No boundary conditions are needed, and one has a perfect control on the average vehicle density.

(ii) The circular road corresponds to an infinite straight road with periodic traffic dynamics.

(iii) Experimental evidence of instabilities in such settings exists [46] [47], and the experimental results can be used to calibrate our model parameters.

3.2 Composition of the traffic

At time $t = 0$: beginning of the observation of the traffic flow, we have the same finite number N ($N \in \mathbb{N}^*$) of vehicles in each lane of the ring-road described in Section 3.1, i.e. we have a total number of $N \times J$ vehicles on the road.

At any time $t \in [0, t_f]$, t_f: end of the observation of the traffic flow, the vehicles **in each lane** $j \in [1, J] \cap \mathbb{N}$ are numbered from 1 to N, such that with $\forall i, i+1, i-1 \in [1, N] \cap \mathbb{N}$ the vehicle numbered $i+1$ (vehicle $i+1$) is the vehicle directly in front of the vehicle numbered i (vehicle i). The vehicle $i+1$ is called the **leader** of the vehicle i. And the vehicle numbered $i-1$ (vehicle $i-1$) is the vehicle for which the leader is the vehicle i. The vehicle $i-1$ is called the **follower** of the vehicle i.

Since the vehicles follow a closed road (closed path), we set the following convention, $\forall t \in [0, t_f]$:

$$\text{vehicle } {}^{j}_{N+1} = \text{ vehicle } {}^{j}_{1}, \quad \forall j \in [1, J] \cap \mathbb{N}. \tag{3.2}$$

With $\forall i \in [1, N] \cap \mathbb{N}$ and $\forall j \in [1, J] \cap \mathbb{N}$, the vehicle ${}^{j}_{i}$ is the vehicle numbered i in the lane j.

We start the numbering of the vehicles from 1 and not zero to avoid confusion when implementing our model in MATLAB, since the first elements of vectors in MATLAB have the index 1 and not 0.

We interest ourselves in the study of the following traffic scenarios (in terms of traffic populations):

(i) A 1-phase traffic flow, with only aggressive cars, which we define later in Remark 3.5.1.

(ii) A 2-phase traffic flow, with collaborative cars, which we define later in Remark 3.5.1, and aggressive cars.

(iii) A 2-phase traffic flow, with cars and trucks.

3.3 Measurements and parameters of the path and the vehicles

In this section, we define the parameters describing the traffic on the ring-road, by introducing the means of characterizing the dynamical properties of each vehicle.

3.3.1 Position

We choose the origin of the position of each vehicle i in each lane j to be whatever the position on the road that the vehicle 1 in that lane j was at at time $t = 0$. The position at time t ($\forall t \in [0, t_f]$) of the point situated in the geometric center of the vehicle i in lane j, $\forall i \in [1, N] \cap \mathbb{N}$ and $\forall j \in [1, J] \cap \mathbb{N}$, is parameterized by $X_i^j(t)$. We call $X_i^j(t)$ the position of the vehicle i in the lane j at time t. We recall the origin of the positions mathematically:

$$X_i^j(0) = 0 \Leftrightarrow i = 1, \quad \forall j \in [1, J] \cap \mathbb{N}. \tag{3.3}$$

The position $X_i^j(t)$ is a curvilinear distance at time t from $X_1^j(0)$, which follows the circular line situated in the middle of the width of lane j, $\forall j \in [1, J] \cap \mathbb{N}$ and $\forall i \in [1, N] \cap \mathbb{N}$ and $\forall t \in [0, t_f]$.

3.3.2 Headway

The headway $H_i^j(t)$ is the distance between the geometric centers of the vehicles $i+1$ and i at time t ($\forall t \in [0, t_f]$), it is given by:

$$H_i^j(t) = X_{i+1}^j(t) - X_i^j(t), \quad \forall i \in [1, N-1] \cap \mathbb{N} \text{ and } \forall j \in [1, J] \cap \mathbb{N}. \tag{3.4}$$

For the case of $i = N$, we refer to the Subsection 3.3.5. The relationship between $H_i^j(t)$ and $h_i^j(t)$, $\forall i \in [1, N] \cap \mathbb{N}$ and $\forall j \in [1, J] \cap \mathbb{N}$, is:

$$h_i^j(t) = H_i^j(t) - \frac{l_{i+1}^j(t) + l_i^j}{2}. \tag{3.5}$$

Where:

- l_i^j : Is the length of the vehicle i in lane j.
- $l_{i+1}^j(t)$: Is the length of the vehicle directly in front of the vehicle i in lane j at time t in the same lane j.

We can easily see that in our closed road we have $\forall t \in [0, t_f]$:

$$\sum_{i=1}^{N} H_i^j(t) = L_j, \quad \forall j \in [1, J] \cap \mathbb{N}. \tag{3.6}$$

3.3.3 Velocity

The velocity at time t ($\forall t \in [0, t_f]$) of the vehicle i in lane j, where $i \in [1, N] \cap \mathbb{N}$ and $j \in [1, J] \cap \mathbb{N}$, is parameterized by $V_i^j(t)$, such that $V_i^j(t)$ is the derivative of $X_i^j(t)$ at time t ($\forall t \in [0, t_f]$).

3.3.4 Acceleration

The acceleration at time t ($\forall t \in [0, t_f]$) of the vehicle i in lane j, where $i \in [1, N] \cap \mathbb{N}$ and $j \in [1, J] \cap \mathbb{N}$, is parameterized by $A_i^j(t)$, such that $A_i^j(t)$ is the derivative of $V_i^j(t)$ at time t ($\forall t \in [0, t_f]$).

We refer to the relation between $V_i^j(t)$ and its derivative $A_i^j(t)$ as the **dynamics** of our system.

3.3.5 Conventions

The first convention (3.2) allows us to define the following conventions for our closed road setting $\forall t \in [0, t_f]$ and $\forall j \in [1, J] \cap \mathbb{N}$:

$$X^j_{N+1}(t) = X^j_1(t), \tag{3.7}$$

$$H^j_N(t) = X^j_{N+1}(t) - X^j_N(t) = X^j_1(t) - X^j_N(t), \tag{3.8}$$

$$V^j_{N+1}(t) = V^j_1(t), \tag{3.9}$$

$$A^j_{N+1}(t) = A^j_1(t). \tag{3.10}$$

The Figure 3.1 shows the configuration of the road at time $t = 0$ for clarification.

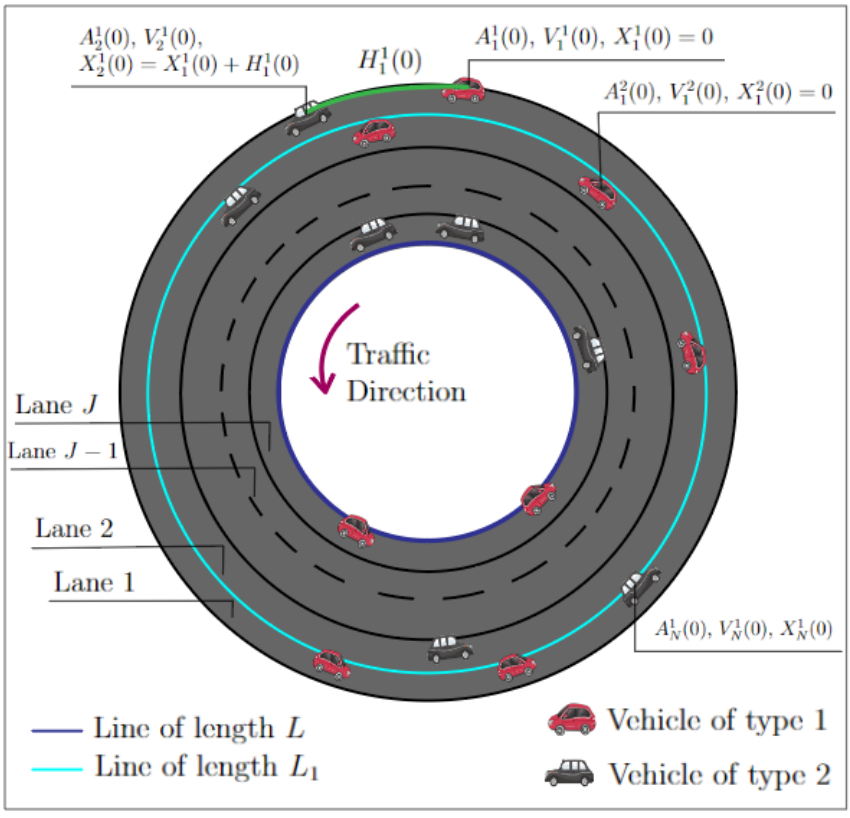

Figure 3.1 – Configuration of the traffic flow at $t = 0$

3.4 The scaling problem: why use a microscopic model

The following explanations are inspired from our article [24].

For a precise measure of fuel consumption, a detailed description of the dynamics and behaviours of each individual vehicle-driver unit is necessary. Therefore, we prefer to adopt a microscopic traffic model for our study. However, our choice is also motivated by other reasons. On one hand, when dealing with heterogeneous traffic flows, which is our case, modeling the different categories of vehicles-drivers with distinct macroscopic models raises the issue of modeling the interactions between these different macroscopic models, and modeling some of the vehicles with macroscopic models and the rest with microscopic models and then coupling the macroscopic and microscopic models, is also a delicate task (but a task that was successfully done in the literature [12, 18, 32, 33]), while the interactions between the different categories of vehicles-drivers is very easily represented in microscopic modeling. On the other hand, mesoscopic models are still limited to laboratory tests and have not been used enough in practical applications. Mesoscopic modeling also tends to be complicated due to the differential approach used and the gas momentum assumption made, and this may pose a challenge in applying them to real life situations [2]. In addition, an approach consisting of starting from a microscopic model and using a mean-field limit to obtain a partial differential equation (PDE) that represents the well-designed behavior of the microscopic system at a larger scale (large number of vehicles) was proposed in [24].

Summary 3.4.1. *Given that:*

(i) We wish to study heterogeneous traffic flows, and it is very simple to model the interactions between the different vehicles-drivers using microscopic modeling.

(ii) Coupling macroscopic models, or macroscopic models with microscopic ones, is a delicate task.

(iii) The mesoscopic models lack realism and real word proven applications.

(iv) We wish to have a high level of precision on our measures of fuel consumption and speed variance.

(v) The possibility of going to the mean field limit of a microscopic model to generalize the obtained results for a large (or infinite) number of vehicles on the road.

We restrain ourselves to a manageable number of vehicles and work at a microscopic scale only.

3.5 The Bando-FTL dynamical model

The model we use to prescribe the dynamics of the vehicles in the traffic flow is the Bando-FTL model, with a constraint on the acceleration (it is bounded), i.e. $\forall i \in [1, N] \cap \mathbb{N}$ and $\forall j \in [1, J] \cap \mathbb{N}$ and $\forall t \in [0, t_f]$:

$$\begin{cases} \dot{X}_i^j(t) = V_i^j(t), \\ f_i^j(H_i^j(t), l_{i+1}^j(t), V_i^j(t), V_{i+1}^j(t)) = \alpha_i^j \left(V_{opt}^{i,j} \left(H_i^j(t) - \dfrac{l_{i+1}^j(t) + l_i^j}{2} \right) - V_i^j(t) \right) \\ \qquad\qquad + \beta_i^j \left(\dfrac{V_{i+1}^j(t) - V_i^j(t)}{\left(H_i^j(t) - \frac{l_{i+1}^j(t) + l_i^j}{2} \right)^2} \right), \\ A_i^j(t) = \dot{V}_i^j(t) = \min(\max(f_i^j(t), -\max_{dec}^{i,j}), \max_{acc}^{i,j}). \end{cases} \tag{3.11}$$

With:

$$V_{opt}^{i,j}(x) = V_{\max}^{i,j} \left(\frac{\tanh\left(\frac{x}{d_0^{i,j}} - 2 \right) + \tanh(2)}{1 + \tanh(2)} \right), \quad x \in \mathbb{R}^+. \tag{3.12}$$

And:

$$\sum_{i=1}^{N} H_i^j(t) = L_j. \tag{3.13}$$

Where:

- α_i^j : Is the weight of the OV/Bando model.
- β_i^j : Is the weight of the FTL model.
- $V_{opt}^{i,j}(x)$: Is the optimal velocity preference function of the vehicle i in lane j.
- $V_{\max}^{i,j}$: Is the maximal preferred speed of the vehicle i in lane j.
- l_i^j : Is the length of the vehicle i in lane j.
- $l_{i+1}^j(t)$: Is the length of the vehicle directly in front of the vehicle i in lane j at time t.
- $d_0^{i,j}$: Is the minimal allowed distance between the vehicle i in lane j and the vehicle directly in front of it in the same lane.

- $\max_{acc}^{i,j}$: Is the maximal acceleration the vehicle i in lane j is capable of.
- $\max_{dec}^{i,j}$: Is the maximal deceleration the vehicle i in lane j is capable of.

Remark 3.5.1. *For the case where in lane $j \in [1, J] \cap \mathbb{N}$: $\alpha_i^j = \alpha^j$ and $\beta_i^j = \beta^j$ and $V_{opt}^{i,j}(x) = V_{opt}^j(x)$ and $l_i^j = l^j$, for $\forall i \in [1, N] \cap \mathbb{N}$, when there are no lane changes, it has been shown (based on the results stated in Subsection 2.7.4) that this model produces stop-and-go waves in lane j if [47]:*

$$\frac{\alpha^j}{2} + \frac{L^2\beta^j}{(N)^2} < \dot{V}_{opt}^j\left(\frac{L}{N} - l^j\right). \tag{3.14}$$

Where $\dot{V}_{opt}^j\left(\frac{L}{N} - l^j\right)$ is the derivative of the function $V_{opt}^j(x)$ at $\frac{L}{N} - l^j$.

We refer to the vehicles satisfying the inequality (3.14) as aggressive vehicles, and to the vehicles satisfying the opposite of the inequality (3.14) as collaborative vehicles.

3.6 Why use the Bando-FTL model

The Bando-FTL model has several advantages regarding the subject of our study:

(i) Not all microscopic models can produce stop-and-go waves (some of them are more realistic than the other ones regarding this point). IDM and Bando-FTL have been shown to do so [24].

(ii) Bando-FTL is generally more robust than IDM. The well-posedness of Bando-FTL and a time delayed version of it have been proven in [16], and the ill-posedness of IDM has been proven in [3]. The Bando part of Bando-FTL enables the uniqueness of the equilibrium flow in single-lane roads, which is what we observe in real life situations.

(iii) Given reasonable initial conditions, Bando-FTL does not require additional safety conditions, since the FTL part already provides a safety criterion by applying a large braking value when a vehicle is too close to the vehicle directly in front of it on the same lane.

For the above reasons, we choose to adopt the Bando-FTL model for our study.

3.7 The lane changing mechanism

All the vehicles in our ring-road can change lane. We base our model on the lane changing mechanism proposed by Treiber et al. in [52]. Mathematically, $\forall i \in [1, N] \cap \mathbb{N}$ and $\forall j \in [1, J] \cap \mathbb{N}$ and $\forall t \in [0, t_f]$, the adopted lane changing mechanism is given by:

$$\begin{cases} \bar{A}_i^j(t) > A_i^j(t) + \Delta_I^{i,j} \text{ (incentive)}, \\ \bar{A}_i^j(t) > -\Delta_s^{i,j}, \quad \bar{A}_{\text{fol}}^{i,j}(t) > -\Delta_s^{i,j} \quad \text{(safety)}, \\ t > t_c + \tau_i^j \quad \text{(cooldown time)}. \end{cases} \tag{3.15}$$

Where:

- $\Delta_I^{i,j}$: Is the acceleration incentive threshold of the vehicle considering a lane change.
- $\Delta_s^{i,j}$: Is the acceleration safety threshold of the vehicle considering a lane change.
- $A_i^j(t)$: Is the acceleration of the vehicle considering a lane change in the original lane at time t.
- $\bar{A}_i^j(t)$: Is the expected acceleration of the vehicle considering a lane change in the new lane at time t.
- $\bar{A}_{\text{fol}}^{i,j}(t)$: Is the expected acceleration of the follower of the vehicle considering a lane change in the new lane at time t.
- t_c : Is the last time that the considered vehicle i in lane j changed lane, $t_c \in [0, t_f]$.
- τ_i^j : Is the cooldown time (the lane change time threshold) of the vehicle considering a lane change.
- t : Is the time $t \in [0, t_f]$ at which the vehicle i in lane j is considering a lane change.

Meaning that a vehicle changes lane if its expected acceleration in the new lane is superior to its acceleration in the original lane by Δ_I, or if it is expected to be decelerating in the new lane with a negative acceleration value that is superior to $-\Delta_s$ and its follower in the new lane is also expected to be decelerating with a negative acceleration value that is superior to $-\Delta_s$. The number of lane changes on the road decreases as the value of the incentive threshold increases. The number of lane changes on the road increases as the value of the safety threshold increases (an increase in the value of the safety threshold means we require less safety measures).

3.8 Why use the Treiber et al. lane changing mechanism

Lane changing models are still poorly understood and compared. Almost all of them have drawbacks. Many models which correct the original ones are emerging, however, not enough reviewed. We did not perform an exhaustive study of the existing lane changing models, and we choose the Treiber et al. model because it is "good enough" for our study.

It has the following advantages [28]:

(i) Both the utility of the original lane and the risk associated with the lane change are determined in terms of longitudinal accelerations calculated with a microscopic traffic model.

(ii) Although the safety criterion prevents critical lane changes and collisions, the incentive criterion takes into account the advantages and disadvantages of other drivers associated with a lane change via a "politeness factor" which is incorporated in its value. It allows one to vary the motivation for lane changing from a purely egoistic to a more cooperative driving behaviour by preventing lane changes for marginal gains if it obstructs other drivers.

(iii) The LC decision-making process is very simple.

(iv) It allows the consideration of drivers with different driving styles on the road (heterogeneous traffic), in a microscopic traffic modeling setting.

And the following principle disadvantages:

(i) It does not account for mandatory lane changes.

(ii) The model parameters are fixed and do not account for the variations in the driver's behaviour over time.

(iii) It assumes that lane changes only occur when they are safe, which in some cases might not be realistic in dense congested traffic scenarios.

3.9 The linearized system around an equilibrium flow

The linearized version of the system of longitudinal dynamics given in Section 3.5 around a considered equilibrium flow $(\bar{v}^j, \bar{h}_i^j)$ (there are no lane changes) is given, $\forall t \in [0, t_f], \forall i \in [1, N] \cap \mathbb{N}$, and $\forall j \in [1, J] \cap \mathbb{N}$, by:

$$h_i^j(t) = H_i^j(t) - \frac{l_{i+1}^j(t) + l_i^j}{2}, \tag{3.16}$$

$$y_i^j(t) = h_i^j(t) - \bar{h}_i^j, \tag{3.17}$$

$$u_i^j(t) = V_i^j(t) - \bar{v}^j, \tag{3.18}$$

$$f_i^j(h_i^j(t), \dot{h}_i^j(t), V_i^j(t)) = \alpha_i^j \left(V_{opt}^{i,j}(h_i^j(t)) - V_i^j(t)\right) + \beta_i^j \left(\frac{\dot{h}_i^j(t)}{(h_i^j(t))^2}\right). \tag{3.19}$$

With $\dot{y}_i^j(t)$ being the derivative of $y_i^j(t)$ at time t and $\dot{h}_i^j(t)$ being the derivative of $h_i^j(t)$ at time t, and:

$$\sum_{i=1}^{N} y_i^j(t) = \sum_{i=1}^{N} h_i^j(t) - \sum_{i=1}^{N} \bar{h}_i^j = 0. \tag{3.20}$$

Which finally gives:

$$\begin{cases} \dot{y}_i^j(t) = u_{i+1}^j(t) - u_i^j(t), \\ \dot{u}_i^j(t) = a_i^{j(1)} y_i^j(t) - a_i^{j(2)} u_i^j(t) + a_i^{j(3)} u_{i+1}^j(t). \end{cases} \tag{3.21}$$

Where at each given time $t \in [0, t_f]$:

$$a_i^{j(1)} = \left.\frac{\partial f_i^j}{\partial x}\right|_{\left(\bar{h}_i^j, 0, \bar{v}^j\right)}, \quad a_i^{j(2)} = \left.\frac{\partial f_i^j}{\partial y} - \frac{\partial f_i^j}{\partial z}\right|_{\left(\bar{h}_i^j, 0, \bar{v}^j\right)}, \quad a_i^{j(3)} = \left.\frac{\partial f_i^j}{\partial y}\right|_{\left(\bar{h}_i^j, 0, \bar{v}^j\right)}. \tag{3.22}$$

It is clear that the constants $a_i^{j(1)}$, $a_i^{j(2)}$, and $a_i^{j(3)}$, are independent of time.

Notation 3.9.1. *We choose to have the below notation, $\forall i \in [1, N] \cap \mathbb{N}$ and $j \in [1, J] \cap \mathbb{N}$:*

$$\begin{aligned} \Lambda_i^j &= \left(a_i^{j(1)}, a_i^{j(2)}, a_i^{j(3)}\right), \\ \Delta_i^j &= (a_i^{j(2)})^2 - (a_i^{j(3)})^2 - 2(a_i^{j(1)}). \end{aligned} \tag{3.23}$$

3.10 The energy consumption model

We define the power consumed by each vehicle i in each lane j at a time t (in $[s]$), $\forall i \in [1, N] \cap \mathbb{N}$ and $\forall j \in [1, J] \cap \mathbb{N}$, based on the $P\Delta P$ model [45]:

$$power_i^j(t) = \left(p_i^j + q_i^j \cdot \left(V_i^j(t)\right)^2 + mass_i^j \cdot \max\left(0, A_i^j(t)\right)\right) \cdot \frac{V_i^j(t)}{1000}, \quad \forall t \in [0, t_f]. \tag{3.24}$$

Where:

- $power_i^j(t)$: Is the power consumed by the vehicle i in lane j at time t, in $[kW]$.
- p_i^j : Is the absorption coefficient for power, of the vehicle i in lane j, in $[N]$.

- q_i^j : Is the absorption coefficient for velocity, of the vehicle i in lane j, in $[N \cdot s^2/m^2]$.
- $mass_i^j$: Is the mass of the vehicle i in lane j, in $[kg]$.

The energy consumption $E^j(t)$ in $[kW \cdot s/m]$, in lane j, at time t in $[s]$, is then given by:

$$E^j(t) = \sum_{i=1}^{N} \frac{power_i^j(t)}{V_i^j(t)}, \quad \forall j \in [1, J] \cap \mathbb{N} \text{ and } \forall t \in [0, t_f]. \tag{3.25}$$

3.11 Why use the $P\Delta P$ fuel consumption model

The authors in [45], test the $P\Delta P$ model on large high resolution Australian data sets and prove its high performance compared to more complex models. The $P\Delta P$ model needs very few inputs (information) to be available and still performs very well.

For this reason, and also because we prefer to use microscopic models in this work, we choose the $P\Delta P$ fuel consumption model.

3.12 The elements of a simulation

For the simulations we refer to in Chapter 4, the time step for a considered simulation is denoted by δt (such that t_f is dividable by δt, and each time instant t_k is given as $t_k = t_{k'-1} + \delta t$, with $k' \in \left[1, \frac{t_f}{\delta t} + 1\right]$ and $t_0 = -\delta t$, which means $k \in \left[1, \frac{t_f}{\delta t}\right]$). For a considered simulation, we choose to have the following definitions, such that S is a natural number dividable by δt.

(i) The instantaneous speed variance is:

$$\text{speedvar}(t_k) = \frac{\sum_{j=1}^{j=J} \frac{\sum_{i=1}^{i=N} \left(V_i^j(t_k) - \frac{\sum_{i=1}^{i=N} V_i^j(t_k)}{N} \right)^2}{N-1}}{J}, \quad \forall k \in \left[1, \frac{t_f}{\delta t}\right]. \tag{3.26}$$

(ii) The speed variance averaged over the last S seconds is:

$$\text{speedvaravrg}(S) = \frac{\sum_{j=1}^{j=J} \frac{1}{S} \int_S^{t_f} \frac{\sum_{i=1}^{i=N} \left(V_i^j(t) - \frac{\sum_{i=1}^{i=N} V_i^j(t)}{N} \right)^2}{N-1} dt}{J}. \tag{3.27}$$

$$\text{speedvaravrg}(S) \approx \frac{\sum_{j=1}^{j=J} \frac{\delta t}{S} \sum_{k=\frac{S}{\delta t}}^{k=\frac{t_f}{\delta t}} \frac{\sum_{i=1}^{i=N} \left(V_i^j(t_k) - \frac{\sum_{i=1}^{i=N} V_i^j(t_k)}{N} \right)^2}{N-1}}{J}. \tag{3.28}$$

It is the approximation (3.28) that we use and refer to as the speed variance over the last S seconds. It quantifies how much is the system far from a state of same velocity for all the vehicles in each lane. Which means that it is an indicator of the presence of stop-and-go waves if its value is not close to 0, and it indicate that we have reached an equilibrium flow if it is equal to 0, or that we are close to an equilibrium flow if its value is close to 0. It is by no means a statistical variance to evaluate the velocity parameter.

(iii) The speed average averaged over the last S seconds is:

$$\text{speedavrg}(S) = \frac{\sum_{j=1}^{j=J} \frac{\delta t}{S} \sum_{k=\frac{S}{\delta t}}^{k=\frac{t_f}{\delta t}} \frac{\sum_{i=1}^{i=N} V_i^j(t_k)}{N}}{J}. \tag{3.29}$$

(iv) The energy consumption averaged over the last S seconds is:

$$\text{energyavrg}(S) = \frac{\sum_{j=1}^{j=J} \frac{\delta t}{S} \sum_{k=\frac{S}{\delta t}}^{k=\frac{t_f}{\delta t}} E_j(t_k)}{J}. \tag{3.30}$$

(v) The number of lane changes over the last S seconds is:

$$\text{Number of lane changes on the whole road during the interval of time } [t_f - S, t_f]. \tag{3.31}$$

If we have Z many simulations with the same parameters but with different (random) initial conditions, for each simulation $z \in [1, Z] \cap \mathbb{N}$, we have an associated speed variance averaged over the last S second $\text{speedvaravrg}_z(S)$, an associated speed average averaged over the last S second $\text{speedavrg}_z(S)$, an associated energy consumption averaged over the last S second $\text{energyavrg}_z(S)$, an associated number of lane changes over the last S seconds, and an associated instantaneous speed variance. It is the averages of these quantities over the Z many simulations that we plot.

Remark 3.12.1. *The trajectories of the vehicles depend on the parameters of the Bando-FTL and the Treiber et al. models. Thus, the quantities (i), (ii), (iii), (iv), and (v), that we have just defined, do too.*

Remark 3.12.2. *The velocity $V_i^j(t)$, $\forall i \in [1, N] \cap \mathbb{N}$ and $\forall j \in [1, J] \cap \mathbb{N}$, depends on the time, on the incentive threshold, and on the safety threshold. Rigorously speaking, it should be written as $V_i^j(t, \Delta_I^{i,j}, \Delta_s^{i,j})$, $\forall i \in [1, N] \cap \mathbb{N}$ and $\forall j \in [1, J] \cap \mathbb{N}$. However, to not complicate the notation we write it as $V_i^j(t)$, $\forall i \in [1, N] \cap \mathbb{N}$ and $\forall j \in [1, J] \cap \mathbb{N}$.*

The following is a simplified summary of the way that a simulation is executed.

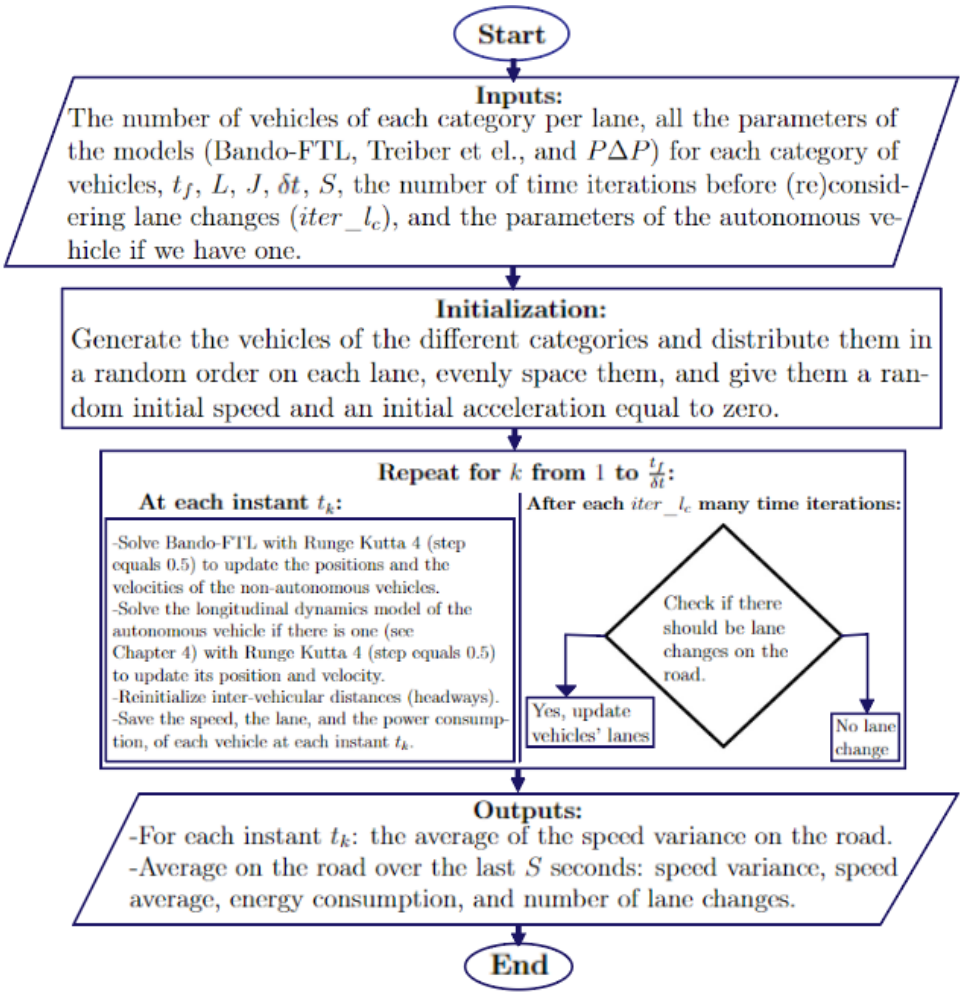

Figure 3.2 – Simplified diagram of the execution of a simulation

Since we perform much more than 20000 simulations on MATLAB, we use computing resources offered by the Office of Advanced Research Computing (OARC) at Rutgers.

N.B. The Matlab code of the simulations that are performed in this study is very long (more than 20 files). Some parts of the code exist already. I: Tinhinane MEZAIR, contributed to each file by making the necessary modifications allowing the integration of multiple types of vehicles (instead of having just one type) and computing the interactions between these different types of vehicles. I: Tinhinane MEZAIR, do not have the full rights on the code, therefore, it cannot be included in this thesis. I: Tinhinane MEZAIR, provide here the necessary explanations that would allow the readers to understand everything that is happening in the simulations, and allow them to obtain the same results if they were to reproduce the study with their own code.

Chapter 4

Dissipating Stop-and-go Waves: State-of-the-art and New Results

In this chapter, we expose existing results and gaps in the literature of dissipating stop-and-go waves in road traffic, we detail the three problematics we contribute to address, and we expose our scientific approach and our findings.

4.1 The problematic of dissipating stop-and-go waves

For a road traffic, to not be at an equilibrium flow is often synonymous to undergoing stop-and-go waves. A direct consequence is the presence of speed variance. The closer is the system to an equilibrium flow, the closer to zero is the speed variance and the smoother are the stop-and-go waves. Smoothing (or dissipating) stop-and-go waves means to bring the system close to an equilibrium flow.

4.2 Existing results and literature gaps

In the literature, the question of dissipating/smoothing (eliminating/reducing) traffic stop-and-go waves has been divided into several sub-questions: (i) dissipating stop-and-go waves in 1-phase traffic flows (homogeneous traffic flows) where only cars are present on the road, (ii) dissipating stop-and-go waves in heterogeneous 2-phase and n-phase traffic flows (with $n > 2$). Below, is the best of our knowledge about the state-of-art.

4.2.1 Dissipating stop-and-go waves in 1-phase traffic flows

Most efforts in this area of research have been centered around using autonomous vehicles. To the best of our knowledge, the state-of-the-art in both theory and experiments is about smoothing stop-and-go waves with a **single autonomous vehicle** in a **single lane road** [13]. The technique is to use two very simple controllers, one proportional and one slightly proportional integral controller. The authors in [13], demonstrated from theoretical analysis and experiments, the efficiency of such simple controllers for dissipating stop-and-go waves in a single-lane ring-road, with a reduction of fuel consumption of up to 40%.

The dissipation/smoothing of stop-and-go waves in a multi-lane road context has, to the best of our knowledge, not been studied theoretically yet. The authors in [19], studied the dissipation of stop-and-go waves with autonomous vehicles in a multi-lane system by performing a small number of numerical simulations (not enough **random** initial conditions to be able to draw conclusions). A multi-lane system is more complex than a single lane one because:

(i) When lane changes are allowed, the dynamics in the different lanes are coupled, therefore, the stability of the equilibrium flow may be impacted, and this may lead to waves which are harder to smooth.

(ii) Choosing different parameters for the lane changing mechanism (incentive threshold, safety threshold, cooldown time), may result in very different systems, and we cannot guarantee that the parameters upon which the study is based are the ground truth ones.

(iii) An autonomous vehicle initially placed on a lane, may impact the dynamics in the other lanes by changing lane, and it may be a positive or a negative impact.

4.2.2 Dissipating stop-and-go waves in multi-phase traffic flows

For these systems, the efforts evolved around the stability analysis of the mixed populations traffic equilibrium point in a **single-lane road**, by varying the proportions of the different categories of vehicles present on the road. The study in [24], showed that for a 2-phase traffic on a single lane where collaborative vehicles (vehicles with parameters α_i^j and β_i^j, with $j = J = 1$ and $i \in [1, N] \cap \mathbb{N}$, which satisfy the opposite of the inequality (3.14)) coexist with aggressive vehicles (vehicles with parameters α_i^j and β_i^j, with $j = J = 1$ and $i \in [1, N] \cap \mathbb{N}$, which satisfy the inequality (3.14)), the higher is the proportion of collaborative vehicles on a **single-lane road** (where all the vehicles are cars) the closer is the system to the equilibrium point (where the speed variance is equal to zero). As shown in Figure 4.1, where the authors ran simulations on a single lane ring-road of $258m$ with 25 cars during $1000s$ and starting close to the equilibrium flow with random initial conditions. These cars start around half their maximal velocity preference, and the maximal velocity preference of each car follows a normal distribution of mean $9.25m/s$ and standard deviation of $1m/s$, with all the cars being initially located within $1m$ from their steady-state location (which corresponds to a uniform spacing). The penetration rate of cars with a collaborative behavior is given by $\left(p = \frac{\text{number of collaborative cars}}{\text{total number of cars}}\right)$. Among the 25 cars, the number of cars with a collaborative behavior was $25(p = 1)$, $12(p = 0.48)$, then $8(p = 0.32)$, $6(p = 0.24)$, $5(p = 0.20)$, $4(p = 0.16)$, $3(p = 0.12)$, $2(p = 0.08)$, $1(p = 0.04)$, $0(p = 0)$. For each of these proportions, the authors ran 40 simulations for which was computed the instantaneous speed variance between cars averaged over the last 100s of each simulation, and then averaged over the 40 simulations.

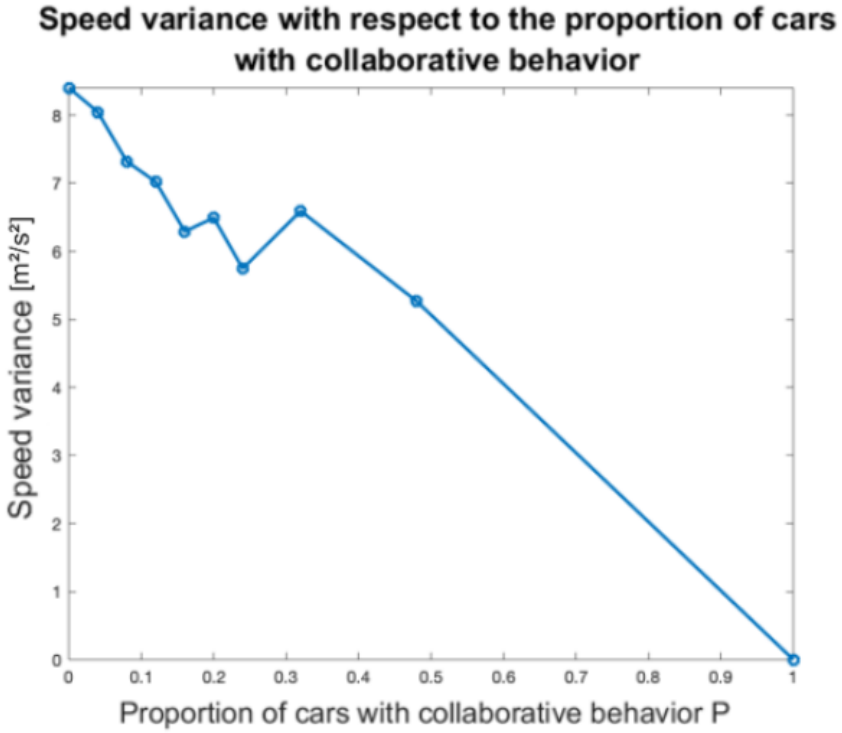

Figure 4.1 – Speed variance with respect to the proportion of cars with a collaborative behavior p (credit: [24])

To the best of our knowledge, the state-of-the-art in this area of research is the results obtained in article [20] about the stability analysis of multi-population traffic flows for **a single lane road** (no lane changes). In the following paragraph, we state their results for a 2-phase traffic flow (whatever are the differences between the two populations of vehicles, the results still hold). They also gave similar results for any number of phases of traffic (still only for single-lane roads) that we will not cover here.

In a 2-phase traffic, Λ_i^j either equals a certain value $\Lambda^1 = (a_1^{(1)}, a_1^{(2)}, a_1^{(3)})$ or a certain value $\Lambda^2 = (a_2^{(1)}, a_2^{(2)}, a_2^{(3)})$, and the same goes for Δ_i^j, which either equals a certain value $\Delta^1 = (a_1^{(2)})^2 - (a_1^{(3)})^2 - 2(a_1^{(1)})$ or a certain value $\Delta^2 = (a_2^{(2)})^2 - (a_2^{(3)})^2 - 2(a_2^{(1)})$, $\forall i \in [1, N] \cap \mathbb{N}$ and $j = J = 1$. The number of vehicles characterized by Δ^1 and Λ^1, i.e. the number of the vehicles of population 1, is denoted by n_1. While the number of vehicles characterized by Δ^2 and Λ^2, i.e. the number of the vehicles of population 2, is denoted by n_2, with $N = n_1 + n_2$. From [20], we have :

Theorem 4.2.2.1. *If $\Delta^1 \geq 0$ and $\Delta^2 \geq 0$, then for any couple $(n_1, n_2) \in \mathbb{N}^2$ and for any order of the vehicles on the road (any way that the vehicles of the two populations are distributed on the road, either clustered or distributed in any other way), the equilibrium flow $(\bar{v}^j, \bar{h}_i^j)$, $\forall i \in [1, N] \cap \mathbb{N}$ and $j = J = 1$, is locally exponentially stable.*

Theorem 4.2.2.2. *If $\Delta^1 \geq 0$ and $\Delta^2 < 0$, then:*
***(i)** If $\Delta^1 > 0$, then there exits a critical penetration rate $\tau_0 \in [0, 1]$ given by:*

$$\tau_0 = 1 - \left(1 + \max\left\{-\frac{H_2(y)}{H_1(y)}; y \in \left]0, \Gamma^2\right]\right\}\right)^{-1}, \tag{4.1}$$

$$H_i(y) = \log\left(\frac{\left(a_i^{(1)}\right)^2 + \left(a_i^{(3)}\right)^2 y}{\left(a_i^{(1)}\right)^2 + \left(\left(a_i^{(2)}\right)^2 - 2a_i^{(1)}\right) y + y^2}\right), \quad \text{for } i \in \{1, 2\}, \tag{4.2}$$

$$\Gamma^2 = \frac{-\left(a_2^{(1)}\right)^2 + \sqrt{\left(a_2^{(1)}\right)^4 - \left(a_2^{(1)}\right)^2 \left(a_2^{(3)}\right)^2 \Delta^2}}{\left(a_2^{(3)}\right)^2} \in \left]0, -\Delta^2\right[. \tag{4.3}$$

Such that if:

$$\tau = \frac{n_1}{n_1 + n_2} > \tau_0. \tag{4.4}$$

For any order of the vehicles on the road, the equilibrium flow is locally exponentially stable.

And if:

$$\tau = \frac{n_1}{n_1 + n_2} < \tau_0. \tag{4.5}$$

Then $\exists M > 0$ *such that for any* $(n_1, n_2) \in \mathbb{N}$ *satisfying* $n_1 + n_2 = M$*, the equilibrium flow is unstable.*

(ii) *If* $\Delta^1 = 0$*, then for any penetration rate:*

$$\tau = \frac{n_1}{n_1 + n_2}, \tag{4.6}$$

$\exists M > 0$*, efficiently computable, such that if* $n_1 + n_2 > M$*, the equilibrium flow is unstable.*

We can deduce from these theorems that in a one lane system, it is possible to calculate a critical penetration rate τ_0 of a certain "good" population of vehicles, introduce it to the traffic and dissipate stop-and-go waves. However, the authors showed that this critical penetration rate is a very large value (it is usually superior to 80%), therefore, this does not represent a realistic strategy to dissipate stop-and-go waves (introducing 80% of good vehicles in a real traffic flow is almost impossible).

Regarding multi-lane systems, there are no such theoretical results available in the literature. The stability analysis of the latter is more complex for the following reasons:

(i) When no lane changes are possible, the equilibrium flow is unique, as seen in Section 2.7.2, and this is partly because the number and order of the vehicles in each lane is invariant over time. However, there may be multiple equilibrium flows in a multi-lane system, and since the stability analysis is usually done on a linearized version of the original nonlinear traffic flow model around an equilibrium flow as in [20], we can only extract local stability results. So even if we find some critical penetration rate of a given population which stabilizes a certain equilibrium flow, it may not work as well if the system starts at a state close to another equilibrium flow, it may even destabilize that other equilibrium flow.

(ii) It is difficult to understand how the dynamics in the different lanes are coupled.

(iii) We have seen from the results of [20], in a one lane setting, that the stability of an equilibrium flow can depend on the total number of vehicles present on the road. Simulations with not "enough" vehicles can give the illusion that the mixed-traffic solution for smoothing stop-and-go waves worked well, but in reality it only worked for that specific number of vehicles. This may also be true for multi-lane systems, which means that results that are obtained from real life field experiments where the number of vehicles is limited may not be generalizable if no mathematical result proves their generalizability. However, numerical simulations, with super calculators, where the number of vehicles is very large, can yield interesting conclusions.

(iv) The results can be sensitive to the lane changing parameters (incentive threshold, safety threshold, cooldown time).

4.3 Addressing the gaps

In the next sections, we address some of the literature gaps we mentioned. We give new results about multi-lane systems, while limiting ourselves to **multi-lane 1-phase traffic flows of cars (aggressive cars)**, **multi-lane 2-phase traffic flows of collaborative cars and aggressive cars**, and **multi-lane 2-phase traffic flows of cars (aggressive cars) and trucks**, since we are limited in time. The difference between collaborative and aggressive cars is in the coefficients α_i^j and β_i^j, while the difference between cars and trucks appears in the coefficients α_i^j and β_i^j and also in the lengths of the vehicles l_i^j, the cooldown times τ_i^j, the masses of the vehicles $mass_i^j$, and the maximal preferred speeds $V_{max}^{i,j}$.

4.4 Multi-lane 1-phase traffic flow of cars

In this section, we study a multi-lane traffic flow composed of one population of aggressive cars. We show that this system presents high speed variance (is far from a desired equilibrium flow of zero speed variance and produces stop-and-go waves), and that it is possible to bring it very close to a desired state of zero speed variance (which means to dissipate stop-and-go waves) just by adding to the multi-lane traffic a single autonomous vehicle (AV) whose acceleration follows an appropriate control law. We also show that this system is very sensitive to lane changing parameters.

The results of this work have been published in The European Physical Journal Special Topics - Springer.

[24] Nicolas Kardous, Amaury Hayat, Sean T. McQuade, Xiaoqian Gong, Sydney Truong, **Tinhinane Mezair**, Paige Arnold, Ryan Delorenzo, Alexandre Bayen, and Benedetto Piccoli. A rigorous multi-population multi-lane hybrid traffic model for dissipation of waves via autonomous vehicles. Eur. Phys. J. Spec. Top., 2022.

4.4.1 Demonstrating the strong influence of the lane changing parameters on the system

To study the effect of the **safety threshold** and **incentive threshold** parameters on the traffic behavior, we run traffic simulations over $1000s$ with different safety and incentive thresholds in a ring road of three lanes. The maximal acceleration allowed for the cars is $2m/s^2$, and the maximal deceleration allowed is $4m/s^2$. In each simulation, all the cars present on the road (all being ordinary cars) have the same safety and incentive thresholds and the same other parameters, and the two lane changing thresholds are varied over the different simulations. The safety threshold ranges from $1m/s^2$ to $4.5m/s^2$, and takes the following consecutive values $1m/s^2$, $1.5m/s^2$, $2m/s^2$, $2.5m/s^2$, $3m/s^2$, $3.5m/s^2$, $4m/s^2$, $4.5m/s^2$. The incentive threshold ranges from $0.5m/s^2$ to $3m/s^2$, and takes the following consecutive values $0.5m/s^2$, $1m/s^2$, $1.5m/s^2$, $2m/s^2$, $2.5m/s^2$, $3m/s^2$.

The explanation for the range on the incentive threshold, is that requiring a maximal value of incentive of $3m/s^2$, that is bigger than the possible maximal acceleration of a car, means that a car can only change lane if its original lane is decelerating and it can accelerate strongly on a neighboring lane, and by varying from $0.5m/s^2$ to $3m/s^2$ we cover all the possible values of the incentive threshold. The explanation for the range on the safety threshold, is that requiring a maximal value of safety of $4.5m/s^2$, that is bigger than the possible maximal deceleration of a car, means that we do not require any safety since the vehicles cannot brake more strongly anyway, and by varying from $1m/s^2$ to $4.5m/s^2$ we cover all the possible values of the safety threshold.

We summarise the parameters of the system that do not vary over the simulations in the Table 4.1. For $\forall i \in [1, N] \cap \mathbb{N}$ and $\forall j \in [1, J] \cap \mathbb{N}$, we have:

Parameter	Value	What it represents
L	$2\pi 41.4$	Length of the road $[m]$
N	24	Number of vehicles per lane
J	3	Number of lanes on the road
l_i^j	4.5	Length of a car $[m]$
$d_0^{i,j}$	2.5	Minimal distance between a car and its leader $[m]$
β_i^j	20	Weight of the FTL model for a car
α_i^j	0.5	Weight of the Bando model for a car
$\max_{dec}^{i,j}$	4	Maximal possible deceleration of a car $[m/s^2]$
$\max_{acc}^{i,j}$	2.5	Maximal possible acceleration of a car $[m/s^2]$
τ_i^j	5	Cooldown time of lane change for a car $[s]$
δt	0.02	Time size of one iteration a simulation $[s]$
t_f	1000	Time duration of the simulation $[s]$
$iter\_l_c$	$1/\delta t = 50$	Number of iterations before considering a new lane change
p_i^j	7.1	Absorption coefficient of a car for power $[N]$
q_i^j	0.6234	Absorption coefficient of a car for power $[N \cdot s^2/m^2]$
$mass_i^j$	2000	Mass of a car $[kg]$

Table 4.1 – Summary of the parameters of the simulations

The chosen values for α_i^j, β_i^j, the length, the mass, the cooldown time, the maximal possible acceleration/deceleration and $d_0^{i,j}$ of a car, are typical values which were proven to generate stop-and-go waves in real life experiments [39]. Whereas the values for p_i^j and q_i^j were suggested by the developers of the $P\Delta P$ model in [45].

For each couple of incentive and safety thresholds, we run 100 simulations with random initial states of the cars. Which means that we run a total of 4800 simulations (the set of safety thresholds contains 8 values, the set of incentive thresholds contains 6 values, which gives $8 \times 6 = 48$ couples of incentive and safety thresholds, and we run 100 simulations for each couple to be able to take the average of the results of the 100 simulations with random initial conditions for each couple and account for the randomness of the results, which finally gives a total of 4800 simulations). These cars start around half their maximal velocity preference, and the maximal velocity preference of each car follows a normal distribution of mean $9.25m/s$ and standard deviation of $1m/s$. All the cars were initially located within $1m$ from their steady-state location (which corresponds to a uniform spacing). For each one of the 100 simulations, the speed, the lane, and the power consumed, at each time step, for each car, were saved and then averaged over the 100 simulations, to calculate the speed variance, speed average, number of lane changes, and the energy consumed, for each car, which were then averaged over all the cars in the three lanes and then only the averages over the last $300s$ were kept (except for the number of lane changes: we keep the total number of lane changes on the road over the last 300s, it is not an average).

The following are the obtained plots for the speed variance (averaged), consumed energy (averaged), speed average (averaged), and number of lane changes, over the last 300s; given by (3.28), (3.29), (3.30), and (3.31), respectively; with respect to the different lane changing parameters.

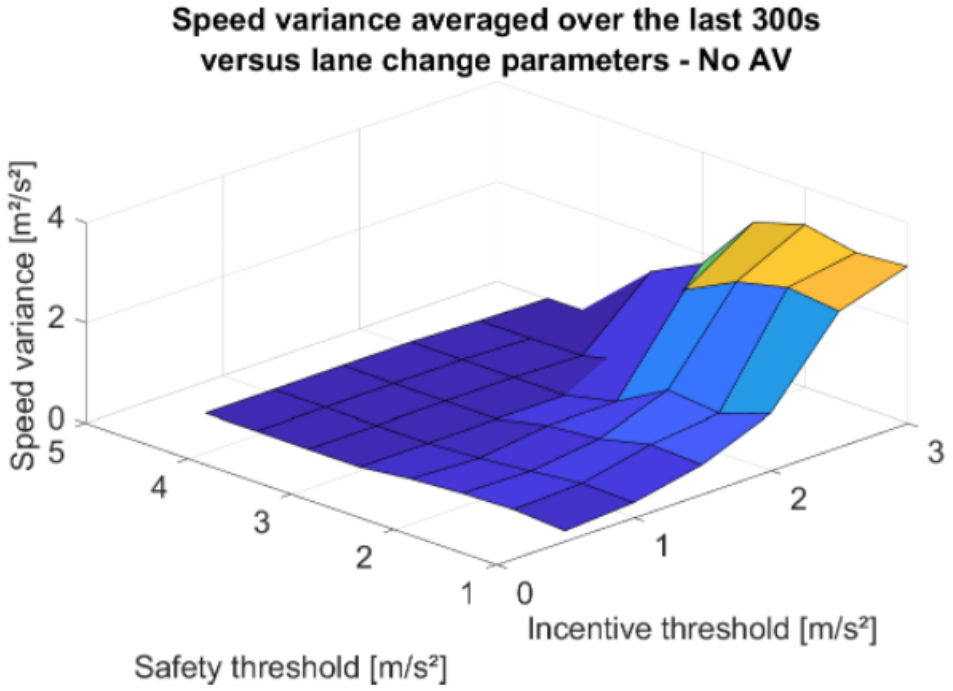

Figure 4.2 – The speed variance averaged over the last 300s with respect to the different lane changing parameters

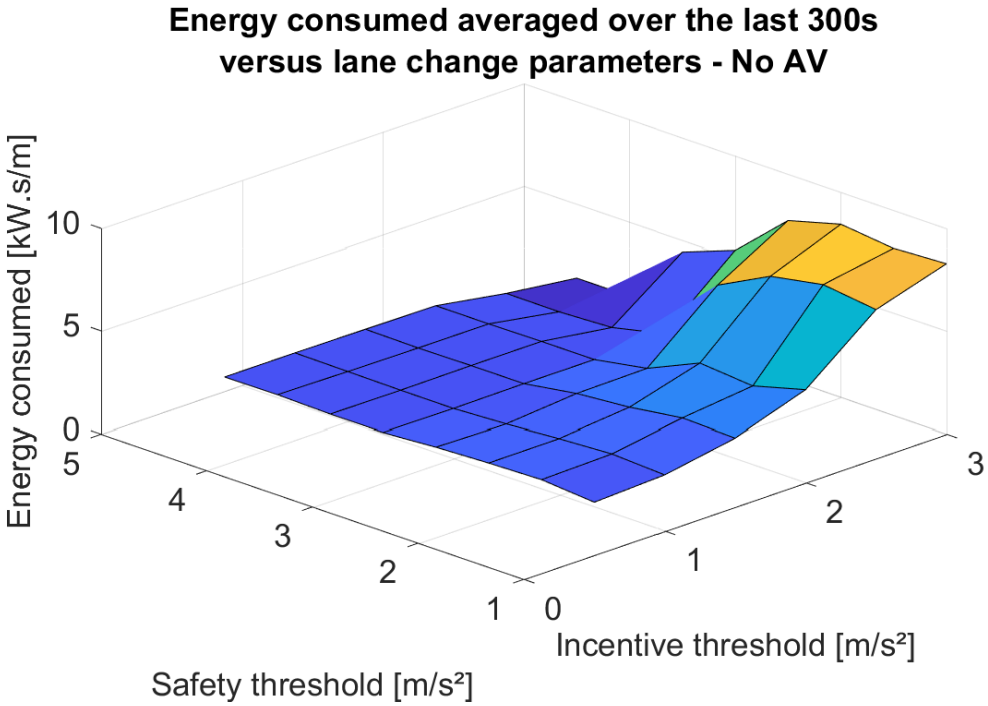

Figure 4.3 – The energy consumption averaged over the last 300s with respect to the different lane changing parameters

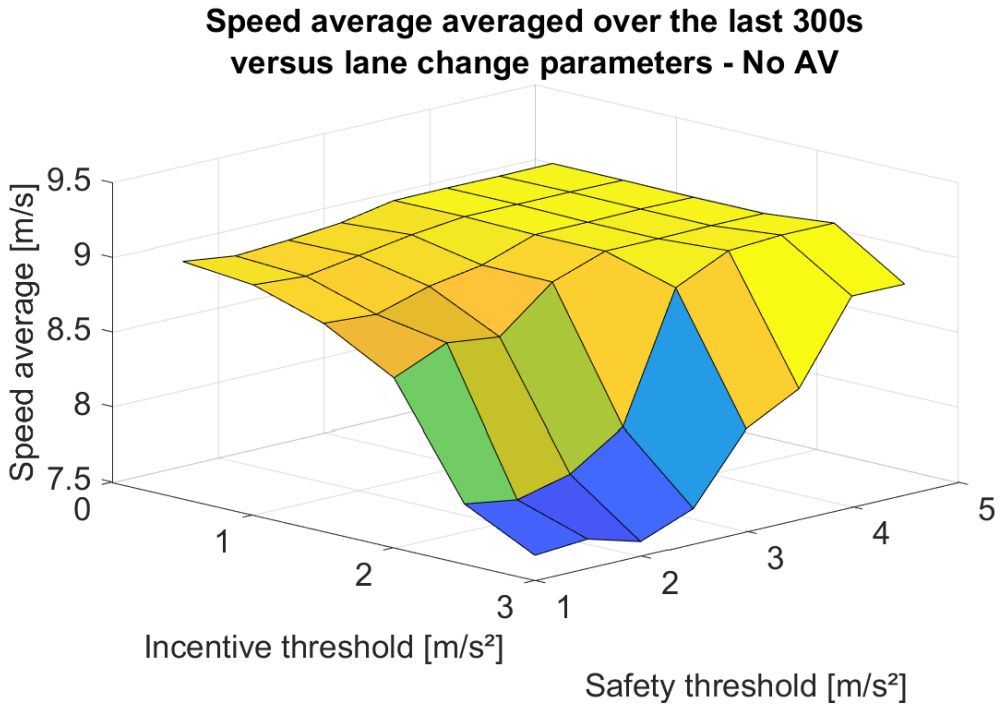

Figure 4.4 – The speed average averaged over the last 300s with respect to the different lane changing parameters

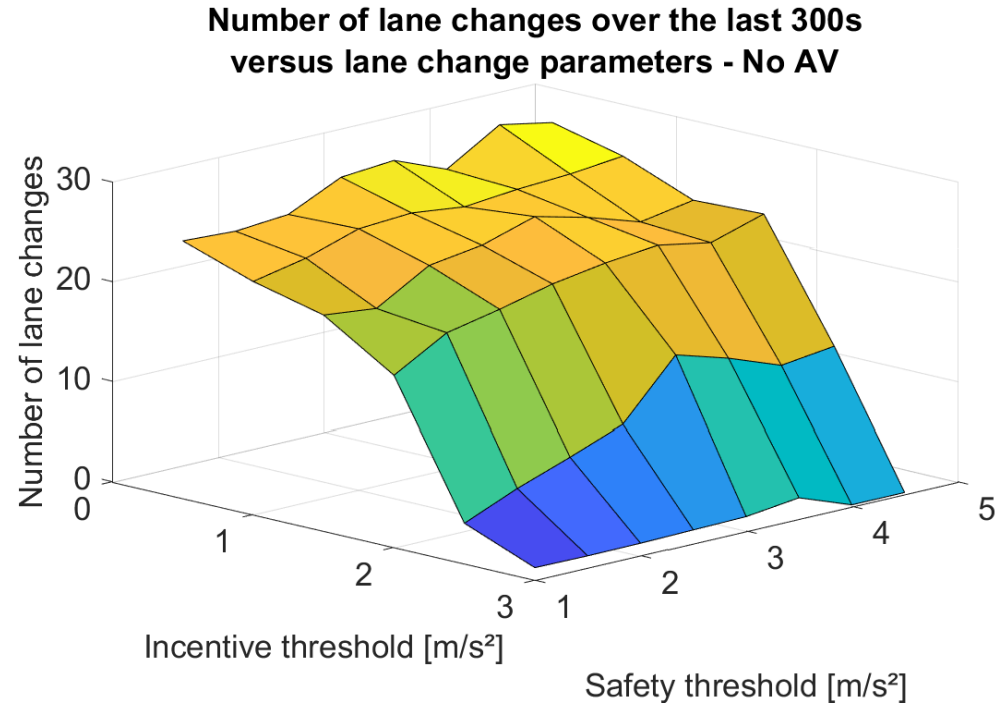

Figure 4.5 – The number of lane changes over the last 300s with respect to the different lane changing parameters

Discussions:

We can see that the traffic flow is very sensitive to the lane changing parameters, the behavior of the traffic changes radically for different values of these parameters.

We expect that the higher the request on the incentive is, the lower the number of lane changes. Similarly, the higher the safety threshold (hence the lower security required), the higher the number of lane changes. These expectations were confirmed in Figure 4.5.

For some combinations of incentive and safety thresholds, the speed variance is very close to 0, which suggests that the system is very close to an equilibrium flow. While for other combinations, the speed variance reaches high values, suggesting that the system undergoes stop-and-go waves. Comparing this to Figure 4.5, one can note that in the area with a very small incentive threshold and a very large safety threshold, there are (logically) a large number of lane changes but no apparent traffic instability, a speed variance close to 0 and a high average velocity. This is something that can seem counter-intuitive. In fact, in this situation lane-changes happen each time there is a slight difference of speed in the lane, and nearly no matter how unsafe it is. Of course, this could contradict real-life experience because in this extreme case the lane-changes are very non-human (they are in particular extremely dangerous).

As expected, the system reaches better (higher) speed averages and better (lower) energy consumption levels for the combinations of parameters leading to low speed variances.

4.4.2 Smoothing the multi-lane system's stop-and-go waves with a single autonomous vehicle

To investigate the possibility of dissipating stop-and-go waves in a **multi-lane** 1-phase traffic system of cars with a **single autonomous car**, we run simulations where we place such a car in the position of the first car in the second lane of a three lane ring road. It first acts like the other cars, and after a certain time $t_{on} \in [0, t_f]$, its acceleration starts following a prescribed control.

Designing the acceleration control law of the autonomous car:

If we consider the autonomous car to be the car initially placed in the position of the first car of the second lane of a ring road, its dynamics, for $t \in [t_{on}, t_f]$, are given by:

$$\begin{cases} \dot{X}_0(t) = V_0(t), \\ \dot{V}_0(t) = u(t, V_0(t)). \end{cases} \qquad \forall t \in [t_{on}, t_f] \tag{4.7}$$

Where $u(t, V_0(t))$ is a chosen control law. Recall that $V_0(t)$ is the velocity of the vehicle that is the vehicle 1 in lane 2 at time $t = 0$.

We could choose $u(t, V_0(t))$ to be the following simple proportional controller:

$$\begin{cases} u(t, V_0(t)) = -k\left(V_0(t) - v_{target}(L_j(t))\right), \\ v_{target}(L_j(t)) = v^*\left(\frac{L_j(t)}{N} - l_0\right). \end{cases}, \quad \forall t \in [t_{on}, t_f] \tag{4.8}$$

With k being a design parameter which can be chosen, such that it represents the inverse of the time necessary for $V_0(t)$ to reach v_{target} at any given time $t \in [t_{on}, t_f]$ for $u(t, V_0(t))$ to be an acceleration, and $v^*\left(\frac{L_j(t)}{N} - l_0\right)$ is the steady-state speed of the system corresponding to the steady-state headway $\frac{L_j(t)}{N} - l_0$. Such that $L_j(t)$ is the length of the lane in which the autonomous car is at the time t, and l_0 is the length of the autonomous car (the vehicle that is the vehicle 1 in lane 2 at time $t = 0$).

However, this ideal very simple control law does not prevent the autonomous car (AV) from crashing into another car. To solve this problem, one could add a safety mechanism where the (AV) would brake if it is too close to its leader. But with such a mechanism, the (AV) would maintain a stop-and-go wave. This is because v_{target} would be too high compared to the current velocity of the cars in front of the (AV). The (AV) would then try to increase its speed until it is too close to the vehicle in front, then it would brake, and then increase its speed again, thus maintaining a stop-and-go wave. Due to this, our control law is instead given by:

$$u(t, V_0(t), \bar{v}_d(t, L_j(t))) = -k\left(V_0(t) - \bar{v}_d(t, L_j(t))\right), \quad \forall t \in [t_{on}, t_f]. \tag{4.9}$$

Where:

$$\begin{cases} \bar{v}_d(t, L_j(t)) = v_{\min} + \left(v^*\left(\frac{L_j(t)}{N} - l_0\right) - v_{\min}\right)\frac{t}{t_{tr}}, & \forall t \in [t_{on}, t_{tr}] \\ \bar{v}_d(t, L_j(t)) = v^*\left(\frac{L_j(t)}{N} - l_0\right), & \forall t \geq t_{tr} \end{cases} \tag{4.10}$$

t_{tr} is the time of transition, and v_{min} is the average velocity at $t = t_{on}$ of the vehicles in the lane where the (AV) is at time $t = t_{on}$. This is only possible because adding the (AV) allows the number of possible steady-states to go from a single steady-state to a continuous range. In control literature, this is referred to as following a continuous path of a steady-state.

In addition to this mechanism, when the (AV) starts to get close to its leading vehicle (the distance between its front and the rear of its leading vehicle is less than $3m$) we change the target speed to the speed of the leading vehicle for safety.

Implementation in MATLAB: The above describes the longitudinal dynamics of the (AV) for $t \geq t_{on}$. We implement this longitudinal control law in MATLAB when introducing the (AV) in the simulations. The **inputs** of this bloc of code are: the time of

activation of the (AV) t_{on}, the design constants k and v_{min}, the time of transition t_{tr}, the length l_0 of the vehicle that is the vehicle 1 in lane 2 at time $t = 0s$, and the lengths of all the lanes of the road. **At each time instant** $t \in [t_{on}, t_f]$, the velocity of the (AV) V_0, its distance to its leading vehicle, and the length of the lane that it is in are measured and injected into the implementation of the equations (4.9)(4.10), while considering the safety mechanism (when the distance between the (AV) and its leading vehicle is smaller than $3m$, change the target speed to the speed of the leading vehicle). The **output** is the acceleration of the (AV) in the lane it is in at this time $t \in [t_{on}, t_f]$.

Designing the lane changing mechanism of the autonomous car:

The (AV) is also capable of changing lane. We allow it to do so following a different lane changing mechanism than the other cars.

The (AV) changes lane when:

(i) The same safety conditions as in (3.15) are satisfied.

(ii) The **speed variance** on a neighboring lane, over the last d_1 seconds, is higher than the speed variance in the original (AV)'s lane, also averaged over the last d_1 seconds. This difference has to be higher than a threshold c_1.

(iii) The (AV) has not been changing lanes in the last d_2 seconds.

We denote the (AV)'s lane at a time t by j_0, the number of vehicles in the lane $j \in \{1, \cdots, 3\}$ at this time t by N_j, and the last time the (AV) changed lane as t_0 ($t_0 = 0$ if the (AV) never changed lane). From this, we have:
- $t > d_1$ and there exists $j \in \{1, \cdots, 3\}$, with $j \neq j_0$, such that:

$$\int_{t-d_1}^{t} \frac{1}{N_j} \sum_{i=1}^{N_j} \left(V_i^j\right)^2(s) - \frac{1}{N_j^2} \left(\sum_{i=1}^{N_j} V_i^j(s) \right)^2 ds > c_1 + \int_{t=d_1}^{t} \frac{1}{N_{j_0}} \sum_{i=1}^{N_{j_0}} \left(V_i^{j_0}\right)^2(s) - \frac{1}{N_{j_0}^2} \left(\sum_{i=1}^{N_{j_0}} V_i^{j_0}(s) \right)^2 ds. \tag{4.11}$$

- $t > d_2$.
- the safety condition (3.15) is satisfied with $i = 1$ and $j = j_0$.

Implementation in MATLAB: The above describes the lateral dynamics of the (AV) for $t \geq t_{on}$. We implement this lateral control law in MATLAB when introducing the (AV) in the simulations. The **inputs** of this bloc of code are: the lane changing safety parameters of the vehicle that is the vehicle 1 in lane 2 for the Treiber et al. model (its safety threshold and cooldown time), the constants d_1, d_2, and c_1. **At each time instant** $t \in [t_{on}, t_f]$, the speed variance over the last d_1 seconds in the lane that the (AV) is in at this time t and in its left and right neighboring lanes (if there is a left or right neighboring lane) are measured, and if there is no vehicle directly next to the (AV) in the neighboring lane(s), we check the conditions (i)(ii)(iii) stated just above to decide on if the (AV) changes lane or not. The **output** is the decision "the (AV) does not just lane", or the new lane of the (AV) if it should be changing lane.

Validating the solution with simulations:

We perform the same simulations as in the Subsection 4.4.1, with the same parameters as in Table 4.1. The only difference, is that starting from a time t_{on}, the car which was initially in the position of the first car of the second lane of the ring road becomes an autonomous car which follows the behavior we just described and has the parameters given in Table 4.2.

Parameter	Value	What it represents
t_{on}	100	Time of activation of the (AV) $[s]$
k	1	Design parameter in the (AV)'s control law $[s^{-1}]$
c_1	0.5	Speed variance threshold for the (AV)'s lane change $[m^2/s^2]$
d_1	10	Time to average speed variance for the (AV)'s lane change $[s]$
d_2	10	(AV)'s cooldown time after a lane change $[s]$
t_{tr}	$0.4t_f$	Time of transition for the (AV)'s control law $[s]$

Table 4.2 – Summary of the parameters of the (AV)

The values of d_2 and d_1 are chosen a bit high, to avoid that the (AV) changes lane constantly and study its performance with a minimum of lane changes. For the parameters k, c_1, and t_{on}, we choose to have a rapid (AV) ($k = 1s^{-1}$), which is very sensitive to speed variance ($c_1 = 0.5m^2/s^2$), activate it early enough to be able to observe its impact on the traffic ($t_{on} = 100s$), and have a time of transition equal to $0.4t_f$ (not too large and not too small).
The following are the obtained plots for the speed variance (averaged), consumed energy (averaged), speed average (averaged), and number of lane changes, over the last $300s$, with respect to the different lane changing parameters, in the presence of the (AV) in the traffic.

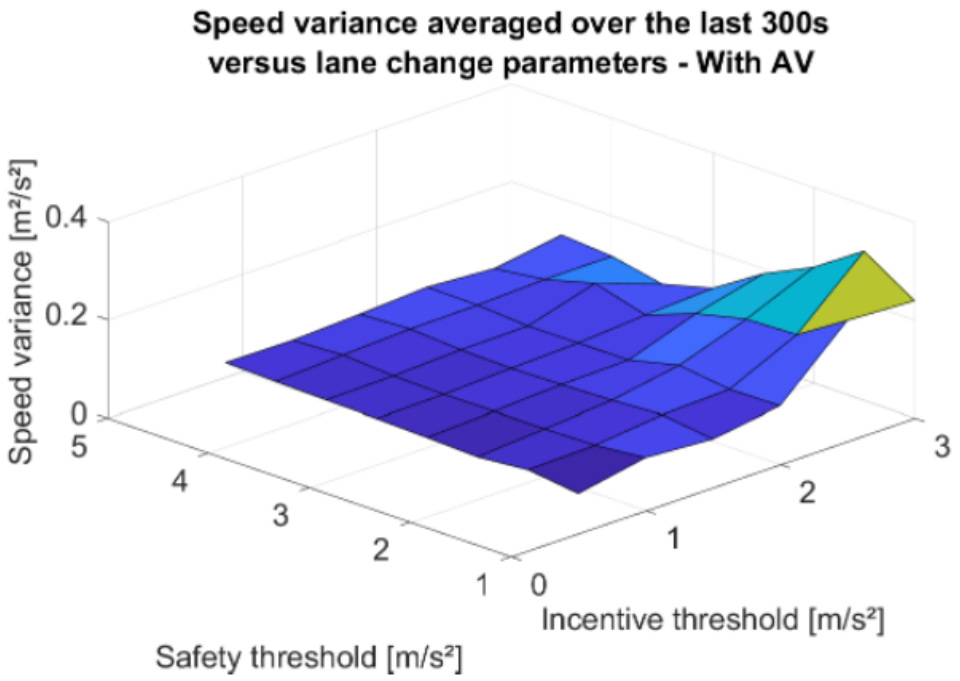

Figure 4.6 – The speed variance averaged over the last 300s with respect to the different lane changing parameters in the presence of (AV)

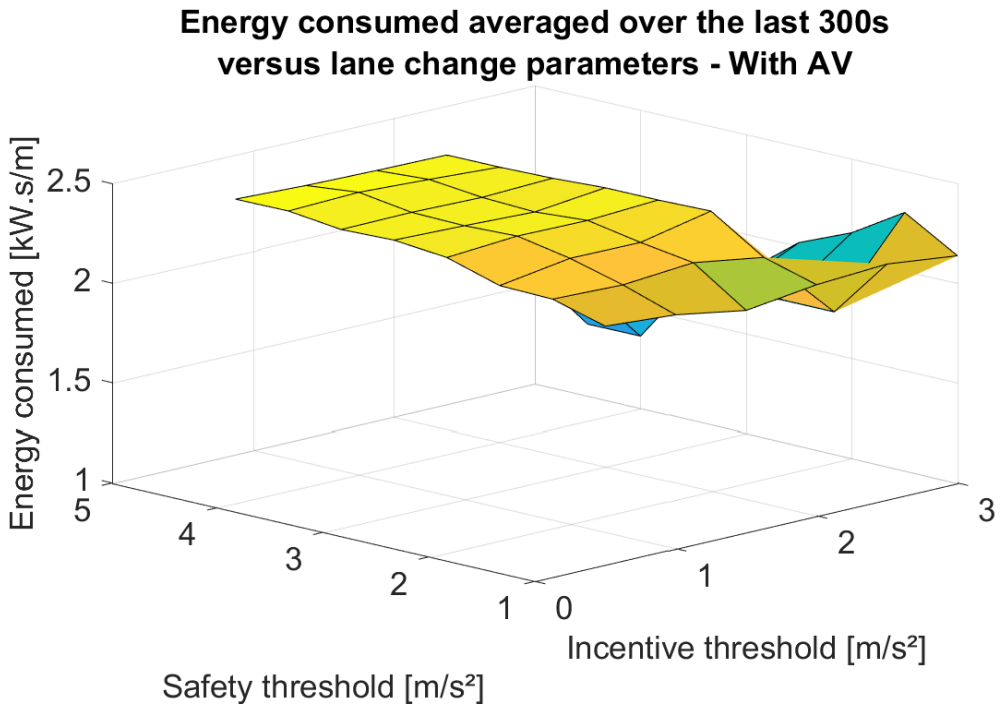

Figure 4.7 – The energy consumption averaged over the last 300s with respect to the different lane changing parameters in the presence of (AV)

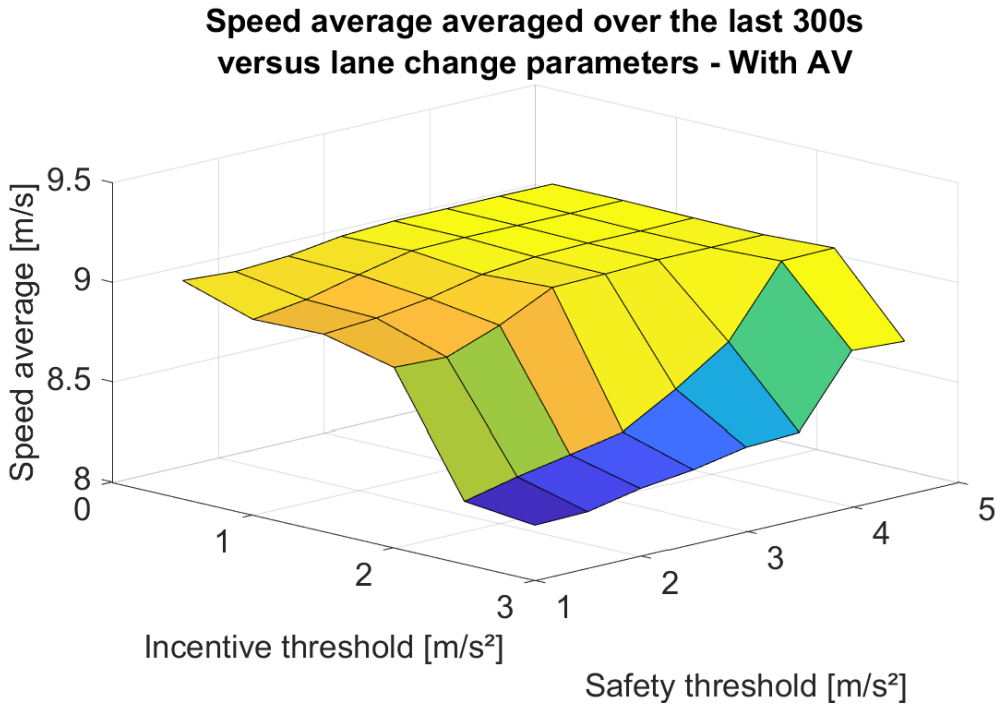

Figure 4.8 – The speed average averaged over the last 300s with respect to the different lane changing parameters in the presence of (AV)

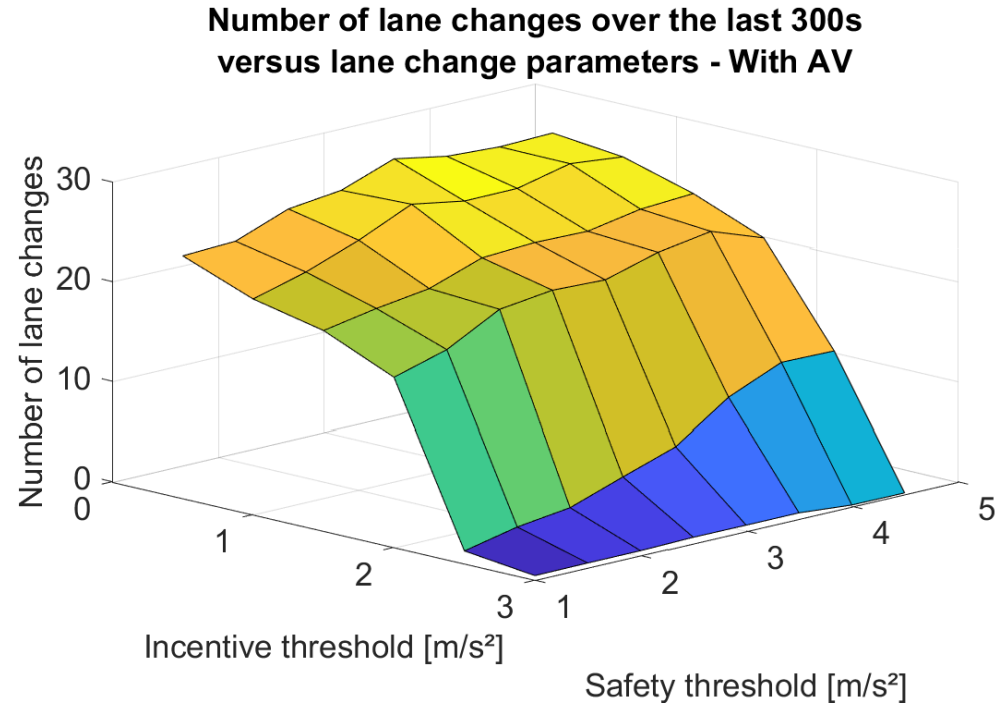

Figure 4.9 – The number of lane changes over the last 300s with respect to the different lane changing parameters in the presence of (AV)

Discussions:

We can see that the plots obtained in the presence of the (AV) follow roughly the same trends as the plots obtained in the absence of the (AV) (Section 4.4.1), but the speed variance is cut to 10% of its value in the absence of the (AV) (reduction of 90%), and the energy consumption is reduced by 75% in the presence of the (AV). We also observe some gain in the speed average and a small reduction of the number of lane changes, in the presence of the (AV). **The dissipation of stop-and-go waves is effective over all the range of the incentive and safety threshold parameters. This control is robust to the change in lane changing parameters. The speed variance never surpasses** $0.4m^2/s^2$ **for all the range of incentive and safety thresholds in the presence of the (AV), while it reaches** $4m^2/s^2$ **in the absence of the (AV)**. In particular, for a safety threshold of $3m/s^2$ and an incentive threshold of $3m/s^2$ we can clearly see, from Figure 4.10 and Figure 4.11, how the instantaneous speed variance (given by (3.26)) rapidly converges to 0 in the three lanes after the activation of the (AV), while staying high in the three lanes in the absence of the (AV).

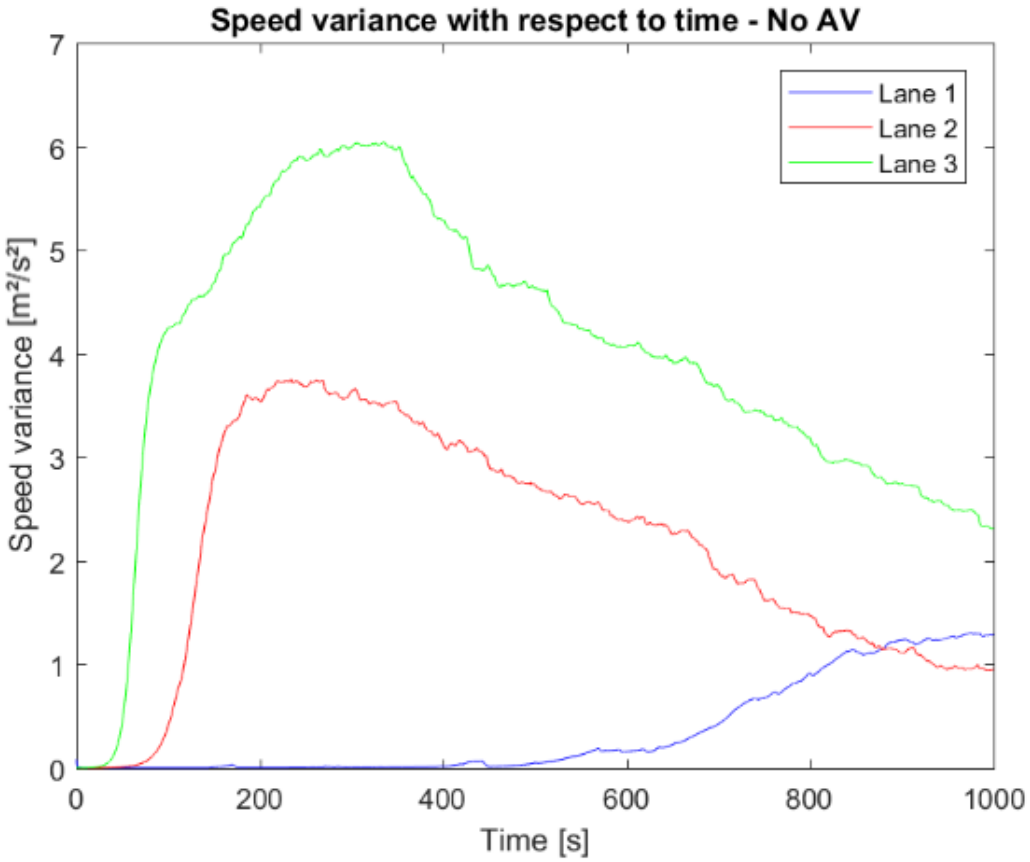

Figure 4.10 – The variation of speed variance with respect to time in the three lanes in the absence of the (AV) for an incentive threshold of $3m/s^2$ and a safety threshold of $3m/s^2$

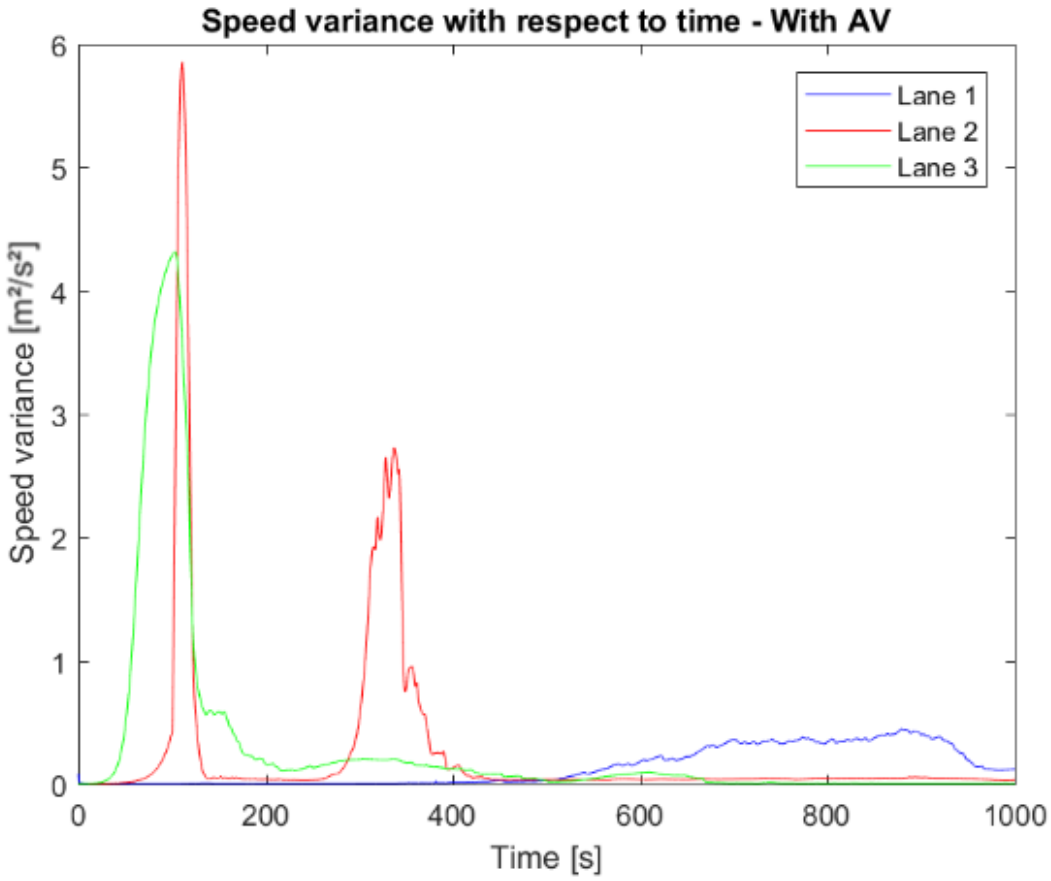

Figure 4.11 – The variation of speed variance with respect to time in the three lanes in the presence of the (AV) for an incentive threshold of $3m/s^2$ and a safety threshold of $3m/s^2$

Recall that $t_{on} = 100s$, which explains that the speed variance quickly drops just after $t = 100s$ in the presence of the (AV). As expected, we see that the (AV) is stabilizing mostly one lane that reaches an equilibrium flow very rapidly, but despite the very weak coupling of the lanes (due to the very small number of lane changes for this couple of incentive and safety thresholds, see Figure 4.5), it is still enough to roughly dissipate the waves that form in the other lanes. On the other hand, when there is no (AV), the speed variance remains high.

4.5 Multi-lane 2-phase traffic flow of collaborative cars and aggressive cars

In this section, we investigate, numerically, if there are similarities between single-lane and multi-lane 2-phase traffic systems where coexist collaborative cars and aggressive cars, which would suggest a possibly easy generalization of the single-lane results of [20] to multi-lane systems.

In a 2-phase traffic, Λ_i^j either equals a certain value $\Lambda^1 = (a_1^{(1)}, a_1^{(2)}, a_1^{(3)})$ or a certain value $\Lambda^2 = (a_2^{(1)}, a_2^{(2)}, a_2^{(3)})$, and the same goes for Δ_i^j, which either equals a certain value $\Delta^1 = (a_1^{(2)})^2 - (a_1^{(3)})^2 - 2(a_1^{(1)})$ or a certain value $\Delta^2 = (a_2^{(2)})^2 - (a_2^{(3)})^2 - 2(a_2^{(1)})$, $\forall i \in [1, N] \cap \mathbb{N}$ and $\forall j \in [1, J] \cap \mathbb{N}$. The number of vehicles characterized by Δ^1 and Λ^1 is denoted by n_1, while the number of vehicles characterized by Δ^2 and Λ^2 is denoted by n_2. In the following, we consider the collaborative cars to be the cars characterized by Λ^1 and Δ^1, and the aggressive cars to be the ones characterized by Λ^2 and Δ^2. The penetration rate of the collaborative cars is considered to be $p = \frac{n_1}{n_1+n_2}$, and the total number of cars per lane is $N = n_1 + n_2$.

4.5.1 A stabilizing proportion of collaborative cars for the multi-lane system

A natural question that may cross our minds is: if there exists a critical penetration rate for multi-lane systems, can it be the same critical penetration rate as for the single-lane versions of these systems?

To answer this question, we perform the same simulations as in the previous section but with different values for the length of the road and the vehicles' parameters. In particular, the aggressive cars all have the exact same parameters as in Table 4.1. The total number of cars (aggressive+collaborative) in each lane is still $N = 24 = n_1 + n_2$, the number of lanes, time length of the simulations, and the time step δt of the simulations, are also the same as in table 4.1. But the collaborative cars differ in the weight of the Bando model, and we have that: $\alpha_i^j = 4, \forall i \in [1, n_1] \cap \mathbb{N}, \forall j \in \{1, 2, 3\}$. Thus, the instability of the aggressive cars only comes from a higher sensitivity to the velocity preference rather than the follow-the-leader behavior. Note that both of the two populations of cars are present since $t = 0s$ of all our simulations.

The critical penetration rate for these exact same parameters in the case of $J = 1$, was found, in [20], to be $\tau_0 = 0.881$. To see if this same penetration rate can also be the "critical" penetration rate in the multi-lane version of the system, we perform two identical batches of simulations (as described above) that just differ in the penetration rate of the collaborative cars. The configuration of each lane is the same as in the one lane of the simulations of [20], except that the vehicles can change lanes. In the Batch 1 of simulations, we have a penetration rate p that is bigger than 0.881, and in the Batch 2 of simulations, we have a penetration rate p that is smaller than 0.881. The length of the road, the number of cars of each population, the total number of cars per lane, and the penetration rate in the two batches of simulations are summarized in the two following tables.

Parameter	Value	What it represents
L	$2\pi 39.7$	Length of the road $[m]$
N	24	Total number of cars per lane
n_1	22	Number of collaborative cars per lane
n_2	2	Number of aggressive cars per lane
p	0.917	Penetration rate of the collaborative cars

Table 4.3 – Summary of the Batch 1 of simulations

Parameter	Value	What it represents
L	$2\pi 39.7$	Length of the road $[m]$
N	24	Total number of cars per lane
n_1	20	Number of collaborative cars per lane
n_2	4	Number of aggressive cars per lane
p	0.833	Penetration rate of the collaborative cars

Table 4.4 – Summary of the Batch 2 of simulations

Let's first recall the simulation results of [20], for a penetration rate of $p = 0.802$ and a penetration rate of $p = 0.882$, in the case of a single-lane road of length $5200m$ with a total number of 500 cars $\left(\frac{5200}{500} = 10.4m\right)$:

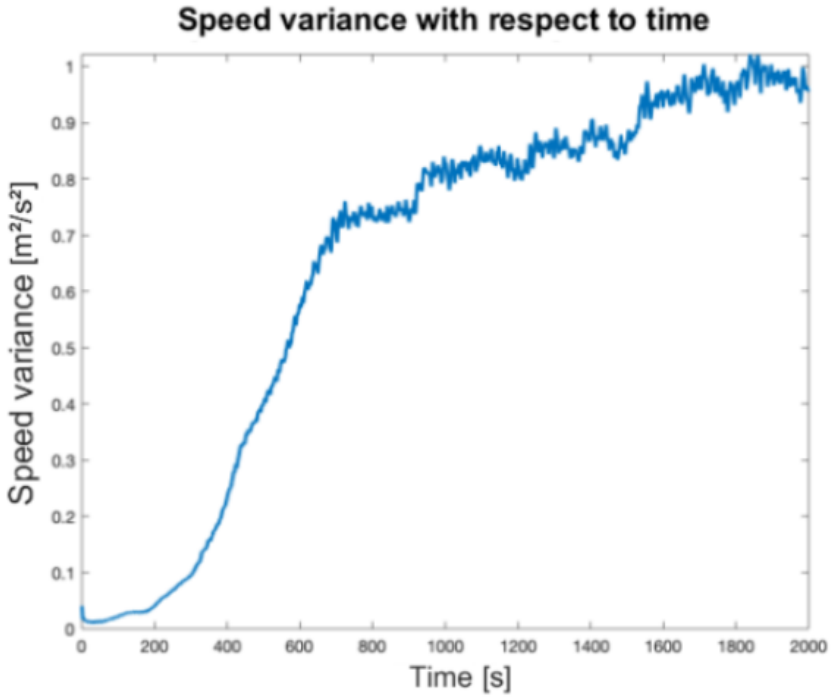

Figure 4.12 – The variation of speed variance with respect to time in the case of a single-lane road with penetration rate p=0.802 (credit: [20])

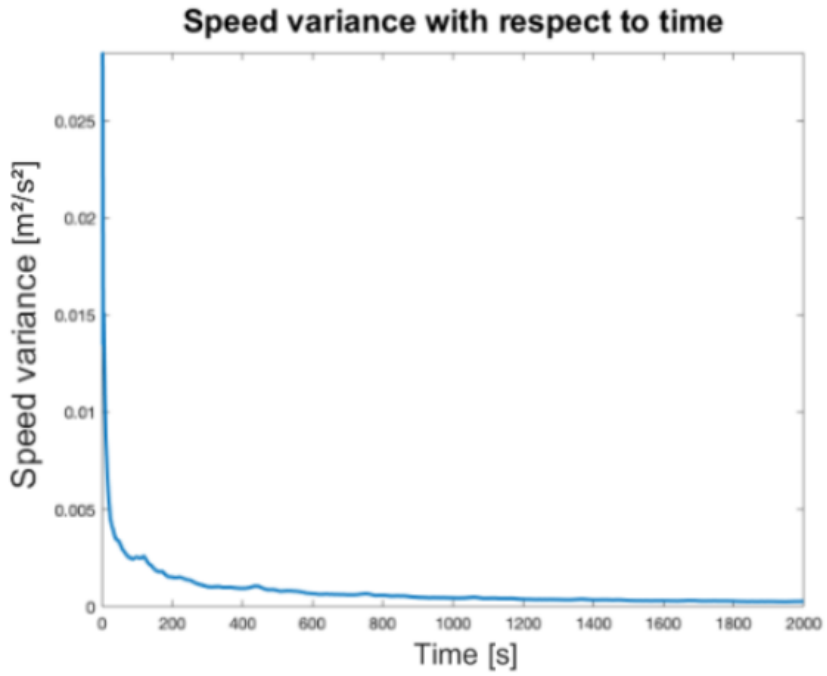

Figure 4.13 – The variation of speed variance with respect to time in the case of a single-lane road with penetration rate p=0.882 (credit: [20])

Note that for the multi-lane simulations, we did not consider such a large number of cars (500 cars) as the computation time would be huge for such a number of cars when there are lane changes. But notice that we keep $\frac{L}{N} = \frac{2\pi 39.7}{24} = 10.4m$ in the two batches of our simulations, which means that we have the same Δ^1 and Δ^2 as in [20], i.e. $\Delta^1 = 7.28$ and $\Delta^2 = -0.84$, with $|\Delta^2| < |\Delta^1|$, which finally gives us the same (supposed) critical penetration rate. Now, let's see the results obtained in our three lanes simulations:

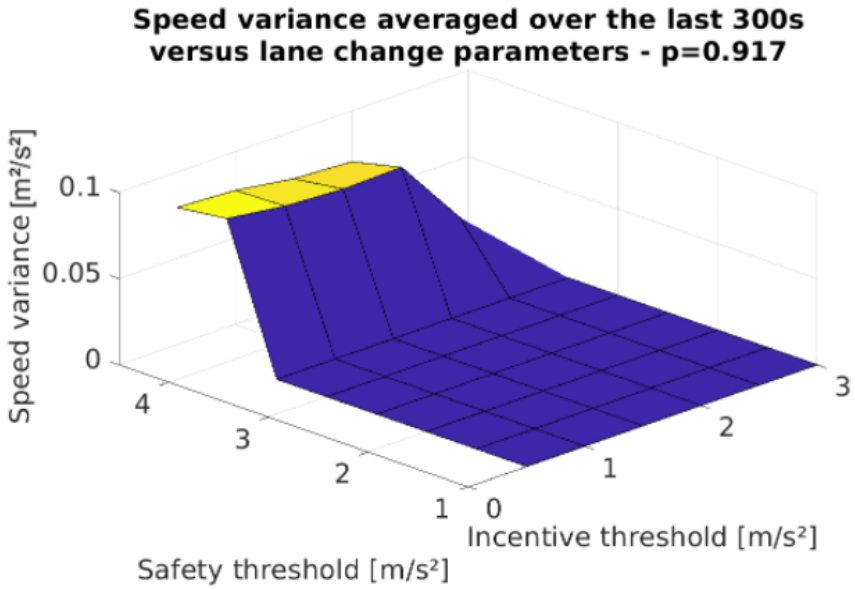

Figure 4.14 – The speed variance averaged over the last 300s with respect to the different lane changing parameters for $p = 0.917$

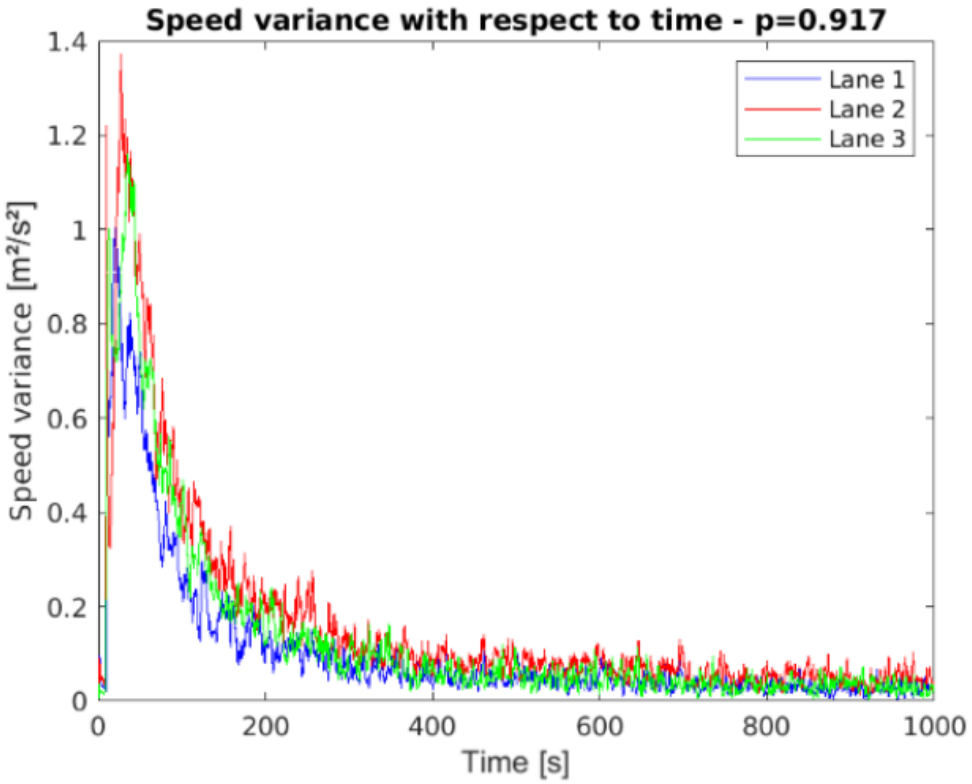

Figure 4.15 – The variation of speed variance with respect to time for $p = 0.917$, an incentive threshold of $2.5m/s^2$, and a safety threshold of $4m/s^2$

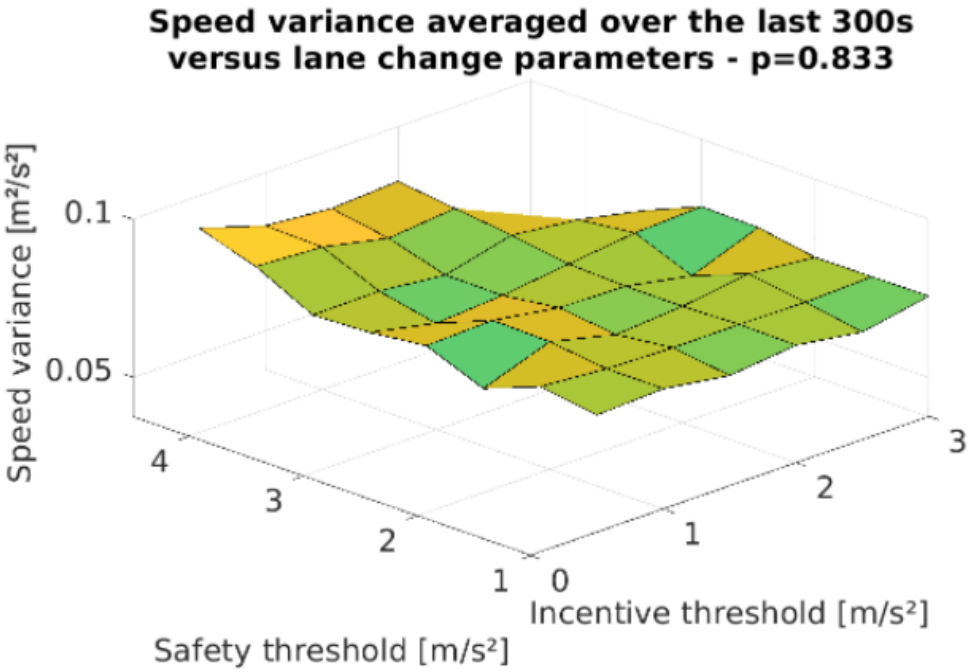

Figure 4.16 – The speed variance averaged over the last 300s with respect to the different lane changing parameters for $p = 0.833$

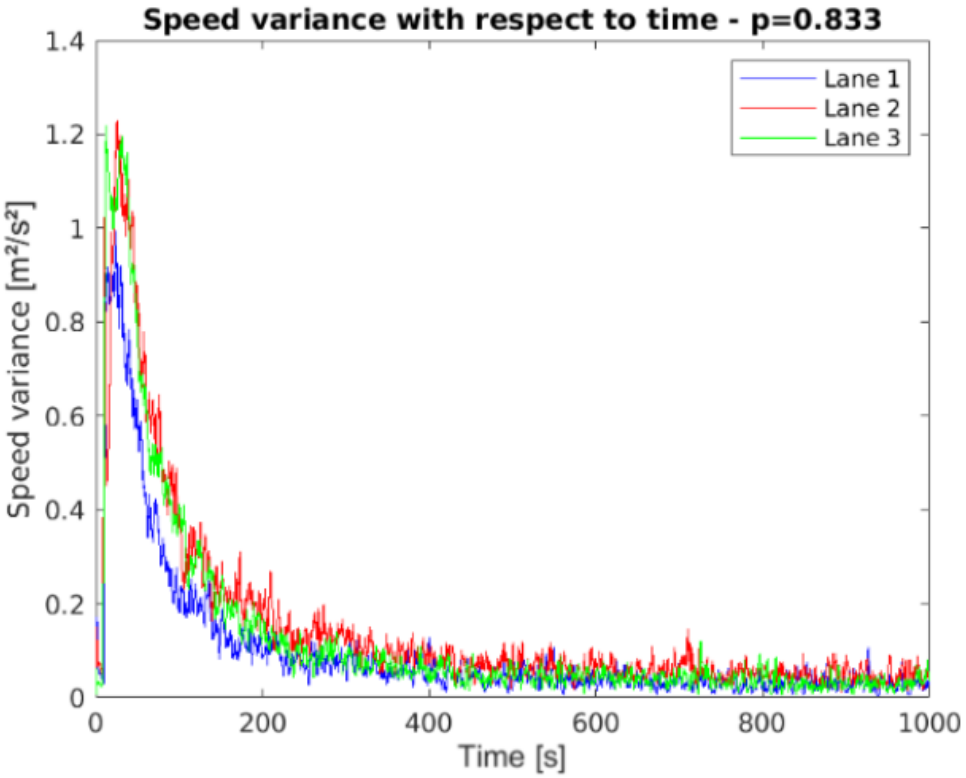

Figure 4.17 – The variation of speed variance with respect to time for $p = 0.833$, an incentive threshold of $2.5m/s^2$, and a safety threshold of $4m/s^2$

Discussions:

We can observe that both $p = 0.917$ (bigger than 0.881) and $p = 0.833$ (smaller than 0.881) seem to stabilize the multi-lane system's steady-state and make the system converge to a state of zero speed variance. Indeed, $p = 0.917$ gives a slightly better performance than $p = 0.833$ over a certain range of lane changing parameters, but this only suggests that the same tendency shown in Figure 4.1 for single-lane systems "may" still hold for multi-lane systems. Therefore, the "critical" penetration rate, which is the penetration rate just before which the system diverges and just after which it converges to the zero speed variance state, seems to not be the same as the one for the single-lane version of the system. **These observations suggest that the critical penetration rate of collaborative cars in multi-lane systems, if it exists; which means: if it is unique and that indeed the same tendency of Figure 4.1 still holds in multi-lane systems (because we know from Section 4.4 that $p = 0$ leads to stop-and-go waves); is smaller than the critical penetration rate for the single-lane version of the system**.

4.5.2 A minimal stabilizing proportion of collaborative cars for the multi-lane system

A single autonomous vehicle following a prescribed acceleration law was shown to be sufficient to dissipate stop-and-go waves in a 1-phase single-lane system with N aggressive cars (penetration rate equal to $\frac{1}{N}$). Similarly, we have shown, in Section 4.4, that a single autonomous vehicle following an appropriate acceleration law can be effective for the dissipation of stop-and-go waves in a 1-phase system with J many lanes and N number of aggressive cars per lane (penetration rate equal to $\frac{1}{J\times N}$). We could ask the following question: if the critical penetration rate of collaborative cars for the dissipation of stop-and-go waves in a given 2-phase single-lane system of collaborative and aggressive cars is τ_0, and we have a multi-lane road with J many lanes each containing this same 2-phase system which requires a critical penetration rate τ_0 to dissipate stop-and-go waves, is it possible in this multi-lane system to dissipate stop-and-go waves with a penetration rate of collaborative cars that equals $\frac{\tau_0}{J}$ instead of τ_0?

To answer this question, we perform two other batches of the same simulations as in Subsection 4.5.1, but with a different number of cars for each of the two populations in each lane, and a different road length. The changed parameters are summarized in the two tables below.

Parameter	Value	What it represents
L	$2\pi 44.69$	Length of the road $[m]$
N	27	Total number of cars per lane
n_1	8	Number of collaborative cars per lane
n_2	19	Number of aggressive cars per lane
p	0.296	Penetration rate of the collaborative cars

Table 4.5 – Summary of the Batch 3 of simulations

Parameter	Value	What it represents
L	$2\pi 44.69$	Length of the road $[m]$
N	27	Total number of cars per lane
n_1	6	Number of collaborative cars per lane
n_2	21	Number of aggressive cars per lane
p	0.222	Penetration rate of the collaborative cars

Table 4.6 – Summary of the Batch 4 of simulations

Explanation: For a single-lane system with $N = 27$ and $p = 0.882$, we have that $n_1 = 23.814$, we take $n_1 = 24$ and $n_2 = 3$. If we distribute the 24 collaborative cars on three lanes, such that $N = 27$ per lane, we would have that $n_1 = 8$ and $n_2 = 19$ per lane, which gives $p = 0.296$. In the Batch 3 of the simulation, we have p=0.296, and in the Batch 4 we have a lower penetration rate. The total number of cars per lane is changed from 24 to 27 in these simulations, just to have a necessary total number of 24 collaborative cars on the road, which is a number that is dividable by 3 (the three lanes). Notice that we still keep $\frac{L}{N} = \frac{2\pi 44.69}{27} = 10.4m$ in Batch 3 and Batch 4.

The following are the obtained plots.

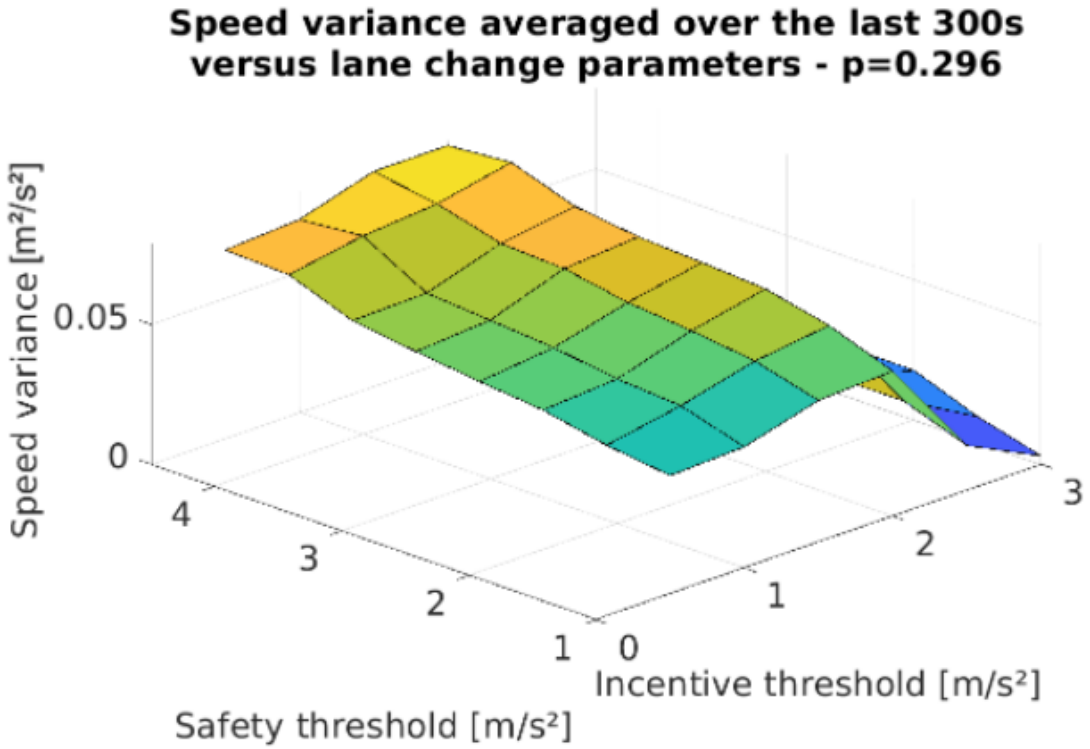

Figure 4.18 – The speed variance averaged over the last 300s with respect to the different lane changing parameters for $p = 0.296$

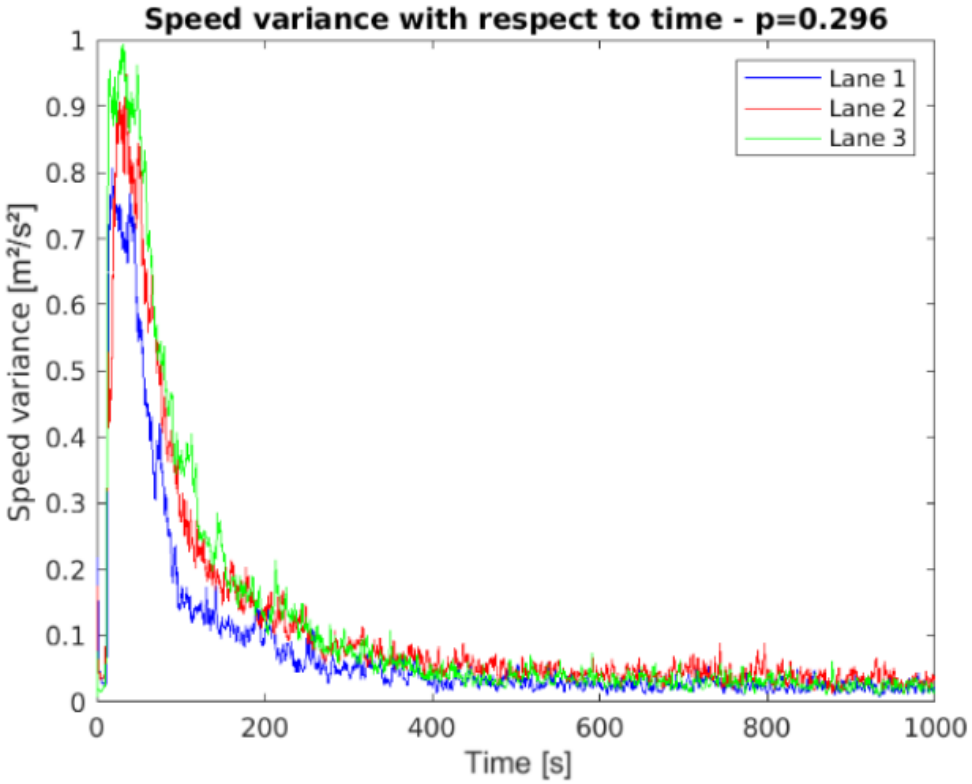

Figure 4.19 – The variation of speed variance with respect to time for $p = 0.296$, an incentive threshold of $2.5m/s^2$, and a safety threshold of $4m/s^2$

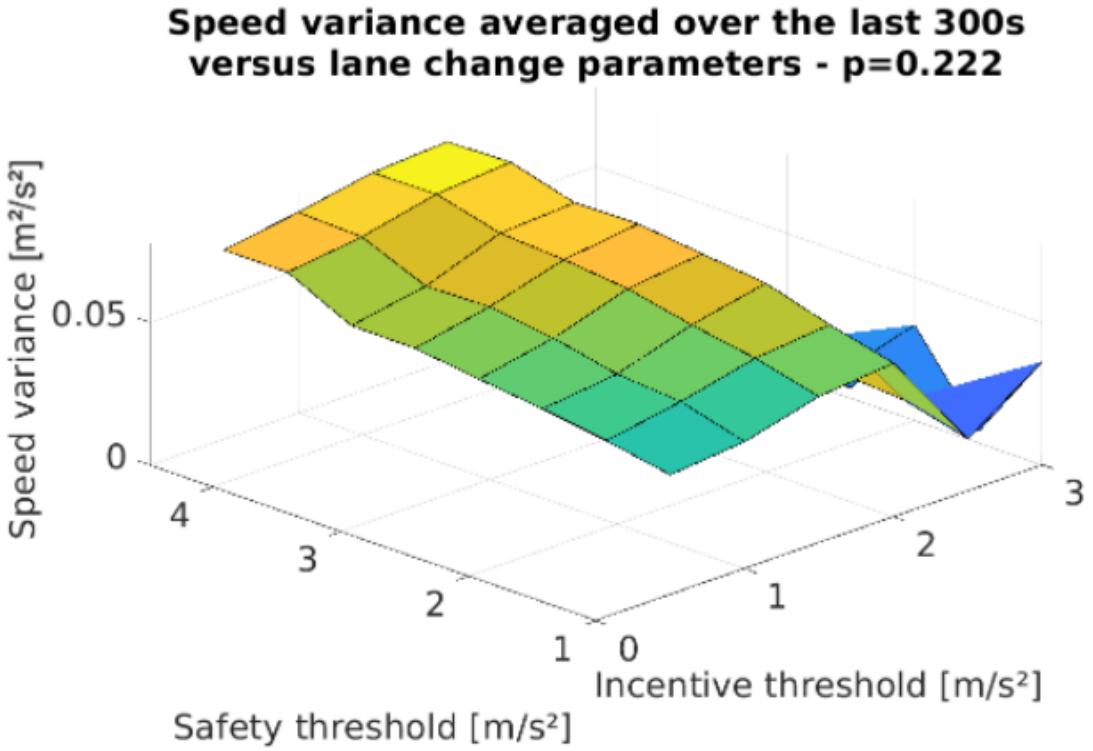

Figure 4.20 – The speed variance averaged over the last 300s with respect to the different lane changing parameters for $p = 0.222$

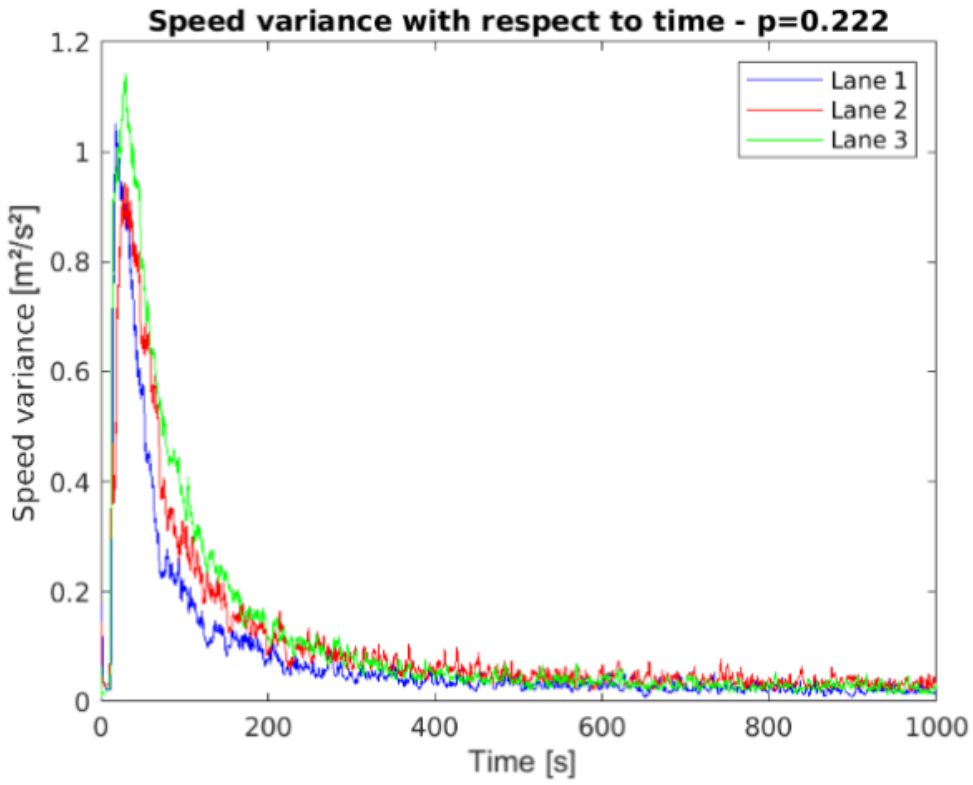

Figure 4.21 – The variation of speed variance with respect to time for $p = 0.222$, an incentive threshold of $2.5m/s^2$, and a safety threshold of $4m/s^2$

Discussions:

We can see that for both $p = 0.296$ and $p = 0.222$, the multi-lane system's speed variance averaged over the last $300s$ is very close to zero for all the range of incentive and safety thresholds, and the present proportion of collaborative cars seems to be able to dissipate stop-and-go waves and make the system converge to a state of zero speed variance. **The answer to the question asked in the beginning of this subsection is: Yes it is possible, and it is even possible with a lower penetration rate than that (we do not know if it is always the case, but we now know that there exists traffic scenarios and lane-changing parameters where it is possible)**.

We explain these results by the fact that in a multi-lane system, the dynamics in the different lanes are coupled, and a single vehicle can have a global effect on the multi-lane road traffic by changing lane.

4.6 Multi-lane 2-phase traffic flow of cars and trucks

In this section, we investigate, numerically, the effect that can have trucks on multi-lane traffic flows when coexisting with aggressive cars, while also studying the effect of lane changing parameters on such systems (**incentive** and **cooldown time** thresholds). We recall that the results of [20] are still valid when studying trucks (heavy weight vehicles, longer than cars) in a single-lane system.

In a 2-phase traffic, Λ_i^j either equals a certain value $\Lambda^1 = (a_1^{(1)}, a_1^{(2)}, a_1^{(3)})$ or a certain value $\Lambda^2 = (a_2^{(1)}, a_2^{(2)}, a_2^{(3)})$, and the same goes for Δ_i^j, which either equals a certain value $\Delta^1 = (a_1^{(2)})^2 - (a_1^{(3)})^2 - 2(a_1^{(1)})$ or a certain value $\Delta^2 = (a_2^{(2)})^2 - (a_2^{(3)})^2 - 2(a_2^{(1)})$, $\forall i \in [1, N] \cap \mathbb{N}$ and $\forall j \in [1, J] \cap \mathbb{N}$. The number of vehicles characterized by Δ^1 and Λ^1 is denoted by n_1, while the number of vehicles characterized by Δ^2 and Λ^2 is denoted by n_2. In the following, we consider the trucks to be the vehicles characterized by Λ^1 and Δ^1, and the aggressive cars to be the ones characterized by Λ^2 and Δ^2. The penetration rate of the trucks is considered to be $p = \frac{n_1}{n_1+n_2}$, and the total number of cars per lane is $N = n_1 + n_2$.

Before being able to start the simulations, we determine the critical penetration rate of the trucks for a single-lane version of the system, using the results of [20], and we know from the previous section that it can give some indications about the minimum number of the vehicles of population 1 (the trucks) in the multi-lane system.

4.6.1 The critical penetration rate of trucks for the single-lane version of the system

We recall that we have $\forall t \in [0, t_f]$ and $\forall i \in [1, N] \cap \mathbb{N}$ and $\forall j \in [1, J] \cap \mathbb{N}$ with $J = 1$:

$$f_i^j(h_i^j(t), \dot{h}_i^j(t), V_i^j(t)) = \alpha_i^j \left(V_{\max}^{i,j} \left(\frac{\tanh\left(\frac{h_i^j(t)}{d_0^{i,j}} - 2\right) + \tanh(2)}{1 + \tanh(2)} \right) - V_i^j(t) \right) + \beta_i^j \left(\frac{\dot{h}_i^j(t)}{(h_i^j(t))^2} \right). \tag{4.12}$$

We consider a 1-phase single-lane (of length L) traffic such that $d_0^{i,j} = d_0 = 2.5m$, $V_{\max}^{i,j} = V_{max}$, $l_i^j = l_v$, $\alpha_i^j = \alpha$, and $\beta_i^j = \beta$, $\forall i \in [1, N] \cap \mathbb{N}$ and $\forall j \in [1, J] \cap \mathbb{N}$, with $J = 1$. We then have $\forall t \in [0, t_f]$ and $\forall i \in [1, N] \cap \mathbb{N}$ and $\forall j \in [1, J] \cap \mathbb{N}$ with $J = 1$:

$$\left.\frac{\partial f_i^j}{\partial x}\right|_{(h_i^j(t), \dot{h}_i^j(t), V_i^j(t))} = \frac{\left(\frac{1}{d_0}\right) \alpha V_{\max} \left(1 - \tanh^2\left(\frac{h_i^j(t)}{d_0} - 2\right)\right)}{1 + \tanh(2)} - 2\beta \frac{\dot{h}_i^j(t)}{(h_i^j(t))^3}, \tag{4.13}$$

$$\left.\frac{\partial f_i^j}{\partial y}\right|_{(h_i^j(t), \dot{h}_i^j(t), V_i^j(t))} = \frac{\beta}{(h_i^j(t))^2}, \tag{4.14}$$

$$\left.\frac{\partial f_i^j}{\partial z}\right|_{(h_i^j(t),\dot{h}_i^j(t),V_i^j(t))} = -\alpha. \tag{4.15}$$

And because it is a 1-phase traffic, at the equilibrium flow we have:

$$\bar{h}_i^j = \bar{h}, \quad \forall i \in [1, N] \cap \mathbb{N}, \forall j \in [1, J] \cap \mathbb{N}, J = 1. \tag{4.16}$$

And:

$$l_v N + N\bar{h} = L, \tag{4.17}$$

$$\bar{h} = \frac{L - l_v N}{N}. \tag{4.18}$$

Just to demonstrate how Δ_2 was calculated in [20], we take $L = 2\pi 39.7$ and $N = 24$, which gives $\frac{L}{N} = 10.4m$.

For the case where the 1-phase single-lane traffic is composed of only aggressive cars, we take $l_v = 4.5m$, which gives $\bar{h} = 5.893m$. And we take $\alpha = 0.5$, $\beta = 20$, and $V_{\max} = 9.25m/s$, which gives $\forall t \in [0, t_f]$ and $\forall i \in [1, N] \cap \mathbb{N}$ and $\forall j \in [1, J] \cap \mathbb{N}$ with $J = 1$:

$$\begin{aligned}
\left.\frac{\partial f_i^j}{\partial x}\right|_{(\bar{h},0,\bar{v})} &= 0.832, \\
\left.\frac{\partial f_i^j}{\partial y}\right|_{(\bar{h},0,\bar{v})} &= 0.576, \\
\left.\frac{\partial f_i^j}{\partial z}\right|_{(\bar{h},0,\bar{v})} &= -0.5.
\end{aligned} \tag{4.19}$$

$$\begin{aligned}
a_2^{(1)} &= 0.832, \\
a_2^{(2)} &= 1.076, \\
a_2^{(3)} &= 0.576, \\
\Delta^2 &= -0.838.
\end{aligned} \tag{4.20}$$

For the case where the 1-phase single-lane traffic is composed of only trucks, we take $l_v = 5.5m$, which gives $\bar{h} = 4.893m$. And we take $\alpha = 4$, $\beta = 20$, and $V_{\max} = 8.33m/s$

(10% less than $V_{\max}$ of cars), which gives $\forall t \in [0, t_f]$ and $\forall i \in [1, N] \cap \mathbb{N}$ and $\forall j \in [1, J] \cap \mathbb{N}$ with $J = 1$:

$$\begin{aligned} \left.\frac{\partial f_i^j}{\partial x}\right|_{(\bar{h},0,\bar{v})} &= 6.772, \\ \left.\frac{\partial f_i^j}{\partial y}\right|_{(\bar{h},0,\bar{v})} &= 0.835, \\ \left.\frac{\partial f_i^j}{\partial z}\right|_{(\bar{h},0,\bar{v})} &= -4. \end{aligned} \tag{4.21}$$

$$\begin{aligned} a_1^{(1)} &= 6.772, \\ a_1^{(2)} &= 4.835, \\ a_1^{(3)} &= 0.835, \\ \Delta^1 &= 9.136. \end{aligned} \tag{4.22}$$

Which then gives:

$$\begin{aligned} H_1(y) &= \log\left(\frac{45.860 + 0.697y}{45.860 + 9.833y + y^2}\right), \\ H_2(y) &= \log\left(\frac{0.692 + 0.332y}{0.692 - 0.506y + y^2}\right), \\ \Gamma^2 &= 0.384 \in \left]0, -\Delta^2\right[. \end{aligned} \tag{4.23}$$

And we have:

$$\tau_0 = 1 - \left(1 + \max\left\{-\frac{H_2(y)}{H_1(y)}; y \in \left]0, \Gamma^2\right]\right\}\right)^{-1}. \tag{4.24}$$

To compute $\max\left\{-\frac{H_2(y)}{H_1(y)}; y \in \left]0, \Gamma^2\right]\right\}$ we use a simple MATLAB script:

```
syms y
m = -log10((0.692+0.332*y)/(0.692-0.506*y+y^2))/log10((45.86+0.697*y)/
(45.86+9.833*y+y^2));
z = 0.001:0.001:0.384;
m_values = subs(m, y, z);
[maxX, maxidx] = max(m_values);
ymax = z(maxidx)
max_m = maxX %the maximum
```

We get:

$$\begin{aligned} \tau_0 &= 1 - \frac{1}{1+6.072}, \\ \tau_0 &= 0.859. \end{aligned} \tag{4.25}$$

Discussions:

We notice that the critical penetration rate for trucks in the 2-phase single-lane traffic flow of trucks and aggressive cars is slightly smaller than the critical penetration rate of collaborative cars in the 2-phase single-lane traffic flow of collaborative and aggressive cars (which was 0.881, for $\frac{L}{N} = 10.4m$). **But as expected, it is still a large value, which means that this is not an efficient strategy to dissipate stop-and-go waves**.

4.6.2 The effect of different incentive thresholds and different trucks' cooldown times

In this subsection, to study the effect of the **incentive** and **cooldown time** thresholds on the multi-lane 2-phase traffic flow of trucks and cars, we perform simulations where we consider that all the vehicles on the road have the same value of the safety threshold $2m/s^2$, and we vary the value of the incentive threshold with all the vehicles on the road having the same incentive threshold value each time. We also consider that the trucks and the cars do not have the same cooldown times. We can observe in real life that trucks wait longer before changing lane again.

All the vehicles on the road have the same parameters as in Table 4.1, except for the trucks, which differ in the parameters summarized in the table below. Such that $\forall i \in [1, n_1] \cap \mathbb{N}$ and $\forall j \in [1, J] \cap \mathbb{N}$ we have:

Parameter	Value	What it represents
α_i^j	4	Weight of the Bando model for a truck
β_i^j	20	Weight of the FTL model for a truck
l_i^j	5.5	Length of a truck $[m]$
$Vmax^{i,j}$	8.33	Maximal preferred speed for a truck $[m/s]$
$mass_i^j$	2400	Mass of a truck $[kg]$
τ_i^j	Varies	Cooldown time of lane change for a truck $[s]$

Table 4.7 – Summary of the trucks' parameters

We continue to take $t_f = 1000s$, $\delta t = 0.02s$, and $J = 3$, and we consider the traffic configuration summarized in the table below:

Parameter	Value	What it represents
L	$2\pi 39.7$	Length of the road $[m]$
N	24	Total number of cars per lane
n_1	21	Number of trucks per lane
n_2	3	Number of aggressive cars per lane
p	0.875	Penetration rate of the trucks

Table 4.8 – Summary of the traffic configuration for $p = 0.875$

We take the set of values for the incentive threshold to be $\{0.5, 1, 1.5, 2, 2.5, 3\}[m/s^2]$ (as in the previous sections), and we take the set of truck cooldown time values to be $\{7, 8, 9, 10, 11, 12, 13, 14\}[s]$. For each couple of these incentive and trucks' cooldown time thresholds, and a fixed safety threshold of value $2m/s^2$, we run 100 simulations with random initial states of the vehicles. These vehicles start around half their maximal velocity preference, and the maximal velocity preference of each vehicle follows a normal distribution of mean $8.33m/s$ for the trucks, and mean $9.25m/s$ for the cars, and a standard deviation of $1m/s$ for both of trucks and cars. All the vehicles were initially located within $1m$ from their steady-state location (which corresponds to a uniform spacing). For each one of the 100 simulations, the speed, the lane, and the power consumed, at each time step for each vehicle, were saved and then averaged over the 100 simulations, to calculate the speed variance, speed average, number of lane changes, and the energy consumed, for each vehicle. Which were then averaged over all the vehicles in the three lanes and then only the averages over the last $300s$ were kept (except for the number of lane changes: we keep the total number of lane changes on the road over the last 300s, it is not an average).

The following are the obtained plots for the speed variance (averaged), consumed energy (averaged), speed average (averaged), and number of lane changes, over the last $300s$, with respect to the different lane changing parameters.

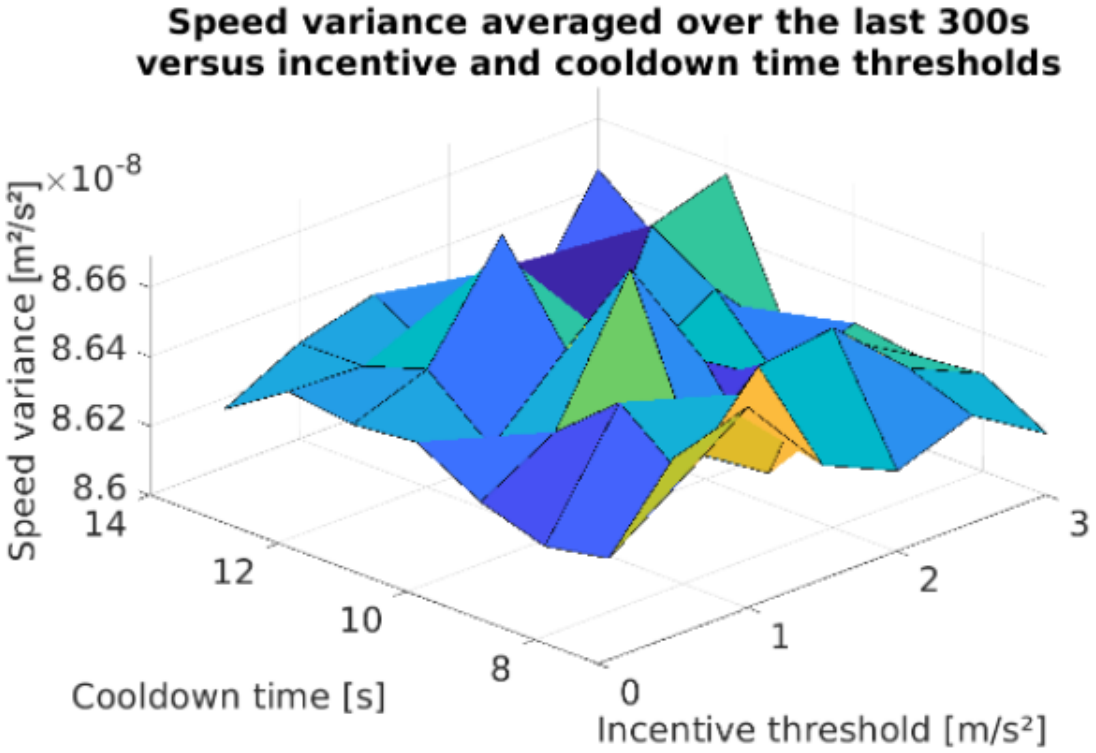

Figure 4.22 – The speed variance averaged over the last 300s with respect to the different lane changing parameters for $p = 0.875$

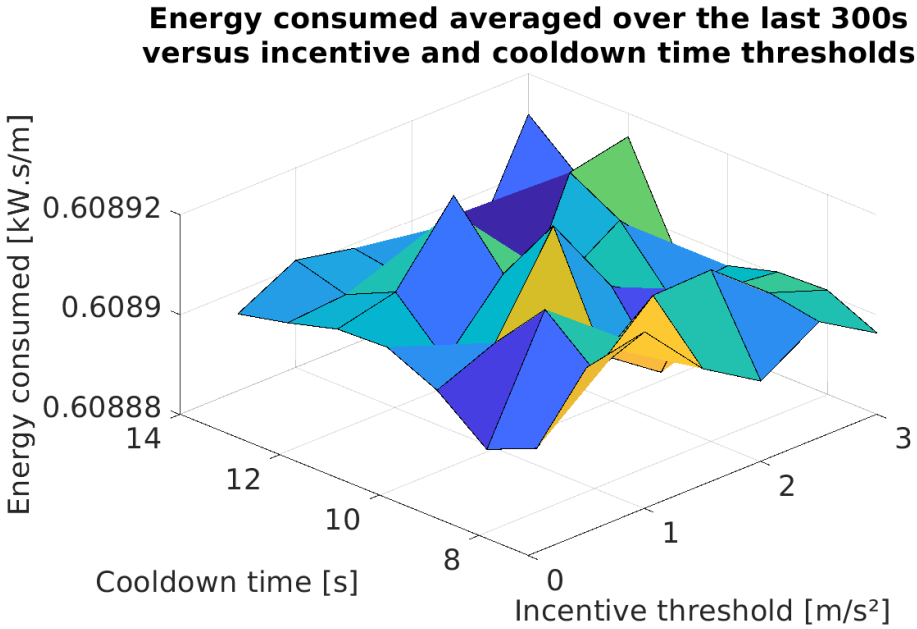

Figure 4.23 – The energy consumption averaged over the last 300s with respect to the different lane changing parameters for $p = 0.875$

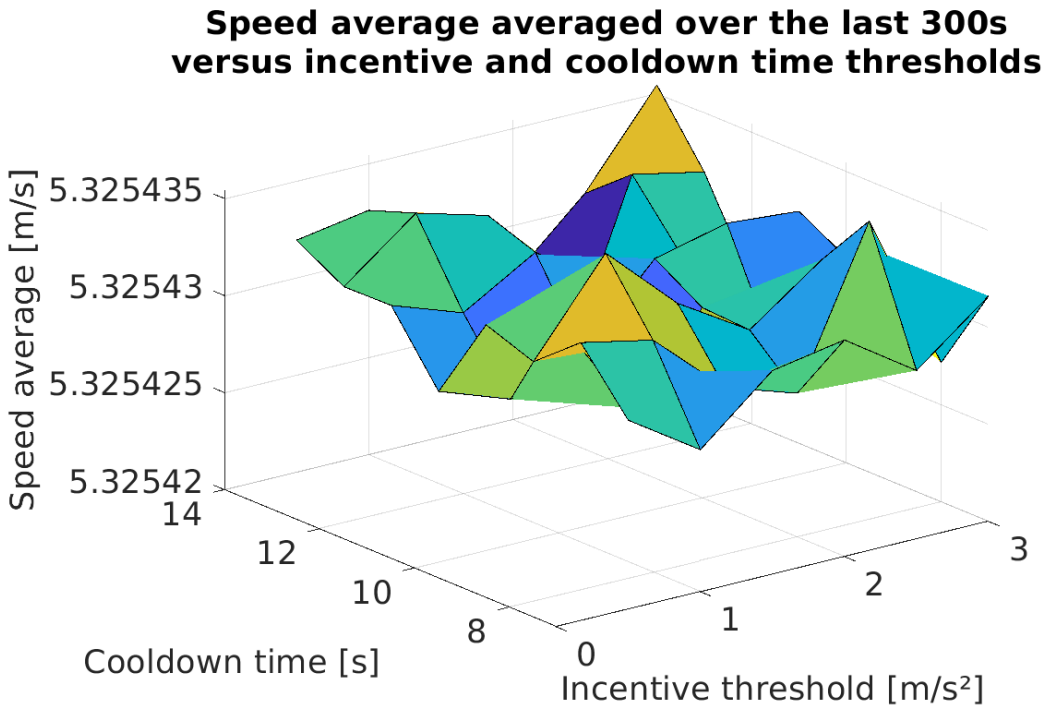

Figure 4.24 – The speed average averaged over the last 300s with respect to the different lane changing parameters for $p = 0.875$

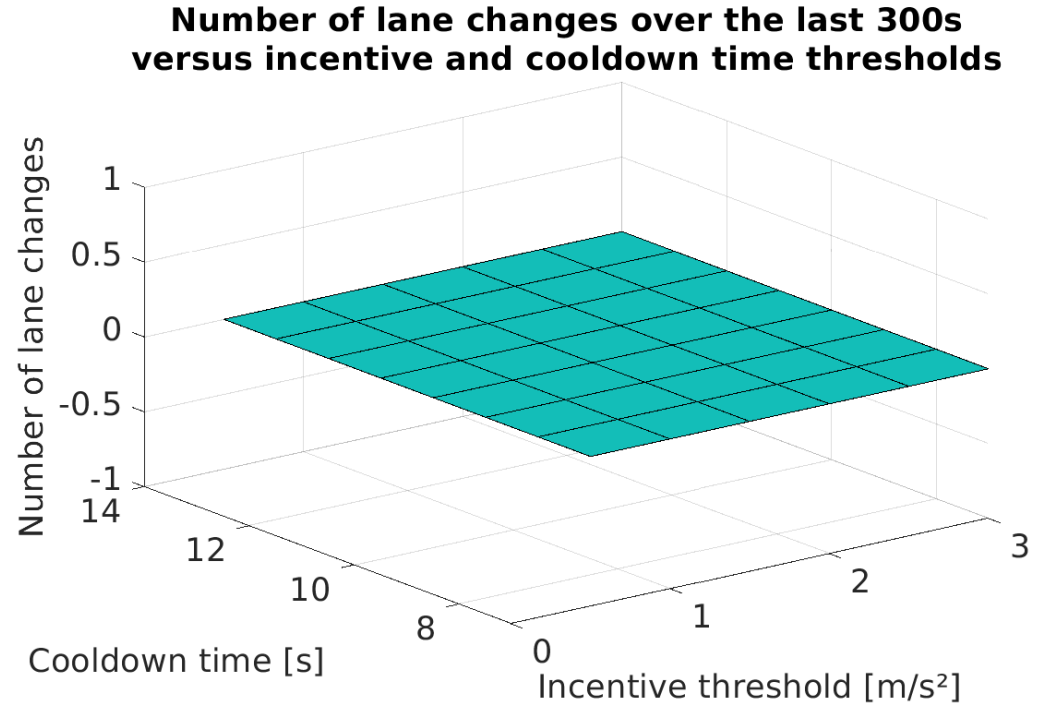

Figure 4.25 – The number of lane changes over the last 300s with respect to the different lane changing parameters for $p = 0.875$

Discussions:

We can observe that for $p = 0.875$, in the 2-phase traffic flow of trucks and cars (a higher penetration rate of trucks than the calculated $\tau_0 = 0.859$ in the previous subsection), the speed variance over the last $300s$ is lower than $8.66 \times 10^{-8} m^2/s^2$ for all the values of incentive and cooldown time thresholds, which is very much lower than the highest speed variance observed over the last $300s$ for $p = 0.917$, in the 2-phase traffic flow of collaborative and aggressive cars. **This suggests that trucks (heavy long vehicles) with the same weights for the Bando and FTL models than the collaborative cars can have a better stabilizing effect on an equilibrium flow than the collaborative cars, in a multi-lane system**. The highest energy consumption value observed for the different incentive and cooldown time thresholds of the 2-phase traffic flow of cars and trucks is cut by 94% of its value in the 1-phase traffic flow of aggressive cars for the value $2m/s^2$ of the safety threshold. However, we can see that the speed average over the last $300s$ for the 2-phase traffic flow of cars and trucks does not exceed $5.4m^2/s^2$, while it reaches $9m^2/s^2$, and exceeds $8m^2/s^2$ for all the range of the incentive threshold when the safety threshold equals $2m/s^2$, when having a single autonomous vehicle in a 1-phase traffic flow of cars. Regarding the number of lane changes over the last $300s$, it equals 0 for all the values of incentive and cooldown time thresholds in the 2-phase traffic flow of cars and trucks. This system is clearly very sensitive to the **value of the cooldown time for the trucks**, and the **value of the incentive threshold** for all the vehicles. For this reason, choosing values that are different than the ground truth for these parameters, can lead to results that are far from the ground truth.

Checking the validity of the results of Subsection 4.5.2 for these systems:

To see if the conclusions we drew in Subsection 4.5.2 still hold for this system, we perform the same simulations as explained in the beginning of this subsection, but with a different traffic configuration to have $p = 0.292$, as summarized in the table below:

Parameter	Value	What it represents
L	$2\pi 39.7$	Length of the road $[m]$
N	24	Total number of cars per lane
n_1	7	Number of trucks per lane
n_2	17	Number of aggressive cars per lane
p	0.292	Penetration rate of the trucks

Table 4.9 – Summary of the traffic configuration for $p = 0.292$

We obtain the following plots.

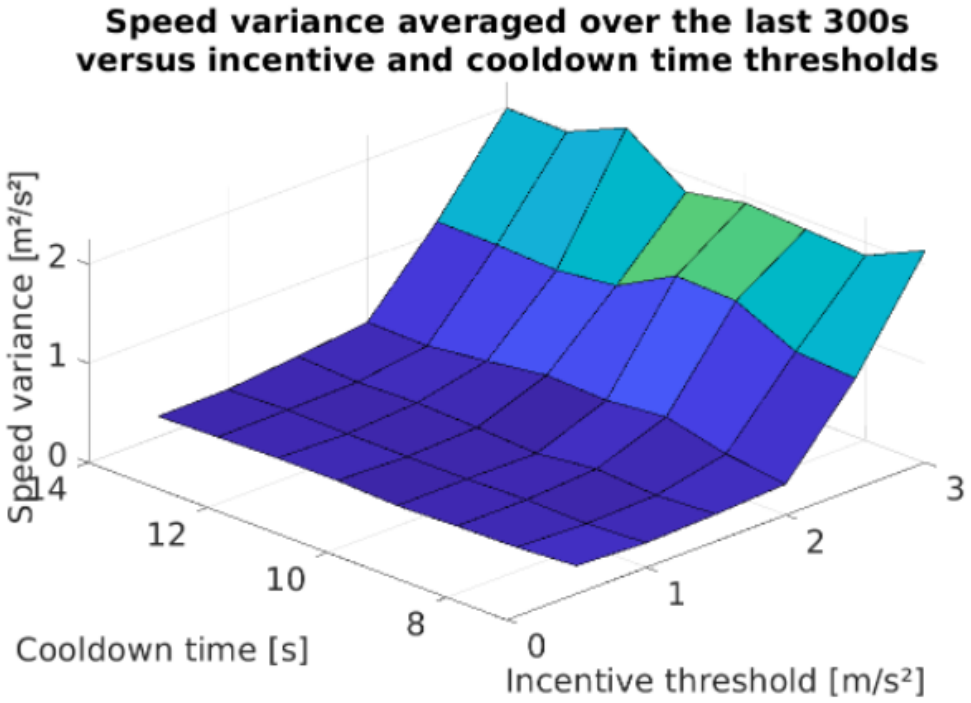

Figure 4.26 – The speed variance averaged over the last 300s with respect to the different lane changing parameters for $p = 0.292$

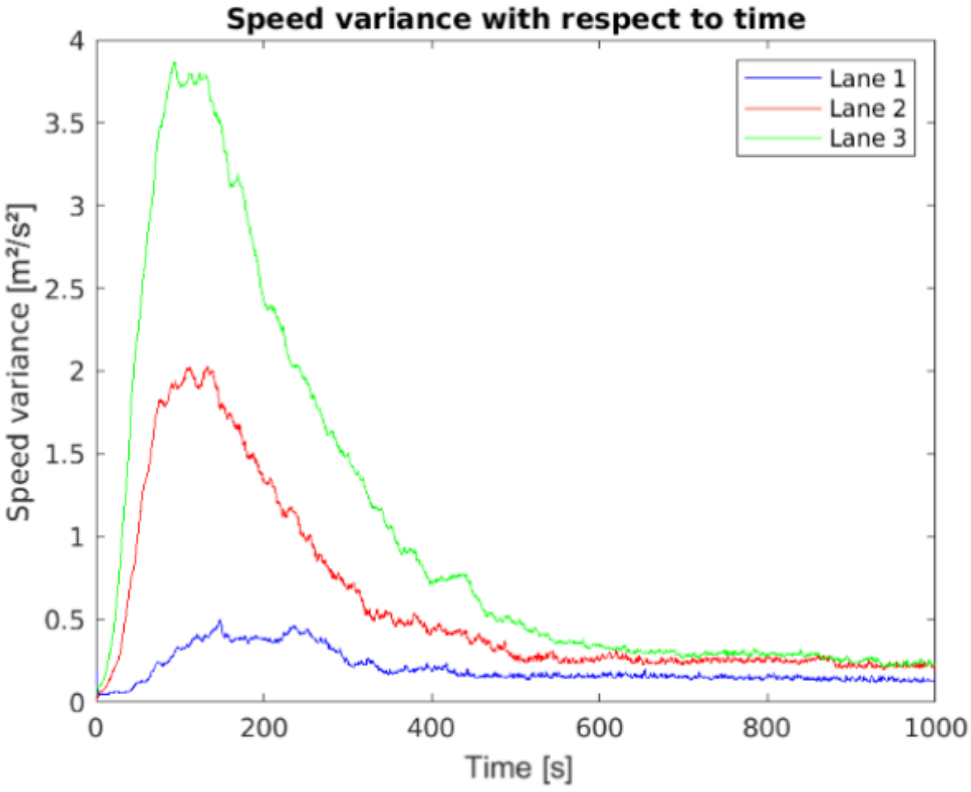

Figure 4.27 – The variation of speed variance with respect to time for $p = 0.292$, an incentive threshold of $2.5m/s^2$, and a cooldown time of trucks of $7s$

Discussions:

Despite having a smaller critical penetration rate for the single-lane version of the 2-phase traffic flow of trucks and aggressive cars than for the 2-phase traffic flow of collaborative and aggressive cars, the speed variance averaged over the last $300s$ for the 2-phase traffic flow of collaborative and aggressive cars does not exceed $0.1m^2/s^2$ for a penetration rate of collaborative cars equal to $p = 0.222$ when the safety threshold equals $2m/s^2$, while it reaches $2m^2/s^2$ when the safety threshold equals $2m/s^2$ and the penetration rate of trucks equals $p = 0.292$, in the 2-phase traffic flow of trucks and aggressive cars. However, $p = 0.292$ **still seems to make the speed variance of this system converge to a value that is very close to zero (or to zero)**. For the large values of the incentive threshold, the system acts like three single-lane roads which are independent (not coupled, not enough lane changes), which explains the speed variance that reaches $2m^2/s^2$.

Conclusions

In this work, we used the Bando-FTL microscopic traffic model with the Treiber et al. lane changing mechanism to describe the dynamics of the vehicles in a multi-lane ring road, and the $P\Delta P$ model to quantify vehicular fuel consumption. We were interested in the problem of dissipating stop-and-go waves in multi-lane road traffic flows and contributing to giving a better understanding of these systems. We showed that multi-lane traffic systems are very sensitive to lane changing parameters, and that it is possible to dissipate stop-and-go waves, in multi-lane 1-phase traffic flows of aggressive cars, by introducing a single autonomous vehicle following a prescribed acceleration law in high congestion, and obtain a reduction in vehicular energy consumption of up to 75%. Moreover, our investigations suggest that, in 2-phase multi-lane traffic flows of collaborative and aggressive cars, in contrast with single-lane systems, a proportion of collaborative cars as low as 22% can be effective to smooth stop-and-go waves. Finally, we studied a multi-lane 2-phase traffic system where coexist trucks (long heavy weight vehicles) with aggressive cars, and we showed that these systems are very sensitive to the trucks' cooldown time lane changing threshold, and that a proportion of 29% of trucks can be efficient to dissipate stop-and-go waves. We explain these low penetration rates of autonomous vehicles, collaborative cars, and trucks, that are effective for dissipating stop-and-go waves and bringing the system to an equilibrium flow, by the fact that in a multi-lane system, the dynamics of the vehicles in the different lanes are coupled, and a single vehicle can have an impact on the whole road by changing lanes.

In future research, one could improve the lane changing mechanism and reproduce our study (as we have seen that the Treiber et al. model was not perfect). We also did not derive rigorous theoretical results about multi-lane road traffic systems. This represents a logical next step.

References

[1] A. B. Abdulla Alalool, H. Khamis, R. Majdalawi, and R. Ainawi. Traffic congestion and long driving hours: Impact on stress, emotional and physical health among drivers in sharjah. In *9th Asia Pacific Global Summit on Healthcare & Immunology*, volume 7. Primary Health Care, 2017.

[2] A. Adebisi. A review of the difference among macroscopic, microscopic and mesoscopic traffic models. Technical report, Florida A&M University, Dec 2017.

[3] S. Albeaik, A. Bayen, M. T. Chiri, X. Gong, A. Hayat, N. Kardous, A. Keimer, S. T. McQuade, B. Piccoli, and Y. You. Limitations and improvements of the intelligent driver model (idm), 2021.

[4] A. Ameri. *Improving the Numerical Stability of Higher Order Methods with Applications to Fluid Dynamics*. PhD thesis, McGill University, Dec 2019.

[5] E. Balal, R. L. Cheu, and T. Sarkodie-Gyan. A binary decision model for discretionary lane changing move based on fuzzy inference system. *Transportation Research Part C: Emerging Technologies*, 67:47–61, 2016.

[6] R. Banerjee and A. Pal. Stabilization of inverted pendulum on cart based on lqg optimal control. In *ICCSDET*, Sep 2019.

[7] N. Bellomo and C. Dogbe. On the modeling of traffic and crowds: A survey of models, speculations, and perspectives. *SIAM Review*, 53(3):409–463, 2011.

[8] S. Bharadwaj, S. Ballare, Rohit, and M. K. Chandel. Impact of congestion on greenhouse gas emissions for road transport in mumbai metropolitan region. *Transportation Research Procedia*, 25:3538–3551, 2017. World Conference on Transport Research - WCTR 2016 Shanghai. 10-15 July 2016.

[9] D. Braess. Über ein paradoxon aus der verkehrsplanung. *Unternehmensforschung Operations Research 12*, 12, 1968.

[10] C. Chicone. *Stability Theory of Ordinary Differential Equations*, pages 8630–8649. Springer New York, New York, NY, 2009.

[11] S. Cui, B. Seibold, R. Stern, and D. B. Work. Stabilizing traffic flow via a single autonomous vehicle: Possibilities and limitations. In *2017 IEEE Intelligent Vehicles Symposium (IV)*, pages 1336–1341, 2017.

[12] M. L. Delle Monache and P. Goatin. Scalar conservation laws with moving constraints arising in traffic flow modeling: an existence result. *Journal of Differential Equations*, 257:4015–4029, 2014.

[13] M. L. Delle Monache, T. Liard, A. Rat, R. E. Stern, R. Bhadani, B. Seibold, J. Sprinkle, D. B. Work, and B. Piccoli. Feedback control algorithms for the dissipation of traffic waves with autonomous vehicles. In *Computational Intelligence and Optimization Methods for Control Engineering*, pages 275–299. Springer, 2019.

[14] M. Di Francesco and M. D. Rosini. Rigorous derivation of nonlinear scalar conservation laws from follow-the-leader type models via many particle limit. *Archive for Rational Mechanics and Analysis*, 217(3):831–871, Jan 2015.

[15] M. Garavello, K. Han, and B. Piccoli. *Models for Vehicular Traffic on Networks*. American Institute of Mathematical Sciences, June 2016.

[16] X. Gong and A. Keimer. On the well-posedness of the "bando-follow the leader" car following model and a time-delayed version. Technical report, School of Mathematical and Statistical Science, Arizona State University, Feb 2022.

[17] Y. Han, A. Hegyi, Y. Yuan, S. Hoogendoorn, M. Papageorgiou, and C. Roncoli. Resolving freeway jam waves by discrete first-order model-based predictive control of variable speed limits. *Transportation Research Part C: Emerging Technologies*, 77:405–420, 2017.

[18] A. Hayat, T. Liard, F. Marcellini, and B. Piccoli. A multiscale second order model for the interaction between AV and traffic flows: analysis and existence of solutions. working paper or preprint, January 2021.

[19] A. Hayat, B. Piccoli, and S. Truong. Dissipation of traffic jams using a single autonomous vehicle on a ring road. working paper or preprint, Sep 2021.

[20] A. Hayat, B. Piccoli, and S. Xiang. Stability of multi-population traffic flows, 2022.

[21] D. Helbing. Traffic and related self-driven many-particle systems. *Rev. Mod. Phys.*, 73:1067–1141, Dec 2001.

[22] Inrix. Leading transportation analytics solutions-inrix. https://inrix.com/. Accessed: 2022-06-19.

[23] I. Izadgoshasb, Y. Y. Lim, L. Tang, R. Padilla, Z. S. Tang, and M. Sedighi. Improving efficiency of piezoelectric based energy harvesting from human motions using double pendulum system. *Energy Conversion and Management*, 184:559–570, Mar 2019.

[24] N. Kardous, A. Hayat, S. T. McQuade, X. Gong, S. Truong, T. Mezair, P. Arnold, R. Delorenzo, A. Bayen, and B. Piccoli. A rigorous multi-population multi-lane hybrid traffic model for dissipation of waves via autonomous vehicles. *Eur. Phys. J. Spec. Top.*, 2022.

[25] A. Katok and B. Hasselblatt. *Introduction to the Modern Theory of Dynamical Systems*. Cambridge University Press, 1995.

[26] S. H. Kellert. *In the wake of chaos : unpredictable order in dynamical systems*. University of Chicago Press, 1993.

[27] F. Kessels. *Mesoscopic Models*, pages 99–106. Springer International Publishing, Cham, 2019.

[28] A. Kesting, M. Treiber, and D. Helbing. General lane-changing model mobil for car-following models. *Transportation Research Record*, 1999:86–94, Jan 2007.

[29] F. Knorr, D. Baselt, M. Schreckenberg, and M. Mauve. Reducing traffic jams via vanets. *IEEE Transactions on Vehicular Technology*, 61:3490–3498, 2012.

[30] K. Konishi, H. Kokame, and K. Hirata. Decentralized delayed-feedback control of an optimal velocity traffic model. *Eur. Phys. J. B*, 15(4):715–722, 2000.

[31] C. E. Lawrence. *An Introduction to Mathematical Optimal Control Theory*. University of California Berkeley, 2013.

[32] T. Liard and B. Piccoli. On entropic solutions to conservation laws coupled with moving bottlenecks. working paper or preprint, June 2019.

[33] T. Liard and B. Piccoli. Well-posedness for scalar conservation laws with moving flux constraints. *SIAM Journal on Applied Mathematics*, 79(2):641–667, 2019.

[34] M. J. Lighthill and G. B. Whitham. On kinematic waves ii. a theory of traffic flow on long crowded roads. *Royal Society*, 229:317–345, 1955.

[35] S. Moridpour, M. Sarvi, and G. Rose. Lane changing models: a critical review. *Transportation Letters*, 2(3):157–173, 2010.

[36] T. Nagatani. Traffic jam and shock formation in stochastic traffic-flow model of a two-lane roadway. *Journal of the Physical Society of Japan*, 63(1):52–58, 1994.

[37] A. Nissan and H. N. Koutsopoulosb. Evaluation of the impact of advisory variable speed limits on motorway capacity and level of service. *Procedia - Social and Behavioral Sciences*, 16:100–109, 2011. 6th International Symposium on Highway Capacity and Quality of Service.

[38] B. Piccoli and A. Tosin. *Vehicular Traffic: A Review of Continuum Mathematical Models*, pages 9727–9749. Springer New York, New York, NY, 2009.

[39] H. Pohlmann and B. Seibold. Simple control options for a vehicle used to dissipate traffic waves. Technical report, UC Berkeley, 2015.

[40] J. Popping. An overview of microscopic and macroscopic traffic models. Bachelor's thesis, mathematics, University of Groningen, 2013.

[41] H. Rakha, K. Ahn, and A. Trani. Comparison of mobile5a, mobile6, vt-micro, and cmem models for estimating hot-stabilized light-duty gasoline vehicle emissions. *Canadian Journal of Civil Engineering*, 30(6):1010–1021, 2003.

[42] P. I. Richards. Shock waves on the highway. *Operations Research*, 4(1):42–51, 1956.

[43] SAE. Taxonomy and definitions for terms related to on-road motor vehicle automated driving systems. Technical report, SAE, 2021.

[44] H. Slamani. Les embouteillages étouffent les villes algériennes : Un lourd coût économique. https://www.elwatan.com/. Accessed: 2022-07-01.

[45] R. Smit. Development and performance of a new vehicle emissions and fuel consumption software (pδp) with a high resolution in time and space. *Atmospheric pollution research*, 4(3):336–345, 2013.

[46] R. E. Stern, S. Cui, M. L. Delle Monache, R. Bhadani, M. Bunting, M. Churchill, N. Hamilton, R. Haulcy, H. Pohlmann, F. Wu, B. Piccoli, B. Seibold, J. Sprinkle, and D. B. Work. Dissipation of stop-and-go waves via control of autonomous vehicles: Field experiments. *Transportation Research Part C: Emerging Technologies*, 89:205–221, April 2018.

[47] Y. Sugiyama, M. Fukui, M. Kikuchi, K. Hasebe, A. Nakayama, K. Nishinari, S. Tadaki, and S. Yukawa. Traffic jams without bottlenecks—experimental evidence for the physical mechanism of the formation of a jam. *New Journal of Physics*, 10(3):033001, Mar 2008.

[48] A. Talebpour and H. S. Mahmassani. Influence of connected and autonomous vehicles on traffic flow stability and throughput. *Transportation Research Part C: Emerging Technologies*, 71:143–163, 2016.

[49] T. Toledo and R. Katz. State dependence in lane-changing models. *Transportation Research Record*, 2124(1):81–88, 2009.

[50] TomTom. Tomtom traffic index-live congestion statistics and historical data. https://www.tomtom.com/en_gb/traffic-index/. Accessed: 2022-06-19.

[51] M. Treiber, A. Hennecke, and D. Helbing. Congested traffic states in empirical observations and microscopic simulations. *Phys. Rev. E*, 62:1805–1824, Aug 2000.

[52] M. Treiber and A. Kesting. Modeling lane-changing decisions with mobil. In Cécile Appert-Rolland, François Chevoir, Philippe Gondret, Sylvain Lassarre, Jean-Patrick Lebacque, and Michael Schreckenberg, editors, *Traffic and Granular Flow '07*, pages 211–221, Berlin, Heidelberg, 2009. Springer Berlin Heidelberg.

[53] E. Trélat. *Contrôle optimal : théorie et applications*. Vuibert, Collection "Mathématiques Concrètes", 2008.

[54] S. Wiggins. *Introduction to Applied Nonlinear Dynamical Systems and Chaos*. Springer, 2003.

[55] Z. Zheng. Recent developments and research needs in modeling lane changing. *Transportation research part B: methodological*, 60:16–32, 2014.